Accepted Manuscript

Exploration of the Molecular Architecture of the Orthosteric Binding Site in the α4β2 Nicotinic Acetylcholine Receptor with Analogs of 3-(Dimethylamino)butyl Dimethylcarbamate (DMABC) and 1-(Pyridin-3-yl)-1,4-diazepane

Tinna B. Bach, Anders A. Jensen, Jette G. Petersen, Troels E. Sørensen, Serena Della Volpe, Jun Liu, Antoni R. Blaazer, Jacqueline E. van Muijlwijk-Koezen, Thomas Balle, Bente Frølund

PII: S0223-5234(15)30156-2

DOI: 10.1016/j.ejmech.2015.07.024

Reference: EJMECH 8008

To appear in: *European Journal of Medicinal Chemistry*

Received Date: 24 February 2015

Revised Date: 10 July 2015

Accepted Date: 13 July 2015

Please cite this article as: T.B. Bach, A.A. Jensen, J.G. Petersen, T.E. Sørensen, S. Della Volpe, J. Liu, A.R. Blaazer, J.E. van Muijlwijk-Koezen, T. Balle, B. Frølund, Exploration of the Molecular Architecture of the Orthosteric Binding Site in the α4β2 Nicotinic Acetylcholine Receptor with Analogs of 3-(Dimethylamino)butyl Dimethylcarbamate (DMABC) and 1-(Pyridin-3-yl)-1,4-diazepane, *European Journal of Medicinal Chemistry* (2015), doi: 10.1016/j.ejmech.2015.07.024.

Graphical abstract

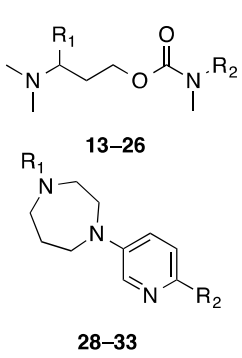

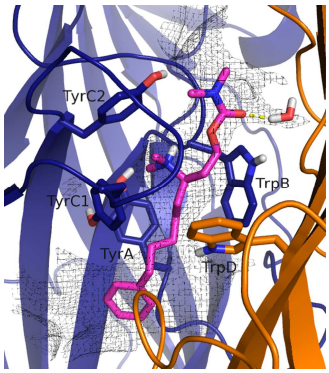

Exploration of the Molecular Architecture of the Orthosteric Binding Site in the α4β2 Nicotinic Acetylcholine Receptor with Analogs of 3-(Dimethylamino)butyl Dimethylcarbamate (DMABC) and 1-(Pyridin-3-yl)-1,4-diazepane

Tinna B. Bach,[#] Anders A. Jensen,[#] Jette G. Petersen,[#] Troels E. Sørensen,[#,†] Serena Della Volpe,[#] Jun Liu,[†] Antoni R. Blaazer,[º] Jacqueline E. van Muijlwijk-Koezen,[º] Thomas Balle,[†,] and Bente Frølund[#,*]*

[#]Department of Drug Design and Pharmacology, Faculty of Health and Medical Sciences, University of Copenhagen, Universitetsparken 2, DK-2100 Copenhagen, Denmark

[†]Faculty of Pharmacy, The University of Sydney, Sydney, NSW 2006, Australia

[º]Division of Medicinal Chemistry, Amsterdam Institute for Molecules, Medicines and Systems, Faculty of Sciences, VU University Amsterdam, De Boelelaan 1105, 1081 HV Amsterdam, The Netherlands

*Corresponding Authors:

Bente Frølund, e-mail: bfr@sund.ku.dk, phone: (+45)35336495

and Thomas Balle, e-mail: thomas.balle@sydney.edu.au, phone (+61)290367035

ABSTRACT

X-ray crystal structures of Acetylcholine binding proteins (AChBPs) have revealed two different possible extensions to the classical ligand binding pocket known to accommodate various nicotinic agonists. One of the pockets is limited in size while the other is of considerable dimensions and protrudes along the interfacial cleft between subunits. To probe these putative extensions in functional nicotinic acetylcholine receptors (nAChRs), elongated analogs of 3-(dimethylamino)butyl dimethylcarbamate (DMABC) and 1-(pyridine-3-yl)-1,4-diazepane were prepared and characterized pharmacologically at neuronal heteromeric nAChRs. Although the new analogs, relative to parent compounds, displayed lower binding affinities, functional characterization of selected compounds revealed that they had retained partial α4β2 nAChR agonist activity. The structure-activity relationship data did not indicate an upper limit to the size of substituents as would have been expected if the bound in the smaller pocket. The data were better in agreement with a binding mode in which substituents protrude along the interfacial cleft of the receptor. This was further supported by docking into a homology model of the α4-β2 nAChR interface and by surface plasmon resonance biosensor analysis of binding of the compounds to acetylcholine-binding proteins, where they exhibit preference for *Lymnaea stagnalis* ACh binding protein (*Ls*-AChBP) over the *Aplysia californa* ACh binding protein (*Ac*-AChBP). These results suggest new opportunities for expanding chemical space in the development of partial agonist and may be of interest in relation to development of novel smoking cessation aids.

Keywords: nACh receptor agonists, structure-activity studies, *Ls*-AChBP, *Ac*-AChBP, Lobeline, DMABC analogs

1. Introduction

The neurotransmitter acetylcholine (ACh, **1**, Figure 1) mediates its physiological effects in the central and peripheral nervous systems through two classes of receptors: the muscarinic and nicotinic ACh receptors (mAChRs and nAChRs, respectively) [1-4]. Central nAChRs are involved in regulation of release of other neurotransmitters, including dopamine, norepinephrine, serotonin, glutamate, and γ-aminobutyric acid [5-8]. The fact that imbalances in the cholinergic system have been proposed to be involved in devastating diseases such as schizophrenia, depression, epilepsy, and Alzheimer's and Parkinson's diseases has spawned the interest in nAChRs as putative drug targets in these disorders [1, 3].

Neuronal nAChRs consist of five subunits that can be either identical (homomeric, α only) or different (heteromeric, combination of α and β subunits) [1][12]. The α4β2 and α7 receptors are the most abundant nAChRs in the brain while α3b4 nAChRs dominate in the autonomic ganglia. [1, 13]. The orthosteric binding sites in the heteromeric receptors are located at the extracellular $\alpha^{(+)}/\beta^{(-)}$ interface (α and β contributing with the principal and complementary binding component, respectively).

ACh binding proteins (AChBPs) have proven valuable as surrogate proteins for structural studies of orthosteric ligand binding to nAChRs [16-20]. The AChBP is a soluble homopentameric protein complex with a structure and fold similar to that of the extracellular domain of the nAChR. Although the overall sequence identities between AChBPs and nAChRs are low (20-24%), the interfacial ACh binding site in the AChBP is highly conserved including the "aromatic box" which consists of five aromatic residues. These residues, TyrA, TrpB, TyrC1, TyrC2 and TrpD, named according to the loop in the orthosteric nAChR site on which they reside [21] (Figure 2A), are strictly conserved among all nAChRs as well as *Ls*-AChBP. In *Ct*- and *Ac*-AChBP TrpD in the nAChR is replaced by an isoleucine and a tyrosine, respectively. From more than 50

AChBP co-crystal structures, it is clear that the binding site is flexible, and that the aromatic box residues play an important role in defining its shape and size. When an agonist binds, as illustrated by (*S*)-nicotine bound to *Ls*-AChBP [24] (Figure 2A), the aromatic residues pack around the ligand to form a closed binding site. In response to more bulky ligands, including antagonists methyllycaconitine [17], α-cobratoxin [25], and α-conotoxin ImI [26], TyrC1 and TyrC2 on the flexible loop C which forms a lid on the binding site can easily be displaced outwards. Two other aromatic box residues observed to adopt alternative conformation in AChBP structures are TyrA and TrpD (TyrD in *Ac*-AChBP). Alternative conformations of these residues have revealed two different extensions to the binding pocket that can accommodate non-classical ligands, including lobeline [17, 20] (**2**, Figure 1 and Figure 2B) and the synthetic compound, 3α-(benzoyloxy)-8β-((*R*)-2-hydroxy-2-phenylethyl)-8α-methyl-8 azoniabicyclo[3.2.1]octane methiodide (**3**, Figure 1 and Figure 2C) [27]. From crystallographic studies of *Ac*-AChBP it is known that a sub-pocket is made accessible by rotameric shift of TyrA upon binding of **2** (Figure 2B) [17]. However, mutational studies indicate that the flip is dependent on specific residues on Loop F on the complementary subunit interface to stabilize the tyrosine in its alternative conformation [27], and it remains unknown if the pocket exists in nAChRs. The second sub-pocket is an extension of the binding site along the dimer interface towards the ion channel and has been observed by co-crystallization of **3** with *Ac*-AChBP [27]. Simultaneous repositioning of TyrA and TyrD in *Ac*-AChBP exposes a narrow cleft where the ligand is wedged between the two aromatic residues (Figure 2C). The existence of this interfacial pocket is also evident from co-crystal structures with MLA and from covalent trapping experiments with a maleimide analog of MLA in both α7 and α4β2 receptors [28, 29], it is evident that the pocket is not an AChBP artifact. The alternative

sub-pockets as extensions to the classical agonist binding site have so far received little attention.

In previous studies, we have explored the medicinal chemistry of 3-(dimethylamino)butyl dimethylcarbamate (**4**, DMABC) and its desmethyl analog **5** [31-33], and 1-(pyridin-3-yl)-1,4-diazepane (**6**) [34] as potent nAChR agonists (Figure 1). Co-crystal structures with *Ls*-AChBP have revealed that both **4** and **6** form direct contacts to TyrA, the residue observed to adopt a flipped state in the *Ac*-AChBP co-crystal structure with **2** [35, 36] (SI Figure 1A,B). Inspired by these co-crystal structures, we have in the present study elaborated on the scaffolds of **4** and **6** to explore possible extensions of the agonist binding pocket and to investigate the structure-activity relationships (SARs) of elongated analogs of these structures at the α4β2 nAChR.

2. Results and discussion

2.1 Ligand design

Based on overlays of AChBP co-crystal structures with **4** and **6** on co-crystal structures with **2** and **3** (Figures 3A-D), we designed a series of ligands with substituents that could protrude towards the two cavities (illustrated in Figures 2B and 2C). In the first series, one of the methyl groups on the basic amine of **4** was replaced with 2-hydroxy-phenethyl and phenylpropyl substituents to give compounds **7** and **8** (Table 1). These compounds were designed to challenge the position of TyrA potentially allowing access to the sub-pocket associated with the binding of **2** (Figure 2B). Along these lines, a series of compounds based on bioisosteric replacements of the dimethylcarbamate moiety with methylcarbamate to give compounds **9**–**12** (Table 1) was also planned. In a second series, the 3-methyl group of **4** was replaced with longer arylalkyl substituents from phenethyl to phenylpentyl to give compounds **13**–**16** and aryl ethers **17**–**21** (Table

1). These compounds were inspired from the overlay of **4** and **3** (Figure 3B) indicating that large substituents in this position could protrude along the interfacial cleft (Figure 2C) without compromising the binding mode of the core agonist fragment. Again, bioisosteric replacements of the dimethylcarbamate with methylcarbamate and an imidazolyloxy moiety were explored resulting in C3 substituted analogs **22**–**27** (Table 1). In a third series, we explored the 1,4-diazepane scaffold of **6**. As *N*-4 forms a hydrogen bond to TyrA in the X-ray structure, substitution in this position could lead to either tyrosine flip exposing the subpocket associated with binding of **2** in *Ac*-AChBP or alternatively a minor change in binding mode allowing the substituent to exit the binding site via the cavity along the interfacial cleft (Figure 3C and 3D). Thus benzyl, phenethyl, phenylpropyl, and phenpropenyl substituents were introduced on the *N*-4 of the 1,4-diazepane to challenge these areas in extension to the orthosteric binding site and resulted in compounds **28**–**33** (Table 2). In the analog series of **6**, we also explored a series of piperazine analogs, **34**–**36**, with benzyl, phenethyl and phenylpropyl substituents on *N*-4 of the piperazine ring (Table 2).

2.2 Chemistry

The syntheses of *N*-arylalkyl analogs of **4** (compounds **7**–**12**) are illustrated in Scheme 1. The synthesis of **9** and **10** was achieved by a three-step procedure starting from methyl acetoacetate and either methyl benzylamine or methyl phenethylamine to yield **38** and **39**. Alcohols **40** and **41** were obtained by reduction with sodium which after treatment with 1,1'-carbonyldiimidazole (CDI) and either methyl- or dimethylamine (in either H_2O or ethanol) gave **9**, **10** and **37**. Products **9** and **37** were exposed to hydrogenolysis that afforded **42** and **43** in good yields which subsequently were reacted with either the appropriate epoxide to give **7** and **11** or subjected to reductive amination to afford **8** and **12**.

The synthesis approaches to C-3-arylalkyl analogs of **4** are presented in Schemes 2 and 3. Target compounds **13**–**15** and **22**–**25** were synthesized starting from **44**–**47** (Scheme 2), which have been previously described [37, 38]. Subsequent Michael addition afforded compounds **48**–**51** that were treated with $LiAlH_4$ to give the alcohols **52**–**55**. Carbamate formations were performed as described above to yield the final compounds. Compound **27** was obtained by reacting the alkoxide of **54** with 2,4,5-tribromo-1-methyl-1*H*-imidazole and subsequent treatment of the product with *n*-BuLi (Scheme 2).

Target compounds **17** and **18** were synthesized from **56**[31] by an Ullmann like reaction, whereas **19-21** were obtained by nucleophilic aromatic substitution with **56** as the nucleophile (Scheme 3). A different approach was applied for the synthesis of the C-3-arylalkyl analogs **16** and **26** to introduce the hydroxyl group in the α position to the phenyl ring (Scheme 3). Alcohol **57**[39] was protected as the tetrahydropyranyl (THP) ether using our previously published procedure [31]. The procedures for the following steps to afford **16** and **26** are described above, and the final target compounds **16** and **26** were obtained after THP-deprotection with *p*-toluenesulfonic acid monohydrate.[31]

The syntheses of the *N*-arylalkyl 3-pyridyl diazacycle analogs are presented in Scheme 4. Analog **28** was synthesized in two steps from **58**[40]. First, intermediate **59** was obtained by a selective bromination in the 6-position of **58** using NBS. Subsequent Boc-deprotection followed by reductive amination afforded the analog. Compounds **29**–**36** were synthesized as described for **28**. All target compounds were characterized pharmacologically as the oxalate salts.

2.3 Pharmacology and SAR discussion

The binding affinities displayed by the target compounds and reference compounds **1**, **2**, and **4-6** in a [^{3}H]-epibatidine competition binding assays to membranes from HEK293 cells stably expressing recombinant rat α4β2, α4β4, and α3β4 nAChRs are presented in Tables 1 and 2. Functional data for selected compounds and reference compounds determined in a fluorescence-based functional assay the FLIPR Membrane Potential Blue assay and in two-electrode-voltage-clamp (TEVC) electrophysiology recordings at nAChR expressed in *Xenopus* oocytes are given in Tables 3 and 4. Dissociation constants determined for **30** and **32** at *Ac*- and *Ls*-AChBP by surface plasmon resonance (SPR) biosensor analyses, respectively, are shown in Table 5.

In the following, SARs have been classified into groups: *N*-arylalkyl analogs of **4** (compounds **7**–**12**); C-3-arylalkyl analogs of **4** (compounds **13**–**26**); and *N*-arylalkyl 3-pyridyl diazacycle analogs (compounds **28**–**36**).

*2.3.1 N-arylalkyl analogs of DMABC (**4**)*

Earlier reported SAR studies for analogs of **4** showed that incorporating the amino group into a piperidine or pyrrolidine ring decreased binding affinities significantly relative to **4** [33]. Based on overlay of the X-ray structure of AChBP co-crystallised with structures **2** and **4** (Figure 3A) this can be rationalized by either a loss of affinity due to the energetic penalty associated with moving TyrA away to allow access to the sub-pocket associated with binding of **2** or, alternatively, by an altered binding mode of the core agonist fragment required to position the increased steric bulk in the sub-pocket associated with binding of **3**. We hypothesized that if the first scenario was in play we should be able to alter the size of the substituent on the basic nitrogen to optimally fit the sub-pocket illustrated in Figure 2B. This should then be reflected in improved

binding affinities up until a certain point after which it should drop drastically. For the second scenario a more flat SAR is to be expected. The resulting *N*-arylalkyl analogs **7**–**12** exhibited binding affinities in the mid-to-high micromolar range corresponding to a reduction in affinity at α4β2 nAChRs of more than 900-fold compared to **4**. No significant recovery of affinity was observed with increasing size of substituents, nor upon incorporation of a hydroxyl group (**7** and **11**) to mimic the hydroxyl group in **2**. Together, this SAR does not suggest that substituents access the subpocket analogous to the one observed upon binding of **2** in *Ac*-AChBP.

*2.3.2 C3-arylalkyl analogs of DMABC (**4**)*

We have previously reported that presence of a small hydrophobic group, preferably a methyl group, at the C-3 carbon of **4** was optimal for nAChR receptor binding and have found that the (*R*)-enantiomer of **4** is significantly more potent than the (*S*)-enantiomer [33]. Introduction of larger hydrophobic substituents, including isopropyl or cyclohexyl, in this position induced a shift from nanomolar to micromolar affinity at the heteromeric nAChRs [33]. Introduction of the more planar cyclopropyl, 3-thiophenyl, and phenyl substituents also led to significant decreases in binding affinity compared to the parent compound, **4** [31]. However, overlay of the X-ray structures of **3** and **4** (Figure 3B) suggested that even larger substituents in the C-3 position of **4** could protrude along the interfacial cleft basically without limitation to length of the substituents. Therefore, arylalkyl chains with varying length were introduced in the C-3 position to probe the effect of larger substituents. The resulting compounds (**13**–**15**) exhibited affinities in the low micromolar range corresponding to 45–95 fold loss in affinity relative to **4**. For the monomethylcarbamates (**22–25**) a decrease in affinities of more than 800-fold relative to **5** was observed. Interestingly, elongation of the alkyl chain from two to five carbons did not affect binding affinity significantly as evident comparing the phenethyl

substituted analog **22** (7.1 μM, α4β2 nAChR) to the phenylpentyl substituent of **25** (2.7 μM, α4β2 nAChR). A similar trend was observed for the dimethylcarbamate analogs **13**–**15**. This indicates that the binding pocket can accommodate substituents with a significant difference in length and is compatible with the flat SAR that was expected for compounds protruding into an interfacial cleft (Figure 2C).

In a previous study, imidazolyloxy moities were shown to be carbamate bioisosteres at the α4β2 nAChRs [35]. Exchange of the carbamate in compound **24** for a 1-methyl-1*H*-imidazoloxy moiety (**27**) yielded the most potent compound of the series with an affinity at the α4β2 nAChR of 0.76 μM and a selectivity for the α4β2 nAChRs over the α4β4 and α3β4 nAChRs, in concordance with data for the parent compounds [35].

To illustrate compatibility of the elongated ligands with a structural model of the receptor, compounds **13**–**15**, **22**–**25**, and **27** were docked into a homology model of the α4β2 nAChR interface constructed using the co-crystal structure of AChBP with **3** to ensure a model with an accessible interfacial cleft. The suggested binding modes of the *R*-enantiomers of these compounds only differed with respect to how far along the interfacial cleft the substituent protruded (Figure 4A). In addition, the binding mode was found not to compromise the binding mode of the parent agonist fragment, **4**, which in a co-crystal structure was identified as the (*R*)-enantiomer [35]. Analogs of **4** with aryl ethers in the C3-position (**17**–**21**) were found to have decreased affinities relative to **4** and corresponding alkyl phenyl analogs with substituents of comparable size as evident by the 14- and 3-fold lower affinity (α4β2 nAChR) of **17** and **20** relative to **22** and **23**. These data are in concordance with observations made from previous C-3 substituted analogs of **4** in which introduction of a hydroxymethyl group in the C-3 position led to a significantly larger decrease in nAChR binding affinity compared to **4**,[31] whereas the binding affinity of the corresponding ethyl analog was much less affected.[41] These data are consistent with a high internal energy of **17** (~10 kJ/mol)

for the conformation resembling the bioactive conformation of **4** [35]. Internal hydrogen bonding from the protonated amine to the ether oxygen is preferred as opposed to the internal hydrogen bond to the carbamate oxygen observed in the bound conformation of **4** (SI Figure 1). As the compounds originally were inspired by **2**, we investigated the effect of a hydroxyl group in the α-position relative to the phenyl ring. In **2**, this is highly favorable and leads to a 25-fold increase in affinity [42]. In the present series the effect was opposite and led to ca. 10-fold decrease in affinity at α4β2 nAChRs (compare **13** and **23** to **16** and **26)**.

2.3.3 N-arylalkyl 3-pyridyl diazacyle analogs

3-Pyridyl substituted diazacycles and diazabicycles are privileged structures and have been the prime scaffolds for synthesis of high affinity α4β2 nAChR agonists. Among these, the scaffold of **6** has been extensively applied in the study of nAChRs in which introduction of various substituents in the 5- and 6-positions on the pyridine ring afforded high-affinity compounds. Especially, rather large substituents including methoxyalkyl groups were allowed in the 5-position but not in the 6-position. Furthermore, analogs of **6** have been reported in which the 1,4-diazepane ring was exchanged for the piperazine ring which generally led to a reduction in α4β2 affinities by up to two orders of magnitude [34]. To our knowledge, the nAChRs have not systematically been challenged by large substituents in the *N*-4 position of the scaffold of **6** and the corresponding piperazine scaffold.

The overlay of X-ray structures of **2** and **6** (Figure 3C) suggested an arylalkyl chain length of approximately 1-2 carbons in the *N*-4 position of **6** to be optimal for reaching into the subpocket associated to the binding of **2**. On the other hand, a chain length of three should be too long. Alternatively, if accessing the interfacial cleft pocket, arylalkyl

substituents could in principle be of any length but would require a slight change in binding mode of the core agonist fragment to allow the substituent to escape the cavity. Introduction of phenylalkyl substituents (benzyl, phenethyl, and phenylpropyl) led to compounds **30**–**32** which displayed 100–150 fold reduced binding affinities at α4β2 nAChRs compared to the parent compound, **6**. Since **6** is a highly potent α4β2 nAChR agonist (Table 2), the *N*-4 substituted analogs still displayed binding affinities in the low to medium nanomolar range. The equivalent series of 1-(pyridin-3-yl)piperazine analogs (**34**–**36**) displayed 5- to 10-fold lower affinity at the three heteromeric nAChRs compared to the 1,4-diazepane containing analogs **30**–**32**. However, a similar SAR pattern was observed for analogs of **6** and the corresponding piperazine analogs indicating a similar binding mode of the analogs in which the benzyl, phenethyl, and phenylpropyl substituents in the *N*-4 positions are tolerated with a flat SAR in agreement with binding along the interfacial cleft as illustrated by docking in Figure 4B.

Based on docking experiments, the analogs **30**–**32** are positioned less optimal for interaction of the core agonist fragment and in particular the protonated *N*-4 with the receptor. This may explain the relatively larger decrease in affinities (>100-fold) compared to the C-3 substituted analogs of **4** which only suffered a ca. 35-fold reduction in affinity and which upon docking had its core agonist part optimally positioned as in the X-ray structure. To probe the importance of reduction of entropic penalty of binding, an alkenyl analog of **32**, **29**, was evaluated. However, **32** and **29** were found equipotent at the receptors indicating that this specific reduction in conformational flexibility is not important for receptor binding. In an attempt to increase binding affinity, a bromine atom was inserted in the 6-position of the pyridine ring of **6**, which previously was found to improve affinity and potency [34, 43]. However, the analog (**28**) exhibited a 10-fold decrease in affinity at the α4β2 nAChRs

compared to **32** which again may be indicative of a slightly shifted binding mode of the core agonist fragment. Introduction of bromine in the meta-position of the phenyl ring of **31** gave compound **33** which was equipotent to **31** at the α4β2 receptors but more than 4-fold more potent at the α3β4 nAChRs compared to **31** indicating room for improvement of affinity in this specific position.

2.3.4 Functional characterization

Selected compounds of the C-3-arylalkyl analogs of **4** and the *N*-arylalkyl 3-pyridyl diazacycle analogs of **6** (Table 3) were characterized functionally at recombinant heteromeric mouse α4β2 and rat α3β4 nAChRs in the FLIPR Membrane Potential Blue assay. Compounds **8**, **12**, **17**, and **20** were devoid of activity at concentrations up to 300 μM (not shown). The results revealed all remaining compounds to be weak agonists except for **29**, which exhibited weak antagonistic properties (Table 3). The pharmacological activity of compounds **30**-**33** could not be determined in the FLIPR Membrane Potential Blue assay. One of these, **30**, was characterized functionally by two-electrode voltage clamp electrophysiological recordings on α4β2 receptors expressed in *Xenopus laevis* oocytes. On oocytes injected with α4 and β2 mRNA in a 1:4 ratio to favor assembly of $(\alpha4)_2(\beta2)_3$ receptors[15] a partial agonist response corresponding to ca 16% of the maximal response of ACh and an EC_{50} value of 1.8 μM were observed. On oocytes injected with α4 and β2 mRNA in a 10:1 ratio favoring expression of $(\alpha4)_3(\beta2)_2$ receptors the response was 6% of the maximal ACh elicited current and a slightly higher EC_{50} of 7.9 μM. (Table 4 and Figure 5).

The agonistic properties of **13**–**15**, **23**, **24**, **27**, **30**, **35**, and **36** are highly interesting and support the docking studies suggesting that the substituted analogs have a binding mode

in which the core agonist fragment of **4** and **6** at least to some degree is conserved because the compounds are still able to act as agonists.

*2.3.5 Characterization of compounds **30** and **32** at Ac-* and *Ls*-AChBP

Since the target compounds were hypothesized to address cavities based on studies of the *Ac*-AChBP and *Ls*-AChBP, we included the two AChBPs in the profiling of benzyl and phenylpropyl *N*-4 substituted analogs of **6** (**30** and **32**) using surface plasmon resonance (SPR) biosensor analyses (Table 5). The reference compounds (*S*)-nicotine and **2** were included in the study, and the data for these compounds were in agreement with data previously reported [27]. The results revealed **30** and **32** to have ~6- and ~50-fold higher affinity for *Ls*- over *Ac*-AChBP, respectively. Being equipotent at the α4β2 nAChRs, **32** (K_d = 0.020 μM) showed an 8-fold higher affinity at *Ls*-AChBP compared to **30** (K_d = 0.16 μM) but despite this deviation the binding affinities obtained for compounds **30** and **32** to *Ls*-AChBP reflected the binding data at α4β2 nAChRs (Table 5). This correlation corresponds well to previous observations made from analogs of **4**[35] and **6**[36] in which high-affinity compounds at the α4β2 receptors were found to hold good affinity at *Ls*-AChBP. Further, as the hydrophobic cavity associated with binding of **2** in *Ac*-AChBP has been suggested not to be present in *Ls*-AChBP it supports our conclusion of a binding mode of elongated nAChR agonists along the interfacial cleft of α4β2 nAChRs.

2.4 Conclusion

N- and C-3-arylalkyl analogs of **4** and *N*-arylalkyl analogs of **6** were designed and synthesized to explore possible extensions to the nAChR agonist binding pocket. Based on X-ray structures of AChBP with **2** and **3**, two such pockets were potentially accessible but the flat SAR for elongated analogs of the compounds investigated here is

best in agreement with binding in one of these pockets that protrudes along the interfacial cleft as observed in the co-crystal structure of **6** with *Ac*-AChBP. To be compatible with binding in the hydrophobic lobeline pocket, a clear optimum in terms of binding affinities for compounds with intermediate size substituents was expected but not observed. The suggested binding mode is further supported by docking and SPR analysis on AChBPs which show preference for *Ls*-AChBP over *Ac*-AChBP. These findings propose a new opportunity for design of partial agonists with properties like **2**, and the fact that agonistic properties were obtained with using both **4** and **6** as starting point suggests that this type of ligands could be generally accessible from agonist scaffolds.

3. Experimental section

3.1 Computational chemistry

3.1.1 Homology modeling

A homology model of the α4β2 nAChR interface was constructed as described by Harpsøe *et al.*[15] with the following exceptions: The *Ac*-AChBP crystal structure used as template was 2Y58[27] instead of 2BYQ[17]. This change necessitated changes in the alignment to accommodate minor differences in sequence between the two templates. These changes included the removal of H1 and S2 in the beginning of the sequence from the alignment (said residues are not present in 2Y58), and changing A43 and A138 to valine (these residues are mutated to valine in 2Y58).

3.1.2 Ligand docking

Initally, the *N*-4 benzyl substituted **6** was docked to the model using the induced fit docking protocol implemented in Schrodinger's Maestro v9.3. Default settings were

used except ligand scaling was set to 0.8 and amino acid residues within 8Å of the docked ligand were sampled. The highest ranking pose with an agonist-like binding mode, i.e. hydrogen bond from pyridine nitrogen to water molecule and hydrogen atom of the protonated *N*-4 of 1,4-diazepane pointing towards the backbone carbonyl oxygen of Trp143, was selected. In subsequent docking runs the Glide v5.8[44] program was used together with the Glide extra precission (XP) scoring function. The binding modes and docking scores were selected based on ranking according to the Glide E-model score.

3.2. Chemistry

3.2.1. General procedures

All reactions involving air sensitive reagents were performed under a nitrogen atmosphere using syringe-septum cap techniques. When using dry solvents, diethyl ether (Et_2O) was stored over sodium wires, and THF was distilled or obtained from a solvent purification system. Furthermore, dry DCM and DMF were either obtained by drying over molecular sieves (4Å) or from a solvent purification system. All other solvents, stated dry, were purchased from a commercial source and stored over molecular sieves (4Å). ^{1}H NMR and ^{13}C NMR spectra were obtained on a Varian Gemini 2000 (300 MHz), Varian Mercury Plus (300 MHz), or Bruker Avance (400 MHz). Data are tabulated in the following order for ^{1}H NMR: chemical shift (δ) (multiplicity (bs, broad singlet; s, singlet; d, doublet; dd, doublet of doublets; dq, dublet of quartets; ddd, doublet of doublet of doublets; dt, doublet of triplets; ddt, doublet of doublet of triplets; dtd, doublet of triplet of doublets; p, pentet; q, quartet; qd, quartet of doublets; t, triplet; td, triplet of doublets; tt, triplet of triplets; m, multiplet; sxt, sextet; sep, septet), coupling constant(s) *J* (Hz), number of protons). The solvent residual peak was used as internal reference. Carbon-fluorine coupling constants observed in ^{13}C

NMR of fluorine containing compounds are stated. Analytical thin-layer chromatography (TLC) was carried out using Merck silica gel 60 F_{254} plates, and the compounds were visualized with UV light (254 nm) and/or $KMnO_4$ spraying reagent. Flash column chromatography (FCC) was performed using Merck silica gel 60 (0.040–0.063 mm). Dry column vacuum chromatography (DCVC) was performed using Merck silica gel 60 (0.015–0.040 mm). Reverse phase column chromatography was performed using Merck LiChroprep RP-18 (0.040–0.063 mm). Liquid chromatography-mass spectrometry (LC-MS) was performed using an Agilent 1200 series system connected to a Bruker Esquire 3000Plus Iontrap MS system with a gradient of water + 0.2% formic acid (Buffer A) and MeCN + 0.2% formic acid (Buffer B). All microwave reactions were carried out in a glass vial using a Biotage Initiator instrument. Elemental analyses were performed by Johannes Theiner, Department of Physical Chemistry, University of Vienna, Austria, and are within ± 0.4% of the theoretical values, unless otherwise stated. Melting points (mp) were determined by OptiMelt from Stanford Research Systems in open capillary tubes and are uncorrected.

3.2.2. General procedure for oxalate salt formation

The free amine (1.0 eq) was dissolved in a small amount of warm acetone to which a solution of oxalic acid (1.1 eq) in warm acetone was added. The mixture was stored at 5 °C until crystallization. If crystallization did not occur a few drops of Et_2O was added.

*3.2.3. 13-((2-Hydroxy-3-phenylpropyl)(methyl)amino)butyl dimethylcarbamate (**7**)*

To a solution of **43** (200 mg, 1.15 mmol) in MeCN (5 mL), $LiClO_4$ (24 mg, 0.23 mmol) and 2-benzyloxirane (185 mg, 1.38 mmol) were added, and the reaction mixture was stirred at reflux overnight. The reaction mixture was diluted with EtOAc (40 mL) and washed with water (30 mL). The water phase was extracted with EtOAc (2 × 40 mL).

The combined organic phases were dried ($MgSO_4$), filtered, and evaporated in vacuo. Purification of the crude product was obtained by DCVC (Heptane:EtOAc:NH_3/100:0:0 to 0:99:1) yielding the product as a clear oil (218 mg, 61%). ^{1}H NMR ($CDCl_3$, 300 MHz) δ 7.39-7.14 (m, 5H), 4.23-4.07 (m, 2H), 3.98-3.82 (m, 1H), 3.05-2.76 (m, 8H), 2.68 (dd, 1H, *J* = 13.6, 5.6 Hz), 2.56-2.12 (m, 5H), 1.73-1.54 (m, 1H), 1.36-1.24 (m, 1H), 1.03 (s, 3H). **3-((2-Hydroxy-3-phenylpropyl)-(methyl)amino)butyl dimethylcarbamate oxalate.** The free amine of **7** (218 mg, 0.71 mmol) was converted into the oxalate salt as described under the general procedure affording white crystals (39 mg, 14%). Mp: n.d. ^{1}H NMR (D_2O, 300 MHz) δ 7.32-7.09 (m, 5H), 4.20-3.87 (m, 3H), 3.63-3.38 (m, 1H), 3.10-2.91 (m, 2H), 2.82-2.66 (m, 12H), 2.21-1.57 (m, 2H), 1.25 (dd, 3H, *J* = 11.1, 6.7 Hz). ^{13}C NMR (D_2O, 75 MHz) δ 165.64 (2C); 157.93, 157.76 (diastereomers); 136.76, 136.69 (diastereomers); 129.52 (2C), 129.39, 128.82 (2C, diastereomers); 127.05; 67.27, 67.09, 66.35, 66.25 (diastereomers); 62.32, 61.88, 61.79, 61.02, 60.52 (diastereomers); 58.57, 57.79, 56.69 (diastereomers); 56.47, 56.09, 54.94 (diastereomers); 40.90, 40.74 (2C, diastereomers); 38.01, 37.28, 36.87 (diastereomers); 36.70, 36.13, 35.74 (diastereomers); 31.17, 31.06, 29.23, 27.95 (diastereomers); 14.27, 13.99, 12.18, 11.65 (diastereomers).

*3.2.4. 3-[Phenylpropyl(methyl)amino]butyl dimethylcarbamate (**8**)*

To a solution of **43** (200 mg, 1.15 mmol) and 3-phenylpropionaldehyde (0.15 mL, 1.15 mmol) dissolved in 1,2-dichloroethane (10 mL) and MeOH (10 mL) was added AcOH (0.07 mL, 1.15 mmol) and $NaBH_3CN$ (109 mg, 1.75 mmol). The reaction mixture was stirred at room temperature for 72 hours. The reaction mixture was quenched by adding saturated aqueous $NaHCO_3$ solution (20 mL) and was then extracted with EtOAc (3 × 30 mL). The organic phases were combined, dried ($MgSO_4$), filtered, and evaporated in vacuo. The crude product was purified by DCVC (Toluene:DCM/100:0 to 95:5)

yielding a pale yellow oil. The product was purified further by extraction: The product was poured into water (30 mL) and then acidified with aqueous HCl solution (30 mL, 2 M), followed by extraction with EtOAc (30 mL). The water phase was then basified with aqueous NaOH solution (30 mL, 2M) and extracted with EtOAc (2 × 60 mL). The combined organic phases were dried ($MgSO_4$), filtered, and evaporated in vacuo yielding the product as a pale yellow oil (127 mg, 38%). ^{1}H NMR (CDCl3, 300 MHz) δ 7.30-7.08 (m, 5H), 4.12-4.00 (m, 2H), 2.85 (s, 6H), 2.70-2.53 (m, 2H), 2.45-2.15 (m, 2H), 2.18 (s, 3H), 1.98-1.61 (m, 4H), 1.60-1.41 (m, 1H), 0.99, 0.97 (2 s, 3H, rotamers).

3-[Phenylpropyl(methyl)amino]butyl dimethylcarbamate oxalate. The free amine of **8** (104 mg, 0.36 mmol) was converted into the oxalate salt as described under the general procedure affording white crystals (28 mg, 27%). Mp: 107.5-108.3 °C. ^{1}H NMR (D_2O, 400 MHz) δ 7.44-7.34 (m, 2H), 7.33-7.26 (m, 3H), 4.24-4.13 (m, 1H), 4.13-4.00 (m, 1H), 3.62-3.50 (m, 1H), 3.23-2.99 (m, 2H), 2.86, 2.84 (2 s, 6H, rotamers), 2.79-2.67 (m, 5H), 2.15-1.71 (m, 4H), 1.34, 1.28 (2 d, 3H, J = 6.8 Hz). ^{13}C NMR (D_2O, 101 MHz) δ 165.54 (2C); 157.78, 157.74 (rotamers); 140.49, 140.42 (rotamers); 128.84 (2C); 128.47; 128.46; 126.58; 61.83 (2C); 58.14, 57.94 (rotamers); 53.29, 52.36 (rotamers); 35.70, 35.14 (rotamers); 31.74 (2C); 30.72; 28.56, 25.74 (rotamers); 13.79, 11.83 (rotamers).

*3.2.5. 3-[Benzyl(methyl)amino]butyl methylcarbamate (**9**)*

A solution of **40** (626 mg, 3.24 mmol) in dry toluene (9 mL) was added CDI (632 mg, 3.90 mmol), stirred for 3 h at rt, and added dry THF (3.3 mL). After further stirring for 2.5 h, methylamine (0.37 mL, 7.0 mmol, 40% in H_2O) was added. The reaction mixture was stirred for 17 h, diluted with EtOAc (9 mL), and washed with brine (8 mL). The organic phase was dried ($MgSO_4$), filtered, and evaporated *in vacuo*. Purification by DCVC (DCM:MeOH:NH_3/100:0:0 to 300:4.5:0.5) afforded the product as a yellow oil

(572 mg, 71%). ^{1}H NMR ($CDCl_3$, 300 MHz) δ 7.34-7.18 (m, 5H), 4.48 (bs, 1H), 4.18 (t, 2H, *J* = 6 Hz), 3.59 (d, 1H, *J* = 12 Hz), 3.46 (d, 1H, *J* = 12 Hz), 2.89-2.82 (m, 1H), 2.80, 2.78 (2 s, 3H, rotamers), 2.14 (s, 3H), 1.91-1.84 (m, 1H), 1.65-1.56 (m, 1H), 1.02 (d, 3H, *J* = 9 Hz). ^{13}C NMR ($CDCl_3$, 75 MHz) δ 157.8, 140.6, 129.1 (2C), 128.5 (2C), 127.1, 63.4, 58.2, 54.5, 36.5, 33.6, 27.9, 13.4. **3-[Benzyl(methyl)amino]butyl methylcarbamate oxalate.** The free amine of **9** (470 mg, 1.89 mmol) was converted into the oxalate salt as described under the general procedure affording white crystals (383 mg, 49%) after recrystallization from acetone. Mp: 118.0-119.8 °C. ^{1}H NMR (D_2O, 300 MHz) δ 7.43-7.40 (m, 5H), 4.32 (dd, 1H, *J* = 12, 3 Hz), 4.21-4.13 (m, 1H), 4.09-3.98 (m, 2H), 3.52-3.38 (m, 1H), 2.68 (s, 3H), 2.61, 2.57 (2 s, 3H, rotamers), 2.45-2.38, 2.28-2.18, 2.09-1.99, 1.90-1.79 (4 m, 2H), 1.34, 1.32 (2 d, 3H, *J* = 6 Hz). ^{13}C NMR (D_2O, 75 MHz) δ 165.8 (2C); 159.0; 130.9 (2C); 130.4; 129.6 (2C); 61.4; 57.7, 57.5 (rotamers); 57.0, 56.5 (rotamers), 35.8, 35.1 (rotamers); 31.0, 29.1 (rotamers); 26.9; 13.9, 12.0 (rotamers).

*3.2.6. 3-[Phenethyl(methyl)amino]butyl methylcarbamate (**10**)*

Compound **10** was prepared as described for **9** from a mixture of **41** (2.96 g, 14.3 mmol), CDI (2.76 g, 17.0 mmol), and methylamine (1.65 mL, 29 mmol, 40% in H_2O). Purification by DCVC (DCM:MeOH:NH_3/100:0:0 to 100:4.5:0.5) afforded the product as a yellow oil (2.95 g, 80%). ^{1}H NMR ($CDCl_3$, 300 MHz) δ 7.22-7.07 (m, 5H), 4.48 (bs, 1H), 3.99 (t, 2H, *J* = 6 Hz), 2.78-2.43 (m, 5H), 2.71, 2.70 (2 s, 3H, rotamers), 2.18 (s, 3H), 1.72 (dq, 1H, *J* = 12, 6 Hz), 1.45 (dq, 1H, *J* = 12, 6 Hz), 0.88 (d, 3H, *J* = 6 Hz). ^{13}C NMR ($CDCl_3$, 75 MHz) δ 157.7, 141.1, 129.1 (2C), 128.7 (2C), 126.3, 63.4, 55.8, 55.4, 37.0, 35.5, 33.4, 31.4, 13.82. **3-[Phenethyl(methyl)amino]butyl methylcarbamate oxalate.** The free amine of **10** (100 mg, 0.38 mmol) was converted into the oxalate salt as described under the general procedure affording white crystals

(103 mg, 77%). Mp: 141.1-142.3 °C. ^{1}H NMR (D_2O, 300 MHz) δ 7.36-7.25 (m, 5H), 4.13-3.95 (m, 2H), 3.62-3.22 (m, 3H), 3.08-2.89 (m, 2H), 2.79, 2.75 (2 s, 3H, rotamers), 2.62, 2.60 (2 s, 3H, rotamers), 2.10-1.95 (m, 1H), 1.89-1.74 (m, 1H), 1.29, 1.26 (2 d, 3H, *J* = 6 Hz). ^{13}C NMR (D_2O, 75 MHz) δ 165.9 (2C); 159.0; 136.2; 129.4 (2C); 129.0 (2C); 127.8; 61.8, 61.5 (rotamers); 59.1, 58.5 (rotamers); 54.8, 53.4 (rotamers); 36.6, 35.5 (rotamers); 30.7, 30.5 (rotamers); 29.4; 26.9; 13.6, 12.0 (rotamers).

*3.2.7. 3-((2-Hydroxy-2-phenethyl)(methyl)amino)butyl methylcarbamate (**11**)*

Compound **11** was prepared as described for **7** from a mixture of **42** (944 mg, 5.93 mmol), $LiClO_4$ (125 mg, 1.17 mmol), and styrene oxide (850 mg, 7.07 mmol). Purification by HPLC (MeOH:H_2O (pH 10)/40:60) yielded the product as a clear oil (84 mg, 58%). ^{1}H NMR ($CDCl_3$, 300 MHz) δ 7.40-7.22 (m, 5H), 4.79 (bs, 1H), 4.70-4.64 (m, 1H), 4.20-4.11 (m, 2H), 2.96-2.74 (m, 1H), 2.81, 2.79 (2 d, 3H, *J* = 6 Hz), 2.65, 2.54 (2 dd, 1H, *J* = 12, 3 Hz), 2.43, 2.39 (2 dd, 1H, *J* = 12, 3 Hz), 2.34, 2.27 (2 s, 3H, rotamers), 1.93-1.75 (m, 1H), 1.68-1.58 (m, 1H), 1.00 (d, 3H, *J* = 6 Hz). ^{13}C NMR ($CDCl_3$, 75 MHz) δ 157.6; 142.8; 128.7 (2C); 127.8; 126.2 (2C); 69.8, 69.4 (diastereomers); 64.7 (diastereomers); 63.2, 63.0 (diastereomers); 60.9 (diastereomers); 57.4, 55.6 (diastereomers); 37.9 (diastereomers); 34.11; 33.7, 33.5 (diastereomers); 27.8; 14.5, 13.7 (diastereomers). **3-((2-Hydroxy-2-phenethyl)(methyl)amino)butyl methylcarbamate oxalate.** The free amine of **11** (65 mg, 0.23 mmol) was converted into the oxalate salt as described under the general procedure affording white crystals (27 mg, 22%). Mp: 80.5-82.9 °C. ^{1}H NMR (D_2O, 300 MHz) δ 4.98-4.94 (m, 1H), 4.06-3.93 (m, 2H), 3.61-3.41 (m, 1H), 3.35-3.11 (m, 2H), 2.84, 2.79, 2.68 (3 s, 3H, diastereomers), 2.52, 2.50 (2 s, 3H, diastereomers), 2.13-1.95 (m, 1H), 1.84-1.61 (m, 1H), 1.26-1.16 (m, 3H). ^{13}C NMR (D_2O, 75 MHz) δ 166.0 (2C); 159.0; 139.5; 129.1 (2C); 126.3 (2C); 126.2; 68.4, 67.4 (diastereomers); 62.0, 61.8 (diastereomers); 61.3;

58.1; 38.1, 36.4 (diastereomers); 31.0, 29.5 (diastereomers); 28.9, 26.9 (diastereomers); 13.7, 12.4 (diastereomers).

*3.2.8. 3-[Phenylpropyl(methyl)amino]butyl methylcarbamate (**12**)*

Compound 12 was prepared as described for **8** from a mixture of **42** (200 mg, 1.25 mmol), 3-phenylpropionaldehyde (0.16 mL, 1.25 mmol), and $NaBH_3CN$ (109 mg, 1.75 mmol) affording the product as a yellow oil (104 mg, 30%). ^1H NMR (CD_3OD, 300 MHz) δ 7.40 - 7.10 (m, 5H), 4.53 (s, 1H), 4.14 (m, 2H), 2.90-2.70 (m, 4H), 2.69-2.51 (m, 2H), 2.49-2.28 (m, 2H), 2.18 (s, 3H), 1.92-1.66 (m, 3H) 1.64 - 1.43 (m, 1H), 0.90, 0.93 (2 s, 3H, rotamers). **3-[Phenylpropyl-(methyl)amino]butyl methylcarbamate oxalate.** The free amine of **12** (104 mg, 0.37 mmol) was converted into the oxalate salt as described under the general procedure affording white crystals (52 mg, 22%). Mp: 121.5-123.3 °C. ^1H NMR (D_2O, 400 MHz) δ 7.43-7.34 (m, 2H), 7.33-7.24 (m, 3H), 4.25-4.14 (m, 1H), 4.12- 3.99 (m, 1H), 3.61-3.48 (m, 1H), 3.22-2.97 (m, 2H), 2.80-2.62 (m, 8H), 2.15-1.95 (m, 3H), 1.93-1.70 (m, 1H), 1.33, 1.27 (2 d, 3H, J = 6.5 Hz). ^{13}C NMR (D_2O, 101 MHz) δ 165.53 (2C); 140.50, 140.45 (rotamers); 128.84 (2C); 128.49; 128.47; 126.58; 118.92; 61.31; 58.12; 53.31; 35.11; 31.74; 30.61; 28.81, 26.64 (rotamers); 25.74, 25.72 (rotamers); 13.60, 11.81 (rotamers).

*3.2.9. 3-(Dimethylamino)-6-phenylhexyl dimethylcarbamate (**13**)*

A solution of **53** (1.52 g, 6.87 mmol) in dry toluene (25 mL) was added CDI (1.34 g, 8.24 mmol). The reaction mixture was stirred for 2 h at rt. The reaction mixture was added THF (20 mL) and stirred for additional one hour. Dimethylamine (8.70 mL, 68.7 mmol, 40% in water) was added the reaction mixture, and stirring continued overnight at rt. The reaction mixture was diluted with EtOAc (25 mL). The water phase was washed with brine (25 mL) and aqueous NaOH solution (1M, 2 × 25 mL). The

combined organic phases were dried ($MgSO_4$), filtered, and evaporated yielding the product as a yellow oil (1.54 g, 77%). ^{1}H NMR ($CDCl_3$, 400 MHz) δ 7.29-7.27 (m, 1H), 7.25 (d, 1H, *J* = 1.8 Hz), 7.18-7.16 (m, 3H), 4.10 (d, 2H, *J* = 13.7 Hz), 2.89 (s, 6H), 2.61 (t, 2H, *J* = 7.6 Hz), 2.52 (t, 1H, *J* = 5.8 Hz), 2.23 (s, 6H), 1.82 (dq, 1H, *J* = 13.6, 6.8 Hz), 1.70-1.64 (m, 2H), 1.57 (t, 2H, *J* = 6.9 Hz), 1.35-1.26 (m, 1H). ^{13}C NMR ($CDCl_3$, 101 MHz) δ 156.86, 142.54, 128.52 (2C), 128.41 (2C), 125.84, 63.91, 61.00, 40.41 (4C), 36.20, 29.48, 29.10, 28.95. **3-(Dimethylamino)-6-phenylhexyl dimethylcarbamate oxalate.** The free amine of **13** (380 mg, 1.30 mmol) was converted into the oxalate salt as described under the general procedure affording white crystals (291 mg, 59%). Mp: 97.9 °C. ^{1}H NMR (D_2O, 400 MHz) δ 7.34-7.29 (m, 2H), 7.24-7.20 (m, 3H), 4.11 (ddd, 1H, *J* = 11.5, 6.6, 4.9 Hz), 4.02 (ddd, 1H, *J* = 11.7, 7.4, 4.5 Hz), 3.28-3.22 (m, 1H), 2.84 (s, 6H), 2.79, 2.77 (2 s, 6H, rotamers), 2.69-2.61 (m, 2H), 2.06 (ddt, 1H, *J* = 15.1, 7.6, 4.9 Hz), 1.93-1.85 (m, 1H), 1.73-1.61 (m, 4H). ^{13}C NMR (D_2O, 101 MHz) δ 165.63 (2C), 157.67, 141.74, 128.69 (2C), 128.55 (2C), 126.23, 63.55 (2C), 62.28, 39.54, 38.77, 34.36 (2C), 27.72, 27.66, 26.70.

*3.2.10. 3-(Dimethylamino)-7-phenylheptyl dimethylcarbamate (**14**)*

Compound **14** was prepared as described for **13** from a mixture of **54** (800 g, 3.40 mmol), CDI (660 g, 4.08 mmol), and dimethylamine (4.3 mL, 34 mmol, 33% in EtOH) yielding the product as a yellow oil (860 mg, 64%). ^{1}H NMR ($CDCl_3$, 400 MHz) δ 7.29-7.27 (m, 2H), 7.17 (dt, 3H, *J* = 1.4, 0.7 Hz), 4.12 (t, 2H, *J* = 6.9 Hz), 2.90 (s, 6H), 2.61 (t, 2H, *J* = 7.8 Hz), 2.49-2.47 (m, 1H), 2.24 (s, 6H), 1.64-1.61 (m, 2H), 1.59-1.52 (m, 2H), 1.42-1.26 (m, 4H). **3-(Dimethylamino)-7-phenylheptyl dimethylcarbamate oxalate.** The free amine of **14** (367 mg, 1.20 mmol) was converted into the oxalate salt as described under the general procedure affording white crystals (346 mg, 94%). Mp: 90.4 °C. ^{1}H NMR (D_2O, 400 MHz) δ 7.42-7.37 (m, 2H), 7.33-7.27 (m, 3H), 4.22 (ddd,

1H, *J* = 11.5, 6.5, 5.1 Hz), 4.13 (ddd, 1H, *J* = 11.7, 7.4, 4.5 Hz), 3.33 (tt, 1H, *J* = 7.6, 5.1 Hz), 2.90 (s, 6H), 2.80, 2.79 (2 s, 6H, rotamers), 2.70 (t, 2H, *J* = 7.4 Hz), 2.15 (ddt, 1H, *J* = 15.0, 7.6, 5.0 Hz), 2.02-1.93 (m, 1H), 1.82-1.68 (m, 4H), 1.43 (dt, 2H, *J* = 15.3, 7.6 Hz). ^{13}C NMR (D_2O, 101 MHz) δ 165.65 (2C), 157.68, 142.65, 128.60 (2C), 128.54 (2C), 125.98, 63.57, 62.20, 39.42 (2C), 38.94 (2C), 34.51, 30.05, 28.18, 27.77, 24.58.

*3.2.11. 3-(Dimethylamino)-8-phenyloctyl dimethylcarbamate (**15**)*

Compound **15** was prepared as described for **13** from a mixture of **55** (488 mg, 1.96 mmol), CDI (381 mg, 2.35 mmol), and dimethylamine (1.75 mL, 9.78 mmol, 33% in EtOH) giving the product as a yellow oil (332 mg, 53%). ^{1}H NMR (CD_3OD, 400 MHz) δ 7.27-7.19 (m, 2H), 7.18-7.10 (m, 3H), 4.10 (td, 2H, *J* = 6.7, 1.9 Hz), 2.89 (s, 6H), 2.61 (t, 2H, *J* = 7.8 Hz), 2.48 (p, 1H, *J* = 6.3 Hz), 2.22 (s, 6H), 1.84 (dq, 1H, *J* = 14.1, 6.3 Hz), 1.67-1.51 (m, 4H), 1.42-1.22 (m, 6H). ^{13}C NMR (CD_3OD, 101 MHz) δ 144.04, 130.08, 129.56 (2C), 129.41 (2C), 126.80, 65.23, 62.32, 40.85 (2C), 37.00, 36.32 (2C) 32.78, 30.74, 30.53, 30.45, 28.13. **3-(Dimethylamino)-8-phenyl-octyl dimethylcarbamate oxalate.** The free amine of **15** (128 mg, 0.40 mmol) was converted into the oxalate salt according to the general procedure affording a white solid (64 mg, 39%). Mp: 84.7-86.0 °C. ^{1}H NMR (D_2O, 400 MHz) δ 7.38-7.32 (m, 2H), 7.30-7.21 (m, 3H), 4.23-4.07 (m, 2H), 3.27 (d, 1H, *J* = 6.8 Hz), 2.87, 2.87 (2 s, 6H, rotamers), 2.80 (dd, 6H, *J* = 6.3, 1.5 Hz), 2.66-2.59 (m, 2H), 2.17-2.06 (m, 1H), 2.01-1.88 (m, 1H), 1.76-1.57 (m, 4H), 1.44-1.28 (m, 4H). ^{13}C NMR (D_2O, 101 MHz) δ 165.64 (2C), 152.37, 143.16, 128.59 (2C), 128.58 (2C), 125.88. 63.53, 62.31, 39.49, 38.87, 35.94, 35.56, 34.84, 34.82, 30.20, 28.28, 27.74, 24.87.

*3.2.12. 3-(Dimethylamino)-6-hydroxy-6-phenylhexyl dimethylcarbamate (**16**)*

To a solution of **61** (0.92 g, 2.34 mmol) in MeOH (50 mL) was added *p*-toluenesulfonic acid monohydrate (0.89 g, 4.68 mmol). The reaction mixture was stirred for 2 h at rt. The reaction mixture was added saturated aqueous $NaHCO_3$ solution (50 mL) and then reduced in vacuo. The remaining mixture was extracted with DCM (3 × 50 mL) and the combined organic phases were dried, filtered, and evaporated in vacuo. The crude product was purified by DCVC (DCM:MeOH:NH_3/90:9:1) yielding the product as a yellow oil (90 mg, 13%). ^{1}H NMR ($CDCl_3$, 400 MHz) δ 7.38-7.19 (m, 5H), 4.81 (dd, 1H, *J* = 6.0, 3.6 Hz), 4.16-4.10 (m, 1H), 4.05-3.99 (m, 1H), 2.89 (s, 6H), 2.56 (tt, 1H, *J* = 9.7, 3.3 Hz), 2.33, 2.25 (2 s, 6H, rotamers), 2.17-2.09 (m, 1H), 1.97-1.87 (m, 2H), 1.60-1.52 (m, 1H), 1.45-1.30 (m, 2H). ^{13}C NMR ($CDCl_3$, 101 MHz) δ 156.66, 145.80, 128.21 (2C), 126.59, 125.74 (2C), 72.17, 63.56, 61.51, 40.08 (4C), 37.21, 27.29, 26.73.

3-(Dimethylamino)-6-hydroxy-6-phenylhexyl dimethylcarbamate oxalate. The free amine of **16** (90 mg, 0.29 mmol) was converted into the oxalate salt as described under the general procedure affording white crystals (67 mg, 58%). Mp: 119.3 °C. ^{1}H NMR (D_2O, 400 MHz) δ 7.51-7.40 (m, 5H), 4.81 (d, 1H, *J* = 6.3 Hz), 4.20 (ddd, 1H, *J* = 11.5, 6.8, 4.9 Hz), 4.12 (ddd, 1H, *J* = 11.7, 7.3, 4.6 Hz), 3.35 (td, 1H, *J* = 6.2, 2.1 Hz), 2.89 (s, 6H), 2.85, 2.80 (2 s, 6H, rotamers), 2.21-2.13 (m, 1H), 2.04-1.68 (m, 5H). ^{13}C NMR (D_2O, 101 MHz) δ 165.69 (2C), 157.66, 142.95, 128.82 (2C), 128.08, 126.02 (2C), 73.01, 63.41, 62.23, 39.47 (2C), 38.87 (2C), 33.63, 27.71, 24.73.

*3.2.13. 3-(Dimethylamino)-4-phenoxybutyl dimethylcarbamate (**17**)*

56[31] (200 mg, 0.98 mmol), CuI (6 mg, 0.03 mmol), 3,4,7,8-tetramethyl-1,10-phenanthroline (15 mg, 0.07 mmol), iodobenzene (73 µL, 0.65 mmol), and Cs_2CO_3 (319 mg, 0.98 mmol) were mixed and added dry toluene (0.50 mL) under nitrogen. The reaction mixture was heated to 110 °C overnight, diluted with EtOAc (15 mL), and filtered through a plug of silica washing additional times with EtOAc. The filtrate was

concentrated *in vacuo* yielding the product as a brown oil (136 mg, 60%). ^{1}H NMR ($CDCl_3$, 300 MHz) δ 7.38-7.28 (m, 2H), 7.05-6.88 (m, 3H), 4.22 (td, 2H, *J* = 6.6, 1.9 Hz), 4.17-4.05 (m, 1H), 4.02-3.96 (m, 1H), 3.05-3.01 (m, 1H), 2.92, 2.89 (2 s, 6H, rotamers), 2.43 (s, 6H), 1.99-1.87 (m, 3H), 1.73-1.56 (m, 3H). **3-(Dimethylamino)-4-phenoxybutyl dimethylcarbamate oxalate.** The free amine of **17** (185 mg, 0.66 mmol) was converted into the oxalate salt as described under the general procedure affording white crystals (66 mg, 27%). Mp: 91.3-92.5 °C. ^{1}H NMR (D_2O, 300 MHz) δ 7.40-7.35 (m, 2H), 7.09-7.00 (m, 3H), 4.46 (dd, 1H, *J* = 11.9, 3.1 Hz), 4.31 (dd, 1H, *J* = 11.9, 6.6 Hz), 4.23 (dd, 2H, *J* = 9.8, 5.7 Hz), 3.84-3.81 (m, 1H), 2.93, 2.88 (2 s, 6H, rotamers), 2.77 (s, 6H), 2.27 (m, 2H). ^{13}C NMR (D_2O, 75 MHz) δ 241.85 (2C), 215.94, 186.69, 144.11 (2C), 136.32, 128.79 (2C), 78.13, 77.16, 76.48, 55.46, 53.41, 50.18, 49.74, 38.60.

3.2.14. 3-(Dimethylamino)-4-(4-fluorophenoxy)butyl dimethylcarbamate (18)

Compound **18** was prepared as described for **17** from a mixture of **56** (200 mg, 0.98 mmol), CuI (6 mg, 0.03 mmol), 3,4,7,8-tetramethyl-1,10-phenanthroline (16 mg, 0.07 mmol), 1-fluoro-4-iodobenzene (76 µL, 0.66 mmol), and Cs_2CO_3 (320 mg, 0.98 mmol). Purification by reverse phase column chromatography (C18 silica) (H_2O:AcOH:MeCN/99.9:0.1:0 to 94.9:0.1:5) followed by basic extraction of the product into EtOAc afforded the product as a yellow oil (46 mg, 23%). ^{1}H NMR (CD_3OD, 300 MHz) δ 7.04-6.90 (m, 3H), 4.19 (t, 2H, *J* = 6.5 Hz), 4.07 (qd, 2H, *J* = 10.3, 5.0 Hz), 3.01-2.97 (m, 1H), 2.88 (s, 5H), 2.37 (s, 6H), 2.01-1.91 (m, 2H). ^{13}C NMR (CD_3OD, 75 MHz) δ 160.06, 158.11 (C-F: ^{1}J = 147 Hz); 156.92; 156.06, 156.03 (C-F: ^{4}J = 2.1 Hz); 116.72, 116.59 (C-F: ^{2}J = 8.5 Hz, 2C); 116.49, 116.41 (C-F: ^{3}J = 5.8 Hz, 2C); 68.59; 64.57; 61.29; 41.61 (2C); 36.57; 36.13; 28.22. **3-(Dimethylamino)-4-(4-fluorophenoxy)butyl dimethylcarbamate oxalate.** The free amine of **18** (46 mg,

0.15 mmol) was converted into the oxalate salt as described under the general procedure affording white crystals (43 mg, 72%). Mp: 97.6-98.3 °C. ^{1}H NMR (D_2O, 300 MHz) δ 7.07-7.00 (m, 2H), 6.97-6.90 (m, 2H), 4.39 (dd, 1H, *J* = 11.8, 3.1 Hz), 4.27-4.12 (m, 4H), 3.78 (qd, 1H, *J* = 6.7, 3.0 Hz), 2.87, 2.82 (2 s, 6H, rotamers), 2.68, 2.66 (2 s, 5H, rotamers), 2.18-2.26 (m, 2H). ^{13}C NMR (D_2O, 75 MHz) δ 165.59; 159.18, 156.04 (C-F: ^{1}J = 245 Hz); 157.52; 153.29, 153.26 (C-F: ^{3}J = 2.3 Hz, 2C); 116.19, 115.80 (C-F: ^{2}J = 21 Hz); 115.88, 115.69 (C-F: ^{2}J = 21 Hz); 64.48; 62.97; 62.24; 41.42; 39.16; 35.96; 35.52; 24.36.

*3.2.15. 3-(Dimethylamino)-4-(pyridin-2-yloxy)butyl dimethylcarbamate (**19**)*

To a suspension of NaH (65 mg, 1.62 mmol, 60% in mineral oil) in dry DMF (6 mL) was dropwisely added **56** (300 mg, 1.47 mmol) at 0 °C. After 1 h of stirring at 0 °C, 2-fluoropyridine (0.25 mL, 2.94 mmol) was added. The reaction mixture was stirred overnight at rt, added water (60 mL), and extracted with Et_2O (2 × 60 mL). The combined organic phases were dried ($MgSO_4$), filtered, and evaporated *in vacuo*. Purification by reverse phase column chromatography (C18 silica) (H_2O:TFA:MeCN/99.9:0.1:0 to 89.9:0.1:10) followed by basic extraction of the product into EtOAc afforded the product as a yellow oil (224 mg, 54%). ^{1}H NMR (CD_3OD, 300 MHz) δ 8.15 (dd, 1H, *J* = 5.1, 1.3 Hz), 7.75 (ddd, 1H, *J* = 8.4, 7.1, 1.9 Hz), 7.04 (ddd, 1H, *J* = 7.1, 5.2, 1.0 Hz), 6.93 (d, 1H, *J* = 8.4 Hz), 4.80 (dd, 1H, *J* = 13.1, 3.0 Hz), 4.63 (dd, 1H, *J* = 13.1, 6.6 Hz), 4.54-4.50 (m, 1H), 4.31-4.24 (m, 2H), 3.86 (qd, 1H, *J* = 6.5, 3.3 Hz), 3.02 (s, 6H), 2.86 (s, 6H), 2.34-2.16 (m, 2H). ^{13}C NMR (CD_3OD, 75 MHz) δ 163.25, 157.57, 147.31, 140.95, 119.18, 112.10, 63.82, 63.12, 62.83, 41.19 (2C), 36.68, 36.15, 26.30. **3-(Dimethylamino)-4-(pyridin-2-yloxy)butyl dimethylcarbamate oxalate.** The free amine of **19** (224 mg, 0.80 mmol) was converted into the oxalate salt as described under the general procedure affording white crystals (141 mg, 47%). Mp:

77.1 °C. ^{1}H NMR (D_2O, 300 MHz) δ 8.08 (dd, 1H, *J* = 5.2, 1.7 Hz), 7.77 (ddd, 1H, *J* = 8.6, 7.1, 1.9 Hz), 7.11-7.07 (m, 1H), 6.94 (dd, 1H, *J* = 8.4, 0.6 Hz), 4.66 (dd, 1H, *J* = 12.6, 2.7 Hz), 4.50 (dd, 1H, *J* = 12.6, 6.1 Hz), 4.26-4.15 (m, 2H), 3.87-3.81 (m, 1H), 2.90 (s, 6H), 2.68, 2.65 (2 s, 5H, rotamers), 2.29-2.17 (m, 2H). ^{13}C NMR (D_2O, 75 MHz) δ 166.09, 161.69 (2C), 157.48, 145.72, 141.37, 118.72, 111.00, 62.85, 62.71, 62.33, 36.02 (2C), 35.51 (2C), 24.62.

*3.2.16. 4-(Benzyloxy)-3-(dimethylamino)butyl dimethylcarbamate (**20**)*

Compound **20** was prepared as described for **19** from a mixture of NaH (44 mg, 1.08 mmol, 60% in mineral oil), **56** (200 mg, 0.98 mmol), and benzyl bromide (0.23 mL, 1.96 mmol) yielding the product as a yellow oil (94 mg, 33%). ^{1}H NMR ($CDCl_3$, 300 MHz) δ 7.38-7.27 (m, 5H), 4.53 (s, 2H), 4.14 (t, 2H, *J* = 6.7 Hz), 3.62-3.47 (m, 2H), 2.92, 2.89 (2 s, 7H, rotamers), 2.37 (s, 6H), 1.92-1.70 (m, 2H). **4-(Benzyloxy)-3-(dimethylamino)butyl dimethylcarbamate oxalate.** The free amine of **20** (94 mg, 0.32 mmol) was converted into the oxalate salt as described under the general procedure affording white crystals (114 mg, 93%). Mp: 79.0-79.7 °C. ^{1}H NMR (D_2O, 300 MHz) δ 7.40-7.34 (m, 5H), 4.58 (d, 2H, *J* = 0.7 Hz), 4.11-3.95 (m, 2H), 3.77 (dd, 1H, *J* = 12.0, 3.7 Hz), 3.65 (dd, 1H, *J* = 12.0, 8.0 Hz), 3.53-3.41 (m, 1H), 2.83-2.73 (m, 12H), 2.18-2.06 (m, 1H), 1.92-1.85 (m, 1H). ^{13}C NMR (D_2O, 75 MHz) δ 165.64, 157.52 (2C), 136.70, 128.85 (2C), 128.69 (2C), 128.62, 73.14, 65.32, 63.14, 62.20, 41.22, 38.02, 36.08, 35.65, 24.02.

*3.2.17. 3-(Dimethylamino)-4-(thiazol-2-yloxy)butyl dimethylcarbamate (**21**)*

Compound **21** was prepared as described for **19** from a mixture of NaH (65 mg, 1.62 mmol, 60% in mineral oil), **56** (300 mg, 1.47 mmol), and 2-bromothiazole (0.26 mL, 2.94 mmol). Purification by reverse phase column chromatography (C18 silica)

(H_2O:AcOH:MeCN/99.9:0.1:0 to 94.9:0.1:5) followed by basic extraction of the product into EtOAc afforded the product as a yellow oil (61 mg, 14%). ^{1}H NMR (CD_3OD, 300 MHz) δ 7.17 (d, 1H, *J* = 3.8 Hz), 6.98 (d, 1H, *J* = 3.8 Hz), 4.88 (dd, 1H, *J* = 12.9, 2.9 Hz), 4.77 (dd, 1H, *J* = 13.0, 6.5 Hz), 4.31-4.25 (m, 2H), 3.97-3.86 (m, 1H), 3.00-2.84 (m, 6H), 2.30-2.19 (m, 2H). ^{13}C NMR (CD_3OD, 75 MHz) δ 174.79, 157.80, 137.69, 114.11, 68.36, 63.84, 62.93, 41.40 (2C), 36.87, 36.35, 26.36. **3-(Dimethylamino)-4-(thiazol-2-yloxy)butyl dimethylcarbamate oxalate.** The free amine of **21** (61 mg, 0.21 mmol) was converted into the oxalate salt as described under the general procedure affording white crystals (53 mg, 66%). Mp: 122.4-122.7 °C. ^{1}H NMR (D_2O, 300 MHz) δ 7.15 (dd, 1H, *J* = 3.9, 0.8 Hz), 6.97 (dd, 1H, *J* = 3.9, 0.9 Hz), 4.81-4.76 (m, 1H), 4.67 (dd, 1H, *J* = 12.6, 6.1 Hz), 4.20 (nonet, 2H, *J* = 5.8 Hz), 3.94-3.84 (m, 1H), 2.94 (s, 6H), 2.78 (s, 6H), 2.30-2.20 (m, 2H). ^{13}C NMR (D_2O, 75 MHz) δ 174.15 (2C), 165.72, 157.52, 136.11, 113.44, 67.29, 62.70, 62.25, 41.08, 39.81, 36.05, 35.57, 24.51.

3.2.18 3-(Dimethylamino)-5-phenylpentyl methylcarbamate (22).

Compound **22** was prepared as described for **13** from a mixture of **52** (500 mg, 2.41 mmol), CDI (469 mg, 2.89 mmol), and methylamine (1.1 mL, 12.06 mmol, 40% in H_2O) affording the product as a yellow oil (360 mg, 57%). ^{1}H NMR (CD_3OD, 400 MHz) δ 7.28-7.23 (m, 2H), 7.21-7.12 (m, 3H), 4.14-4.04 (m, 2H), 2.69 (s, 3H), 2.66-2.60 (m, 2H), 2.52 (t, 1H, *J* = 6.3 Hz), 2.22 (s, 6H), 1.92-1.79 (m, 2H), 1.70-1.52 (m, 2H). ^{13}C NMR (CD_3OD, 101 MHz) δ 143.70, 129.58 (2C), 129.52 (2C), 126.96, 64.19, 61.48, 40.74 (2C), 34.35, 30.27, 32.93, 27.55. **3-(Dimethylamino)-5-phenylpentyl methylcarbamate oxalate.** The free amine of **22** (200 mg, 0.76 mmol) was converted into the oxalate salt according to the general procedure affording a white solid (182 mg, 68%). Mp: 136.0-136.7 °C. ^{1}H NMR (D_2O, 400 MHz) δ 7.34-7.27 (m, 2H), 7.25-7.18

(m, 3H), 4.16-4.06 (m, 1H), 4.02-3.92 (m, 1H), 3.22-3.11 (m, 1H), 2.70 (d, 6H, *J* = 11.3 Hz), 2.59 (s, 3H), 2.10-1.94 (m, 2H), 1.93-1.83 (m, 1H). ^{13}C NMR (D_2O, 101 MHz) δ. 165.48 (2C), 158.61, 140.04, 128.79 (2C), 128.45 (2C), 126.54, 62.40, 61.14, 39.49, 38.70, 31.10, 27.83, 29.35, 26.53.

*3.2.19. 3-(Dimethylamino)-6-phenylhexyl methylcarbamate (**23**)*

Compound **23** was prepared as described for **13** from a mixture of **53** (1.48 g, 6.67 mmol), CDI (1.30 g, 8.00 mmol), and methylamine (5.80 mL, 68.7 mmol, 40% in H_2O) affording the product as a yellow oil (1.49 g, 80%). ^{1}H NMR ($CDCl_3$, 400 MHz) δ 7.29-7.27 (m, 1H), 7.25 (d, 1H, *J* = 1.8 Hz), 7.19-7.16 (m, 3H), 4.60 (s, 1H), 4.10 (t, 2H, *J* = 6.8 Hz), 2.79, 2.78 (2 s, 3H, rotamers), 2.61 (t, 2H, *J* = 7.6 Hz), 2.51 (t, 1H, *J* = 6.0 Hz), 2.23 (s, 6H), 1.78 (dq, 1H, *J* = 13.3, 6.6 Hz), 1.69-1.64 (m, 2H), 1.61-1.53 (m, 2H), 1.32-1.27 (m, 1H). ^{13}C NMR ($CDCl_3$, 101 MHz) δ 157.39, 142.52, 128.54 (2C), 128.42 (2C), 125.84, 63.44, 61.02, 40.44 (3C), 36.17, 29.15, 28.90, 27.64. **3-(Dimethylamino)-6-phenylhexyl methylcarbamate oxalate.** The free amine of **23** (362 mg, 1.30 mmol) was converted into the oxalate salt as described under the general procedure affording white crystals (291 mg, 61%). Mp: 91.8 °C. ^{1}H NMR (D_2O, 400 MHz) δ 7.34-7.30 (m, 2H), 7.25-7.20 (m, 3H), 4.14-4.07 (m, 1H), 4.04-3.98 (m, 1H), 3.26-3.23 (m, 1H), 2.78, 2.76 (2 s, 6H, rotamers), 2.65 (t, 2H, *J* = 3.1 Hz), 2.63 (s, 3H), 2.06-1.98 (m, 1H), 1.92-1.84 (m, 1H), 1.68-1.58 (m, 4H). ^{13}C NMR (D_2O, 101 MHz) δ 165.68 (2C), 158.70, 141.78, 128.69 (2C), 128.57 (2C), 126.22, 63.57, 61.66, 39.34, 39.07, 34.37, 30.23, 27.68, 27.57, 26.71.

*3.2.20. 3-(Dimethylamino)-7-phenylheptyl methylcarbamate (**24**)*

Compound **24** was prepared as described for **13** from a mixture of **54** (970 mg, 4.12 mmol), CDI (800 mg, 4.95 mmol), and methylamine (4.0 mL, 41.2 mmol, 40% in H_2O)

yielding the product as a yellow oil (890 mg, 73%). ^{1}H NMR ($CDCl_3$, 400 MHz) δ 7.29-7.28 (m, 2H), 7.19-7.17 (m, 3H), 4.60 (s, 1H), 4.13-4.09 (m, 2H), 2.83-2.77 (m, 3H), 2.61 (t, 2H, *J* = 7.8 Hz), 2.48-2.43 (m, 1H), 2.24 (s, 6H), 1.64-1.60 (m, 2H), 1.56-1.49 (m, 2H), 1.40-1.33 (m, 2H), 1.30-1.23 (m, 2H). ^{13}C NMR ($CDCl_3$, 101 MHz) δ 157.33, 142.64, 128.51 (2C), 128.43 (2C), 125.83, 63.17, 61.46, 40.42 (2C), 35.99, 31.73, 29.17, 27.64, 26.74, 25.67. **3-(Dimethylamino)-7-phenylheptyl methylcarbamate oxalate.** The free amine of **24** (409 mg, 1.40 mmol) was converted into the oxalate salt as described under the general procedure affording white crystals (224 mg, 55%). Mp: 87.1 °C. ^{1}H NMR (D_2O, 400 MHz) δ 7.42-7.38 (m, 2H), 7.33-7.27 (m, 3H), 4.22 (dt, 1H, *J* = 11.4, 5.7 Hz), 4.12 (ddd, 1H, *J* = 11.4, 7.4, 4.5 Hz), 3.32 (p, 1H, *J* = 5.4 Hz), 2.83 (s, 6H), 2.72-2.68 (m, 6H), 2.14-2.07 (m, 1H), 2.00-1.93 (m, 1H), 1.82-1.66 (m, 4H), 1.42 (dt, 2H, *J* = 15.0, 7.5 Hz). ^{13}C NMR (D_2O, 101 MHz) δ 165.51 (2C), 158.71, 142.69, 128.61 (2C), 128.56 (2C), 125.97, 63.65, 61.64, 39.33, 39.10, 34.51, 30.09, 28.06, 27.75, 26.63, 24.54.

*3.2.21. 3-(Dimethylamino)-8-phenyloctyl methylcarbamate (**25**)*

Compound **25** was prepared as described for **13** from a mixture of **55** (470 g, 1.89 mmol), CDI (370 g, 2.26 mmol), and methylamine (0.80 mL, 9.42 mmol, 40% in H_2O) furnishing the product as a yellow oil (425 mg, 73%). ^{1}H NMR (CD_3OD, 400 MHz) δ 7.27-7.20 (m, 2H), 7.18-7.10 (m, 3H), 4.11-4.03 (m, 2H), 2.68 (s, 3H), 2.61 (t, 2H, *J* = 7.5 Hz), 2.21 (s, 6H), 1.80 (sxt, 1H, *J* = 6.5 Hz), 1.68-1.49 (m, 4H), 1.26 (bs, 6H). ^{13}C NMR (CD_3OD, 101 MHz) δ 129.56 (2C), 129.41 (2C), 129.37, 126.79, 64.27, 62.22, 40.84 (2C), 37.00, 32.79, 30.79, 30.57, 30.53, 28.13, 27.54. **3-(Dimethylamino)-8-phenyloctyl methylcarbamate oxalate.** The free amine of **25** (212 mg, 0.69 mmol) was converted into the oxalate salt according to the general procedure yielding a white solid (213 mg, 78%). Mp: 98.2-98.7 °C. ^{1}H NMR (D_2O, 400 MHz) δ 7.34-7.27 (m, 2H),

7.25-7.17 (m, 3H), 4.19-3.99 (m, 2H), 3.20 (bs, 1H), 2.73 (s, 6H), 2.64 (s, 3H), 2.57 (t, 2H, *J* = 7.4 Hz), 2.09-1.95 (m, 1H), 1.92-1.81 (m, 1H), 1.70-1.60 (m, 1H), 1.60-1.54 (m, 3H), 1.39-1.24 (m, 4H). ^{13}C NMR (D_2O, 101 MHz) δ 165.64 (2C), 158.71, 143.17, 128.59 (2C), 128.58 (2C), 125.88, 63.61, 61.71, 39.36, 39.07, 34.85, 30.24, 28.16, 27.80, 27.75, 26.66, 24.89.

*3.2.22. 3-(Dimethylamino)-6-hydroxy-6-phenylhexyl methylcarbamate (**26**)*

Compound **26** was prepared as described for **16** from a mixture of **60** (1.08 g, 2.85 mmol) and *p*-toluenesulfonic acid monohydrate (1.08 g, 5.70 mmol yielding the product as a yellow oil (0.50 g, 60%). ^{1}H NMR ($CDCl_3$, 400 MHz) δ 7.39-7.19 (m, 10H, diastereomers); 4.80 (dd, 1H, *J* = 6.1, 3.6 Hz), 4.66-4.58 (m, 1H) (diastereomers); 4.15-4.10, 4.05-4.00 (2m, 2H, diastereomers); 2.80, 2.79 (2 s, 6H, diastereomers); 2.57-2.52 (m, 2H, diastereomers); 2.30, 2.23 (2 s, 6H, diastereomers); 2.15-1.85 (m, 6H, diastereomers); 1.73-1.63 (m, 2H, diastereomers); 1.59-1.51 (m, 1H, diastereomers); 1.45-1.29 (m, 3H, diastereomers). ^{13}C NMR ($CDCl_3$, 101 MHz) δ 145.92, 145.64 (diastereomers); 128.08, 128.06 (2C, diastereomers); 126.69, 126.45 (diastereomers); 125.65, 125.57 (2C, diastereomers); 74.64, 72.06 (diastereomers); 62.90; 61.98, 61.16 (diastereomers); 40.10, 36.96 (diastereomers); 39.93, 39.50 (diastereomers); 30.26, 27.04 (diastereomers); 27.49; 26.58, 26.41 (diastereomers). **3-(Dimethylamino)-6-hydroxy-6-phenylhexyl methylcarbamate oxalate.** The free amine of **26** (100 mg, 0.34 mmol) was converted into the oxalate salt as described under the general procedure affording white crystals (86 mg, 66%). Mp: 90.3 °C. ^{1}H NMR (D_2O, 400 MHz) δ 7.50-7.34 (m, 5H), 4.22-4.11 (m, 1H), 4.10-4.00 (m, 1H), 3.36-3.25 (m, 1H), 2.78, 2.75 (2 s, 6H, rotamers), 2.68 (s, 3H), 2.18-2.01 (m, 1H), 2.01-1.80 (m, 4H), 1.79-1.47 (m, 2H). ^{13}C NMR (D_2O, 101 MHz) δ 158.71, 158.68 (diastereomers); 142.96, 142.88 (diastereomers); 128.83 (2C); 128.11, 128.08 (diastereomers); 126.12, 126.07 (2C,

diastereomers); 73.29, 73.05 (diastereomers); 63.69, 63.45 (diastereomers); 61.63, 61.62 (diastereomers); 39.35, 39.20 (diastereomers); 33.83, 33.61 (2C, diastereomers); 27.73, 27.64 (diastereomers); 26.75, 26.62 (diastereomers); 24.74, 24.56 (diastereomers).

*3.2.23. N,N-Dimethyl-1-((1-methyl-1H-imidazol-2-yl)oxy)-7-phenylheptan-3-amine (**27**)*

To a stirred suspension of NaH (68 mg, 1.71 mmol, 60% in mineral oil) in dry THF (5 mL) at 0 °C was added a dry THF (6 mL) solution of **54** (268 mg, 1.14 mmol). After 30 min of stirring at 0 °C, 2,4,5-tribromo-1-methyl-1*H*-imidazole[45] (399 mg, 1.10 mmol) was added. The reaction mixture was refluxed overnight, then cooled, and poured into ice water (~10 mL). The resulting mixture was extracted with EtOAc (2 × 10 mL). The combined organic phases were extracted with aq HCl solution (1M, 2 × 6 mL). The combined water phases were basified to pH 14 with a concentrated aq NaOH solution and extracted with EtOAc (3 × 10 mL). The combined organic phases were dried ($MgSO_4$), filtered, and evaporated *in vacuo*. Purification by DCVC (DCM:MeOH:NH_3/100:0:0 to 100:13:1) gave 1-((4,5-dibromo-1-methyl-1*H*-imidazol-2-yl)oxy-*N*,*N*-dimethyl-7-phenylheptan-3-amine as a yellow oil (155 mg, 29%). ^{1}H NMR (CD_3OD, 400 MHz) δ 7.26-7.20 (m, 3H), 7.18-7.10 (m, 3H), 4.41-4.29 (m, 2H), 3.36 (s, 3H), 2.62 (t, 3H, *J* = 7.5 Hz), 2.33 (s, 6H), 2.00 (dq, 1H, *J* = 14.4, 7.8 Hz), 1.81 (dq, 1H, *J* = 7.8, 6.8 Hz), 1.69-1.61 (m, 4H), 1.39-1.37 (m, 2H). ^{13}C NMR (CD_3OD, 101 MHz) δ 129.55 (2C), 129.44 (2C), 126.85, 110.88, 69.83, 62.27, 40.79 (2C), 36.88, 32.82, 31.03, 30.32, 27.78. A stirred solution of 1-((4,5-dibromo-1-methyl-1*H*-imidazol-2-yl)oxy-*N*,*N*-dimethyl-7-phenylheptan-3-amine (178 mg, 0.38 mmol) in dry THF (2 mL) was cooled to -78 °C and dropwisely added *n*-BuLi (0.95 ml, 2.27 mmol, 2.4M in hexane). After 15 min of stirring at -78 °C, the reaction mixture was added sat. aq $NaHCO_3$ solution (3.5 mL) and then extracted with DCM (3 × 7 mL). The combined organic phases were dried ($MgSO_4$), filtered, and evaporated *in vacuo*. Purification by

DCVC (DCM:MeOH:NH_3/100:0:0 to 100:2.8:0.3) gave **27** as a yellow oil (52 mg, 44%). ^{1}H NMR (CD_3OD, 400 MHz) δ 7.26-7.20 (m, 2H), 7.17-7.10 (m, 3H), 6.64 (d, 1H, *J* = 1.8 Hz), 6.52 (d, 1H, *J* = 1.8 Hz), 4.38-4.26 (m, 2H), 3.37 (s, 3H), 2.64-2.58 (m, 3H), 2.24 (s, 6H), 1.95 (d, 1H, *J* = 6.3 Hz), 1.75 (d, 1H, *J* = 6.5 Hz), 1.63 (d, 3H, *J* = 7.5 Hz), 1.42-1.33 (m, 3H). ^{13}C NMR (CD_3OD, 101 MHz) δ 129.55 (2C), 129.43 (2C), 126.82, 122.83, 117.76, 69.45, 62.12, 40.82, 36.91, 32.91, 30.91 30.63, 30.40, 27.86. The product was not converted into the oxalate salt but tested pharmacologically as the oil.

*3.2.24. 1-(6-Bromopyridin-3-yl)-4-(3-phenylpropyl)-1,4-diazepane (**28**)*

A solution of **58** (598 mg, 1.68 mmol) and TFA (2.58 mL, 33.7 mmol) in DCM (20 mL) was stirred at rt for 16 h. The reaction mixture was evaporated *in vacuo*. The residue was added aq NaOH solution (4M, 20 mL) and extracted with DCM (3 × 100 mL). The combined organic phases were dried ($MgSO_4$), filtered, and evaporated *in vacuo* giving 1-(6-bromopyridin-3-yl)-1,4-diazepane as a yellow oil (274 mg, 64%) that crystallizes over time. ^{1}H NMR ($CDCl_3$, 400 MHz) δ 7.84 (d, 1H, *J* = 3.3 Hz), 7.23 (dd, 1H, *J* = 8.8, 0.5 Hz), 6.86 (dd, 1H, *J* = 8.9, 3.4 Hz), 3.54 (dt, 4H, *J* = 16.7, 5.8 Hz), 3.08-3.00 (m, 2H), 2.89-2.80 (m, 2H), 2.28 (bs, 1H), 1.97-1.85 (m, 2H). ^{13}C NMR ($CDCl_3$, 101 MHz) δ 143.90, 133.91, 127.59, 126.76, 121.08, 51.71, 47.95, 47.91, 47.89, 28.92. To a solution 1-(6-bromopyridin-3-yl)-1,4-diazepane (274 mg, 1.07 mmol) and phenylpropanal (157 µL, 1.07 mmol, 90%) in dry DCE (10 mL) was added freshly grinded $NaBH(OAc)_3$ (340 mg, 1.61 mmol). The reaction mixture was stirred overnight at rt. Sat. aq $NaHCO_3$ solution (10 mL) was added to the reaction mixture that was extracted with DCM (2 × 5 mL). The combined organic phases were washed with sat. aq $NaHCO_3$ solution (10 mL), dried ($MgSO_4$), filtered, and evaporated *in vacuo*. Purification by DCVC (DCM:MeOH:NH_3/100:0:0 to 97.5:2.25:0.25) afforded the

product as a yellow oil (362 mg, 90%). ^{1}H NMR ($CDCl_3$, 400 MHz) δ 7.87 (d, 1H, *J* = 3.3 Hz), 7.35-7.29 (m, 3H), 7.26-7.18 (m, 4H), 6.88 (dd, 1H, *J* = 8.8, 3.3 Hz), 3.55 (t, 2H, *J* = 5.0 Hz), 3.51 (t, 2H, *J* = 6.2 Hz), 2.84-2.77 (m, 2H), 2.70-2.61 (m, 4H), 2.55 (t, 2H, *J* = 7.3 Hz), 2.03-1.95 (m, 2H), 1.84 (p, 2H, *J* = 7.5 Hz). ^{13}C NMR ($CDCl_3$, 101 MHz) δ 144.39, 142.02, 133.91, 128.35 (2C), 128.29 (2C), 127.43, 126.68, 125.76, 121.05, 57.05, 54.62, 54.38, 48.90, 47.94, 33.43, 29.08, 27.24. **1-(6-Bromopyridin-3-yl)-4-(3-phenylpropyl)-1,4-diazepane oxalate.** The free amine of **28** (283 mg, 0.71 mmol) was converted into the oxalate salt as described under the general procedure with the exception that 2.0 eq of oxalic acid was added. Salt formation afforded white crystals (293 mg, 81%). Mp: 95.3 °C. ^{1}H NMR (D_2O, 400 MHz) δ 7.81 (d, 1H, *J* = 3.3 Hz), 7.47 (d, 1H, *J* = 9.0 Hz), 7.36-7.29 (m, 2H), 7.28-7.17 (m, 4H), 3.80-3.59 (m, 3H), 3.58-3.40 (m, 3H), 3.37-3.18 (m, 2H), 3.17-3.05 (m, 2H), 2.70 (t, 2H, *J* = 7.2 Hz), 2.23-2.11 (m, 2H), 2.10-1.99 (m, 2H). ^{13}C NMR (D_2O, 101 MHz) δ 165.13 (2C), 144.54, 141.60, 140.28, 132.31, 132.27, 128.78 (2C), 128.45 (2C), 126.58, 124.32, 55.70, 54.01, 53.58, 46.36, 43.48, 31.72, 25.26, 23.62.

*3.2.25. 1-Cinnamyl-4-(pyridin-3-yl)-1,4-diazepane (**29**)*

Compound **29** was prepared as described for **28** from a mixture of 1-(pyridin-3-yl)-1,4-diazepane (100 mg, 0.56 mmol), cinnamaldehyde (0.076 mL, 0.56 mmol, 93%), and $NaBH(OAc)_3$ (178 mg, 0.84 mmol). Purification by DCVC (DCM:MeOH:NH_3/100:0:0 to 100:2.3:0.3) afforded the product as a yellow oil (90 mg, 55%). ^{1}H NMR ($CDCl_3$, 400 MHz) δ 8.14 (d, 1H, *J* = 3.0 Hz), 7.94 (dd, 1H, *J* = 4.8, 1.3 Hz), 7.41-7.36 (m, 2H), 7.35-7.30 (m, 2H), 7.27-7.22 (m, 1H), 7.11 (ddd, 1H, *J* = 4.0 Hz), 6.95 (ddd, 1H, *J* = 8.6, 3.2, 1.3 Hz), 6.52 (d, 1H, *J* =16.1 Hz), 6.30 (dt, 1H, *J* = 9.0, 6.5 Hz), 3.61 (t, 2H, *J* = 4.8 Hz), 3.54 (t, 2H, *J* = 6.3 Hz), 3.33 (d, 2H, *J* = 6.3 Hz) 2.91-2.82 (m, 2H), 2.75-2.67 (m, 2H), 2.09-2.00 (m, 2H). ^{13}C NMR ($CDCl_3$, 101 MHz) δ 144.90, 137.30,

136.79, 134.41, 133.02, 128.58 (2C), 127.58, 126.33, 123.54 (2C), 120.59, 117.73, 60.72, 55.14, 54.66, 48.51, 47.67, 27.52. **1-Cinnamyl-4-(pyridin-3-yl)-1,4-diazepane oxalate.** The free amine of **29** (78 mg, 0.27 mmol) was converted into the oxalate salt according to the general procedure with the exception that 2.0 eq of oxalic acid was added. Salt formation yielded a yellow solid (58 mg, 56%). Mp: 63.0-63.9 °C. ^{1}H NMR (D_2O, 400 MHz) δ 8.15 (d, 1H, *J* = 2.5 Hz), 8.03 (d, 1H, *J* = 5.5 Hz), 7.89 (dd, 1H, *J* = 6.0, 3.0 Hz), 7.83-7.77 (m, 1H), 7.54 (d, 2H, *J* = 7.5 Hz), 7.47-7.37 (m, 3H), 6.93 (d, 1H, *J* = 15.8 Hz), 6.33 (p, 1H, *J* = 7.5 Hz), 4.01 (d, 2H, *J* = 7.3 Hz), 3.97-3.89 (m, 2H), 3.85-3.70 (m, 2H), 3.70-3.50 (m, 2H), 3.45-3.20 (m, 2H), 2.45-2.25 (m, 2H). ^{13}C NMR (D_2O, 101 MHz) δ 165.13 (2C), 147.02, 140.87, 135.16, 129.27, 129.02 (2C), 128.51, 127.60, 127.16, 126.97 (2C), 124.90, 116.31, 59.44, 53.58, 53.46, 46.69, 43.39, 23.76.

*3.2.26. 1-Benzyl-4-(pyridin-3-yl)-1,4-diazepane (**30**)*

58 was deprotected as described for **28** from a mixture of **58** (948 mg, 3.42 mmol) and TFA (5.23 mL, 68.4 mmol) yielding 1-(pyridin-3-yl)-1,4-diazepane as a yellow oil (507 mg, 84%). ^{1}H NMR ($CDCl_3$, 400 MHz) δ 8.13 (d, 1H, *J* = 3.1 Hz), 7.92 (dd, 1H, *J* = 4.5, 1.3 Hz), 7.10 (dd, 1H, *J* = 8.5, 4.6 Hz), 6.95 (ddd, 1H, *J* = 8.6, 3.1, 1.3 Hz), 3.62-3.54 (m, 4H), 3.05 (t, 2H, *J* = 5.3 Hz), 2.85 (t, 2H, *J* = 5.8 Hz), 2.07 (s, 1H), 1.93 (p, 2H, *J* = 6.0 Hz). ^{13}C NMR ($CDCl_3$, 101 MHz) δ 144.40, 137.49, 134.54, 123.84, 117.91, 51.45, 48.19, 47.93, 47.89, 29.24. Compound **30** was prepared as described for **28** from a mixture of 1-(pyridin-3-yl)-1,4-diazepane (100 mg, 0.56 mmol), benzaldehyde (57 μL, 0.56 mmol), and $NaBH(OAc)_3$ (178 mg, 0.84 mmol) affording the product as a yellow oil (104 mg, 69%). ^{1}H NMR ($CDCl_3$, 400 MHz) δ 8.12 (d, 1H, *J* = 3.0 Hz), 7.93 (dd, 1H, *J* = 4.6, 1.3 Hz), 7.34-7.28 (m, 4H), 7.28-7.23 (m, 2H), 7.10 (ddd, 1H, *J* = 8.5, 4.6, 0.6 Hz), 6.94 (ddd, 1H, *J* = 8.6, 3.1, 1.3 Hz), 3.65 (s, 2H), 3.54 (dt, 4H, *J* = 13.3, 5.6 Hz), 2.78 (t, 2H, *J* = 5.0 Hz), 2.65 (t, 2H, *J* = 5.6 Hz), 1.98 (p, 2H,

J = 5.9 Hz). ^{13}C NMR ($CDCl_3$, 101 MHz) δ 145.07, 138.94, 137.23, 134.47, 128.97 (2C), 128.44 (2C), 127.27, 123.72, 117.93, 62.48, 55.07, 54.75, 48.74, 47.99, 27.62. **1-Benzyl-4-(pyridin-3-yl)-1,4-diazepane oxalate.** The free amine of **30** (104 mg, 0.39 mmol) was converted into the oxalate salt as described under the general procedure affording an orange solid (113 mg, 81%). Mp: 124.0-124.8 °C. ^{1}H NMR (D_2O, 400 MHz) δ 8.16 (d, 1H, *J* = 3.0 Hz), 8.06 (d, 1H, *J* = 5.3 Hz), 7.89 (ddd, 1H, *J* = 9.1, 3.0, 1.1 Hz), 7.82 (dd, 1H, *J* = 9.0, 5.3 Hz), 7.60-7.53 (m, 5H), 4.44 (s, 2H), 3.92 (t, 2H, *J* = 4.6 Hz), 3.78 (s, 4H), 3.62 (t, 2H, *J* = 6.1 Hz), 3.59-3.44 (m, 3H), 2.40-2.34 (m, 2H). ^{13}C NMR (D_2O, 101 MHz) δ 170.15 (2C), 147.06, 131.23 (2C), 130.32, 129.34 (2C), 128.79, 128.58, 127.42, 127.07, 124.30, 61.07, 53.93, 53.71, 46.61, 42.97, 23.45.

*3.2.27. 1-Phenethyl-4-(pyridin-3-yl)-1,4-diazepane (**31**)*

Compound **31** was prepared as described for **28** from a mixture of 1-(pyridin-3-yl)-1,4-diazepane (100 mg, 0.56 mmol), 2-phenylacetaldehyde (65 μL, 0.56 mmol), and $NaBH(OAc)_3$ (178 mg, 0.84 mmol). Purification by DCVC (DCM:MeOH:NH_3/100:0:0 to 95:4.5:0.5) afforded the product as a brown oil (124 mg, 79%). ^{1}H NMR ($CDCl_3$, 400 MHz) δ 8.20 (d, 1H, *J* = 3.0 Hz), 7.99 (dd, 1H, *J* = 4.6, 1.3 Hz), 7.37-7.32 (m, 2H), 7.30-7.23 (m, 3H), 7.16 (ddd, 1H, *J* = 8.5, 4.6, 0.6 Hz), 7.01 (ddd, 1H, *J* = 8.6, 3.1, 1.3 Hz), 3.63 (t, 2H, *J* = 5.0 Hz), 3.57 (t, 2H, *J* = 6.3 Hz), 2.94-2.91 (m, 2H), 2.88-2.80 (m, 4H), 2.77-2.75 (m, 2H), 2.05 (p, 2H, *J* = 5.9 Hz). ^{13}C NMR ($CDCl_3$, 101 MHz) δ 144.86, 140.32, 137.19, 134.40, 128.71 (2C), 128.40 (2C), 126.04, 123.60, 117.75, 59.88, 54.95, 54.49, 48.76, 47.73, 34.09, 27.52. **1-Phenethyl-4-(pyridin-3-yl)-1,4-diazepane oxalate.** The free amine of **31** (124 mg, 0.44 mmol) was converted into the oxalate salt as described under the general procedure affording an orange solid (98 mg, 60%). Mp: 173.1-173.9 °C. ^{1}H NMR (D_2O, 400 MHz) δ 8.18 (d, 1H, *J* = 3.0 Hz), 8.08-8.07 (m, 1H), 7.92 (ddd, 1H, *J* = 9.1, 3.0, 1.0 Hz), 7.83 (dd, 1H, *J* = 9.0, 5.4 Hz), 7.46-

7.41 (m, 2H), 7.40-7.35 (m, 3H), 3.97 (t, 2H, *J* = 4.7 Hz), 3.86-3.59 (m, 4H), 3.58-3.32 (m, 4H), 3.18-3.12 (m, 2H), 2.43-2.33 (m, 2H). ^{13}C NMR (D_2O, 101 MHz): δ 168.31 (2C), 146.99, 136.16, 129.13 (2C), 128.81 (2C), 128.57, 127.54, 127.44, 127.15, 124.27, 58.02, 54.10, 54.07, 46.60, 43.24, 30.05, 23.55.

*3.2.28. 1-(3-Phenylpropyl)-4-(pyridin-3-yl)-1,4-diazepane (**32**)*

Compound **32** was prepared as described for **28** from a mixture of 1-(pyridin-3-yl)-1,4-diazepane (100 mg, 0.56 mmol), 3-phenylpropanal (82 μL, 0.56 mmol, 90%), and $NaBH(OAc)_3$ (178 mg, 0.84 mmol) yielding the product as an orange oil (121 mg, 73%). ^{1}H NMR ($CDCl_3$, 400 MHz) δ 8.12 (d, 1H, *J* = 2.9 Hz), 7.92 (dd, 1H, *J* = 4.6, 1.3 Hz), 7.29-7.25 (m, 3H), 7.20-7.14 (m, 3H), 7.09 (ddd, 1H, *J* = 8.5, 4.6, 0.7 Hz), 6.93 (ddd, 1H, *J* = 8.6, 3.1, 1.3 Hz), 3.56 (t, 2H, *J* = 4.9 Hz), 3.50 (t, 2H, *J* = 6.3 Hz), 2.80-2.77 (m, 2H), 2.66-2.59 (m, 4H), 2.52 (t, 2H, *J* = 7.4 Hz), 2.01-1.96 (m, 2H), 1.81 (p, 2H, *J* = 7.5 Hz). ^{13}C NMR ($CDCl_3$, 101 MHz) δ 144.99, 142.16, 137.31, 134.48, 128.53 (2C), 128.47 (2C), 125.94, 123.73, 117.92, 57.23, 55.07, 54.54, 48.64, 47.86, 33.63, 29.12, 27.45. **1-(3-Phenylpropyl)-4-(pyridin-3-yl)-1,4-diazepane oxalate.** The free amine of **32** (121 mg, 0.41 mmol) was converted into the oxalate salt as described under the general procedure affording a yellow solid (55 mg, 35%). Mp: 59.3-60.3 °C. ^{1}H NMR (D_2O, 400 MHz) δ 8.13 (d, 1H, *J* = 2.9 Hz), 8.07 (d, 1H, *J* = 5.2 Hz), 7.88 (ddd, 1H, *J* = 9.1, 2.9, 1.0 Hz), 7.82 (dd, 1H, *J* = 9.0, 5.3 Hz), 7.40-7.37 (m, 2H), 7.32-7.28 (m, 3H), 3.89 (t, 2H, *J* = 4.7 Hz), 3.68-3.56 (m, 4H), 3.50-3.25 (m, 2H), 3.22-3.18 (m, 2H), 2.75 (t, 2H, *J* = 7.3 Hz), 2.33-2.27 (m, 2H), 2.16-2.08 (m, 2H). ^{13}C NMR (D_2O, 101 MHz) δ 168.27 (2C), 146.92, 140.37, 128.79 (2C), 128.58 (2C), 128.50, 127.55, 127.16, 126.57, 124.21, 56.08, 54.04, 53.59, 46.51, 43.18, 31.71, 25.31, 23.47.

*3.2.29. 1-(3-Bromophenethyl)-4-(pyridin-3-yl)-1,4-diazepane (**33**)*

Compound **33** was prepared as described for **28** from a mixture of 1-(pyridin-3-yl)-1,4-diazepane (281 mg, 1.59 mmol), 2-(3-bromophenyl)acetaldehyde[46] (411 mg, 2.07 mmol), and $NaBH(OAc)_3$ (506 mg, 2.39 mmol) giving the product as a yellow oil (179 mg, 31%). ^{1}H NMR ($CDCl_3$, 400 MHz) δ 8.12 (d, 1H, *J* = 2.9 Hz), 7.92 (dd, 1H, *J* = 4.6, 1.3 Hz), 7.33-7.29 (m, 2H), 7.14-7.07 (m, 3H), 6.93 (ddd, 1H, *J* = 8.6, 3.1, 1.3 Hz), 3.57 (t, 2H, *J* = 4.9 Hz), 3.50 (t, 2H, *J* = 6.3 Hz), 2.86 (t, 2H, *J* = 4.9 Hz), 2.75 (s, 4H), 2.70 (t, 2H, *J* = 5.5 Hz), 2.03-1.97 (m, 2H). ^{13}C NMR ($CDCl_3$, 101 MHz) δ 144.90, 142.58, 137.47, 134.50, 131.89, 130.09, 129.37, 127.51, 123.76, 122.55, 117.97, 59.56, 55.11, 54.55, 48.68, 47.81, 33.69, 27.40. **1-(3-Bromophenethyl)-4-(pyridin-3-yl)-1,4-diazepane oxalate.** The free amine of **33** (180 mg, 0.50 mmol) was converted into the oxalate salt as described under the general procedure with the exception that 2.0 eq of oxalic acid was added. Salt formation afforded a yellow solid (183 mg, 74%). Mp: 130.5-131.4 °C. ^{1}H NMR (D_2O, 400 MHz) δ 8.18 (d, 1H, *J* = 3.0 Hz), 8.08-8.07 (m, 1H), 7.92 (ddd, 1H, *J* = 9.1, 3.0, 1.0 Hz), 7.84 (dd, 1H, *J* = 9.0, 5.4 Hz), 7.55-7.52 (m, 2H), 7.35-7.32 (m, 2H), 3.97-3.94 (m, 2H), 3.71-3.49 (m, 8H), 3.16-3.12 (m, 2H), 2.41-2.35 (m, 2H). ^{13}C NMR (D_2O, 101 MHz) δ 165.98 (2C), 146.99, 138.45, 131.63, 130.76, 130.36, 128.58, 127.65, 127.58, 127.18, 124.21, 122.22, 57.67, 54.12 (2C), 46.60, 43.22, 29.62, 23.55.

*3.2.30. 1-Benzyl-4-(pyridin-3-yl)piperazine (**34**)*

62[40] was deprotected as described for **28** from a mixture of **62** (0.77 g, 2.92 mmol) and TFA (4.5 mL, 58.4 mmol) yielding 1-(pyridin-3-yl)piperazine as a yellow oil (410 mg, 86%). ^{1}H NMR ($CDCl_3$, 400 MHz) δ 8.31 (dd, 1H, *J* = 2.6, 1.1 Hz), 8.10 (dd, 1H, *J* = 4.0, 2.0 Hz), 7.19-7.13 (m, 2H), 3.17 (dd, 4H, *J* = 6.2, 3.8 Hz), 3.05 (dd, 4H, *J* = 6.2, 3.9 Hz), 1.85 (s, 1H). ^{13}C NMR ($CDCl_3$, 101 MHz) δ 147.53, 140.91, 138.86, 123.58, 122.49, 49.79 (2C), 46.08 (2C). Compound **34** was prepared as described for **28** from a

mixture of 1-(pyridin-3-yl)piperazine (100 mg, 0.61 mmol), benzaldehyde (62 µL, 0.61 mmol), and $NaBH(OAc)_3$ (195 mg, 0.92 mmol). Purification by DCVC (DCM:MeOH:NH_3/100:0:0 to 92.5:6.75:0.75) afforded the product as a brown oil (80 mg, 52%). ^{1}H NMR ($CDCl_3$, 400 MHz) δ 8.30 (dd, 1H, *J* = 2.6, 1.1 Hz), 8.09 (dd, 1H, *J* = 4.0, 2.0 Hz), 7.36-7.27 (m, 5H), 7.15 (dt, 2H, *J* = 4.2, 1.6 Hz), 3.57 (s, 2H), 3.23 (t, 4H, *J* = 5.1 Hz), 2.62 (t, 4H, *J* = 5.1 Hz). ^{13}C NMR ($CDCl_3$, 101 MHz) δ 147.15, 140.76, 138.72, 138.01, 129.30 (2C), 128.45 (2C), 127.35, 123.56, 122.36, 63.16, 52.95 (2C), 48.62 (2C). **1-Benzyl-4-(pyridin-3-yl)piperazine oxalate.** The free amine of **34** (80 mg, 0.32 mmol) was converted into the oxalate salt as described under the general procedure with the exception that 2.1 eq of oxalic acid was added. Salt formation afforded yellow crystals (99 mg, 90%). Mp: 148.3 °C. ^{1}H NMR (D_2O, 400 MHz) δ 8.38 (d, 1H, *J* = 2.9 Hz), 8.23 (dt, 1H, *J* = 5.5, 0.8 Hz), 8.14 (ddd, 1H, *J* = 9.0, 2.9, 1.0 Hz), 7.91 (dd, 1H, *J* = 9.0, 5.6 Hz), 7.61-7.56 (m, 5H), 4.48 (s, 2H), 4.11 (d, 2H, *J* = 9.0 Hz), 3.71 (d, 2H, *J* = 8.7 Hz), 3.38 (d, 4H, *J* = 9.1 Hz). ^{13}C NMR (D_2O, 101 MHz) δ 165.07 (2C), 147.60, 131.37, 131.31, 131.23 (2C), 130.42, 129.36 (2C), 128.00, 127.70, 127.34, 60.52, 50.46 (2C), 44.04 (2C).

*3.2.31. 1-Phenethyl-4-(pyridin-3-yl)piperazine (**35**)*

Compound **35** was prepared as described for **28** from a mixture of 1-(pyridin-3-yl)piperazine (100 mg, 0.61 mmol), 2-phenylacetaldehyde (71 µL, 0.61 mmol), and $NaBH(OAc)_3$ (195 mg, 0.92 mmol). Purification by DCVC (DCM:MeOH:NH_3/100:0:0 to 92.5:6.75:0.75) afforded the product as a brown oil (90 mg, 55%). ^{1}H NMR ($CDCl_3$, 400 MHz) δ 8.21 (bs, 2H), 7.32-7.28 (m, 2H), 7.24-7.18 (m, 5H), 3.26 (t, 4H, *J* = 5.1 Hz), 2.85 (dd, 2H, *J* = 9.9, 6.3 Hz), 2.71-2.65 (m, 6H). ^{13}C NMR ($CDCl_3$, 101 MHz) δ 147.09, 140.79, 140.25, 138.68, 128.83 (2C), 128.57 (2C), 126.28, 123.60, 122.44, 60.53, 53.07 (2C), 48.60 (2C), 33.73. **1-Phenethyl-4-(pyridin-3-yl)piperazine oxalate.**

The free amine of **35** (40 mg, 0.15 mmol) was converted into the oxalate salt as described under the general procedure with the exception that 2.1 eq of oxalic acid was added. Salt formation afforded yellow crystals (31 mg, 58%). Mp: 150.7 °C. ^{1}H NMR (D_2O, 400 MHz) δ 8.40 (d, 1H, *J* = 2.9 Hz), 8.24 (d, 1H, *J* = 5.5 Hz), 8.15 (ddd, 1H, *J* = 9.0, 2.9, 1.0 Hz), 7.92 (dd, 1H, *J* = 9.0, 5.5 Hz), 7.49-7.38 (m, 5H), 4.12 (d, 2H, *J* = 12.0 Hz), 3.84 (d, 2H, *J* = 10.4 Hz), 3.59-3.55 (m, 2H), 3.41 (p, 4H, *J* = 12.6 Hz), 3.19 (dd, 2H, *J* = 9.4, 6.8 Hz). ^{13}C NMR (D_2O, 101 MHz) δ 147.60, 136.01, 131.36, 131.32, 129.13 (2C), 128.79 (2C), 127.69, 127.46, 127.35, 57.51, 51.01 (2C), 44.05 (2C), 29.62.

*3.2.32. 1-(3-Phenylpropyl)-4-(pyridin-3-yl)piperazine (**36**)*

Compound **36** was prepared as described for **28** from a mixture of 1-(pyridin-3-yl)piperazine (200 mg, 1.23 mmol), 3-phenylpropanal (163 µL, 1.23 mmol), and $NaBH(OAc)_3$ (392 mg, 1.85 mmol). Purification by DCVC (DCM:MeOH:NH_3/100:0:0 to 95:4.5:0.5) afforded the product as a brown oil (200 mg, 58%). ^{1}H NMR ($CDCl_3$, 400 MHz) δ 8.31 (dd, 1H, *J* = 2.7, 0.9 Hz), 8.09 (dd, 1H, *J* = 4.1, 1.8 Hz), 7.31-7.26 (m, 2H), 7.21-7.15 (m, 5H), 3.23 (t, 4H, *J* = 5.1 Hz), 2.67 (t, 2H, *J* = 7.7 Hz), 2.60 (t, 4H, *J* = 5.1 Hz), 2.45-2.41 (m, 2H), 1.86 (dt, 2H, *J* = 15.2, 7.6 Hz). ^{13}C NMR ($CDCl_3$, 101 MHz) δ 147.11, 142.19, 140.79, 138.71, 128.55 (2C), 128.47 (2C), 125.95, 123.55, 122.33, 58.03, 53.08 (2C), 48.62 (2C), 33.78, 28.69. **1-(3-Phenylpropyl)-4-(pyridin-3-yl)piperazine oxalate.** The free amine of **36** (200 mg, 0.71 mmol) was converted into the oxalate salt as described under the general procedure with the exception that 2.1 eq of oxalic acid was added. Salt formation afforded yellow crystals (242 mg, 92%). Mp: 154.2 °C. ^{1}H NMR (D_2O, 400 MHz) δ 8.40-8.38 (m, 1H), 8.25-8.22 (m, 1H), 8.15-8.12 (m, 1H), 7.93-7.89 (m, 1H), 7.46-7.32 (m, 5H), 4.11-4.06 (m, 2H), 3.78-3.72 (m, 2H), 3.44-3.36 (m, 2H), 3.32-3.22 (m, 4H), 2.81-2.76 (m, 2H), 2.20-2.11 (m, 2H). ^{13}C NMR

(D_2O, 101 MHz) δ 165.52 (2C), 147.61, 140.42, 131.34 (2C), 128.83 (2C), 128.51 (2C), 127.70, 127.33, 126.60, 56.23, 50.87 (2C), 44.10 (2C), 31.68, 24.94.

*3.2.33. 3-[Benzyl(methyl)amino]butyl dimethylcarbamate (**37**)*

Compound **37** was prepared as described for **9** from a mixture of **40** (6.47 g, 33.5 mmol), CDI (7.05 g, 43.5 mmol), and dimethylamine (15.1 mL, 77.0 mmol, 33% in ethanol (EtOH)). Purification by FCC (EtOAc:heptane/0:100 to 100:0) afforded the product as a yellow oil (7.48 g, 85%). ^{1}H NMR ($CDCl_3$, 400 MHz) δ 7.35-7.15 (m, 5H), 4.23-4.10 (m, 2H), 3.58 (d, 1H, *J* = 13.3 Hz), 3.47 (d, 1H, *J* = 13.6 Hz), 2.95-2.70 (m, 7H), 2.14 (s, 3H), 1.95-1.82 (m, 1H), 1.65-1.55 (m, 1H), 1.02, 1.00 (2 s, 3H, rotamers). ^{13}C NMR ($CDCl_3$, 101 MHz) δ 156.74, 140.01, 128.59 (2C), 128.10 (2C), 126.65, 63.36, 57.85, 53.97, 36.28, 36.02, 35.72, 33.14, 13.04.

*3.2.34. Methyl 3-[benzyl(methyl)amino]but-2-enoate (**38**)*

To a stirred suspension of methyl acetoacetate (5.00 g, 43.1 mmol) in toluene (100 mL) containing AcOH (2.15 mL) was added methyl benzylamine (10.4 g, 85.8 mmol), and the mixture was stirred at room temperature (rt) for 5 days. The reaction mixture was washed with saturated (sat.) aqueous (aq) $NaHCO_3$ solution (2 × 100 mL), and the organic phase dried ($MgSO_4$), filtered, and evaporated *in vacuo*. Purification by Kugelrohr distillation (0.4 mmHg, 200 °C) afforded the product as a yellow oil (9.34 g, >99%). ^{1}H NMR ($CDCl_3$, 300 MHz) δ 7.35-7.23 (m, 3H), 7.09 (d, 2H, *J* = 9 Hz), 4.71 (s, 1H), 4.49 (s, 2H), 3.62 (s, 3H), 2.90 (s, 3H), 2.53 (s, 3H). ^{13}C NMR ($CDCl_3$, 75 MHz) δ 170.0, 161.8, 137.7, 129.2 (2C), 127.8, 126.6 (2C), 84.9, 55.3, 50.5, 38.9, 15.6.

*3.2.35. Methyl 3-[phenethyl(methyl)amino]but-2-enoate (**39**)*

Compound **39** was prepared as described for **38** from a mixture of methyl acetoacetate (5.00 g, 43.1 mmol), AcOH (2.15 mL), and methyl phenethylamine (11.6 g, 85.8 mmol) yielding the product as a yellow oil (9.57 g, 93%). ^{1}H NMR ($CDCl_3$, 300 MHz) δ 7.31-7.13 (m, 5H), 4.60 (s, 1H), 3.62 (s, 3H), 3.48 (t, 2H, *J* = 8 Hz), 2.83-2.78 (m, 5H), 2.40 (s, 3H). ^{13}C NMR ($CDCl_3$, 75 MHz) δ 170.0, 161.3, 138.9, 129.1 (2C), 129.1 (2C), 127.0, 84.3, 54.1, 50.5, 38.9, 34.8, 15.5.

*3.2.36. 3-[Benzyl(methyl)amino]butan-1-ol (**40**)*

38 (4.25 g, 19.4 mmol) dissolved in dry *i*-PrOH (19 mL) and dry THF (48 mL) was treated with sodium (3.84 g, 166 mmol) at 0 °C. The reaction mixture was allowed to warm to rt over 17 h. The reaction mixture was poured into sat. aq NH_4Cl solution (50 mL), extracted with DCM (3 × 50 mL), and the organic phase evaporated *in vacuo*. The residue was dissolved in aq HCl solution (4M, 20 mL) and washed with Et_2O (2 × 20 mL). The water phase was neutralized with solid $NaHCO_3$ and extracted with DCM (3× 20 mL). The combined organic phases were dried ($MgSO_4$), filtered, and evaporated *in vacuo*. Purification by DCVC (DCM:MeOH:NH_3/100:0:0 to 100:4.5:0.5) afforded the product as a brown oil (880 mg, 24%). ^{1}H NMR ($CDCl_3$, 300 MHz) δ 7.33-7.25 (m, 5H), 5.99 (bs, 1H), 3.81-3.77 (m, 2H), 3.70 (d, 1H, *J* = 12 Hz), 3.52 (d, 1H, *J* = 12 Hz), 3.11-3.00 (m, 1H), 2.19 (s, 3H), 2.01-2.87 (m, 1H), 1.34 (dq, 1H, *J* = 15, 3 Hz), 1.02 (d, 3H, *J* = 6 Hz). ^{13}C NMR ($CDCl_3$, 75 MHz) δ 138.9, 129.4 (2C), 128.9 (2C), 127.6, 64.5, 59.7, 59.2, 35.7, 34.6, 12.4.

*3.2.37. 3-[Phenethyl(methyl)amino]butan-1-ol (**41**)*

Compound **41** was prepared as described for **40** from a mixture of **39** (5.00 g, 21.4 mmol) and sodium (4.43 g, 193 mmol). Purification by DCVC (DCM:MeOH:NH_3/100:0:0 to 100:9:1) yielded the product as a yellow oil (2.97 g,

67%). ^{1}H NMR ($CDCl_3$, 300 MHz) δ 7.31-7.10 (m, 5H), 5.84 (bs, 1H), 3.84-3.70 (m, 2H), 3.05-2.96 (m, 1H), 2.82-2.71 (m, 2H), 2.62-2.55 (m, 2H), 2.29 (s, 3H), 1.92-1.78 (m, 1H), 1.30 (dq, 1H, *J* = 12, 3 Hz), 0.93 (d, 3H, *J* = 6 Hz). ^{13}C NMR ($CDCl_3$, 75 MHz) δ 140.2, 129.1 (2C), 129.1 (2C), 126.9, 65.5, 62.7, 60.6, 36.4, 35.4, 34.7, 13.0.

*3.2.38. 3-(Methylamino)butyl methylcarbamate acetate (**42**)*

9 (645 mg, 2.59 mmol), AcOH (6 mL), and Pd/C (32 mg, 5% w/w) were added to a flask that was evacuated and flushed with H_2 and stirred at rt for 52 h under a positive pressure of H_2. The reaction mixture was diluted with EtOAc and filtered through a plug of Celite. The filtrate was evaporated *in vacuo* to give the product as a brown oil (645 mg, quantitative). ^{1}H NMR (D_2O, 300 MHz) δ 4.20-4.05 (m, 2H), 3.36-3.29 (m, 1H), 2.64 (s, 6H), 2.11-1.98 (m, 1H), 1.90 (s, 3H), 1.90-1.82 (m, 1H), 1.29 (d, 3H, *J* = 9 Hz). ^{13}C NMR (D_2O, 75 MHz) δ 178.1, 157.4, 61.3, 53.0, 32.3, 30.2, 27.8, 23.8, 16.1. **42** (3.40 g, 15.6 mmol) was dissolved in aq NaOH solution (2M, 70 mL) and extracted with EtOAc (3 x 70 mL). The combined organic phases were dried ($MgSO_4$), filtered, and evaporated *in vacuo* affording the free amine of **42** (2.03 g, 82%).

*3.2.39. 3-(Methylamino)butyl dimethylcarbamate (**43**)*

Compound **43** was prepared as described for **42** from a mixture of **37** (2.53 g, 9.59 mmol) and Pd/C (127 mg, 5% w/w). Basic extraction afforded the free amine of **43** as a transparent oil (170 mg, 69%). ^{1}H NMR ($CDCl_3$, 400 MHz) δ 4.17-4.03 (m, 2H), 2.87 (s, 6H), 2.65 (sxt, 1H, *J* = 6.3 Hz), 2.38 (s, 3H), 1.92 (bs, 1H), 1.86-1.73 (m, 1H), 1.66-1.54 (m, 1H), 1.07, 1.05 (2 s, 3H, rotamers). ^{13}C NMR ($CDCl_3$, 101 MHz) δ 156.58, 62.80, 60.27, 52.20, 35.78, 33.49 (2C), 19.73.

*3.2.40. Ethyl-3-(dimethylamino)-5-phenylpentanoate (**48**)*

To **44**[38] (2.08 g, 10.2 mmol) was added dimethylamine (7.28 mL, 40.8 mmol, 33% in EtOH), and the reaction mixture was stirred for 4 days at rt. The solvent was evaporated in vacuo giving the product as a yellow oil (2.30 g, 91%). ^{1}H NMR (CD_3OD, 400 MHz) δ 7.28-7.22 (m, 2H), 7.21-7.11 (m, 3H), 4.11 (q, 2H, *J* = 6.8 Hz), 2.98 (p, 1H, *J* = 6.4 Hz) 2.64 (t, 2H, *J* = 7.9 Hz), 2.57 (dd, 1H, *J* = 14.8, 6.0 Hz), 2.29 (dd, 1H, *J* = 14.8, 7.3 Hz), 2.23 (s, 6H), 1.90-1.79 (m, 1H), 1.69-1.58 (m, 1H), 1.23 (t, 4H, *J* = 7.0 Hz). ^{13}C NMR (CD_3OD, 101 MHz) δ 174.84, 143.47, 129.58 (2C), 129.52 (2C), 127.01, 61.89, 61.77, 40.68 (2C), 35.32, 34.21, 34.00, 14.61.

*3.2.41. Ethyl 3-(dimethylamino)-6-phenylhexanoate (**49**)*

Compound **49** was prepared as described for **48** from a mixture of dimethylamine (11.7 mL, 65.4 mmol, 33% in EtOH) and **45**[37, 38] (3.57 g, 16.4 mmol) yielding the product as a yellow oil (4.05 g, 94%). ^{1}H NMR ($CDCl_3$, 400 MHz) δ 7.28-7.26 (m, 1H), 7.25 (t, 1H, *J* = 2.2 Hz), 7.18-7.15 (m, 3H), 4.12 (q, 2H, *J* = 7.1 Hz), 3.06-2.99 (m, 1H), 2.62 (t, 2H, *J* = 7.7 Hz), 2.51 (dd, 1H, *J* = 14.4, 5.7 Hz), 2.23 (s, 6H), 2.16 (dd, 1H, *J* = 14.2, 7.7 Hz), 1.74-1.62 (m, 2H), 1.60-1.52 (m, 1H), 1.40-1.31 (m, 1H), 1.23 (t, 3H, *J* = 7.1 Hz). ^{13}C NMR ($CDCl_3$, 101 MHz) δ 173.32, 142.46, 128.54 (2C), 128.40 (2C), 125.83, 61.13, 60.53, 40.39 (2C), 35.96, 34.33, 30.83, 28.51, 14.34.

*3.2.42. Ethyl 3-(dimethylamino)-7-phenylheptanoate (**50**)*

Compound **50** was prepared as described for **48** from a mixture of dimethylamine (8.0 mL, 51 mmol, 33% in EtOH) and **46**[37, 38] (2.98 g, 12.8 mmol) furnishing the product as a yellow oil (3.52 g, 99%). ^{1}H NMR ($CDCl_3$, 400 MHz) δ 7.29-7.26 (m, 2H), 7.19-7.16 (m, 3H), 4.12 (q, 2H, *J* = 7.1 Hz), 2.98 (dt, 1H, *J* = 13.6, 7.1 Hz), 2.61 (t, 2H, *J* = 7.8 Hz), 2.50 (dd, 1H, *J* = 14.5, 6.0 Hz), 2.23 (s, 6H), 2.15 (dd, 1H, *J* = 14.5, 7.5 Hz), 1.66-1.59 (m, 3H), 1.42-1.30 (m, 3H), 1.25 (t, 3H, *J* = 7.1 Hz). ^{13}C NMR ($CDCl_3$, 101

MHz) δ 173.25, 142.77, 128.52 (2C), 128.39 (2C), 125.77, 61.18, 60.51, 40.40 (2C), 36.01, 34.44, 31.67, 31.03, 26.53, 14.36.

*3.2.43. Ethyl-3-(dimethylamino)-8-phenyloctanoate (**51**)*

Compound **51** was prepared as described for **48** from a mixture of dimethylamine (4.85 mL, 27.2 mmol, 33% in EtOH) and **47**[37, 38] (1.12 g, 4.50 mmol) furnishing the product as a yellow oil (1.18 g, 90%). ^{1}H NMR (CD_3OD, 400 MHz) δ 7.27-7.20 (m, 2H), 7.18-7.10 (m, 3H), 4.11 (q, 2H, *J* = 7.3 Hz), 3.55-3.35 (m, 1H), 3.00-2.75 (m, 1H), 2.65-2.50 (m, 7H), 2.50-2.40 (m, 1H), 1.90-1.77 (m, 1H), 1.63 (p, 2H, *J* = 7.4 Hz), 1.57-1.47 (m, 1H), 1.45-1.32 (m, 5H), 1.28 (t, 3H, *J* = 7.3 Hz). ^{13}C NMR (CD_3OD, 101 MHz) δ 144.24, 129.76 (2C), 129.62 (2C), 127.01, 62.74, 61.98, 40.98, 40.94, 37.17, 35.81, 32.95, 27.94, 30.57, 32.22, 14.84.

*3.2.44. 3-(Dimethylamino)-5-phenylpentan-1-ol (**52**)*

A mixture of **48** (2.30 g, 9.22 mmol) in dry Et_2O (12 mL) was slowly added to a slurry mixture of $LiAlH_4$ (0.70 g, 18.5 mmol) in dry Et_2O (12 mL) at 0 °C. The reaction mixture was allowed to reach rt and stirring was continued overnight. H_2O (2 mL), aq NaOH solution (5M, 1 mL), and H_2O (4 mL) were slowly added at 0 °C. The precipitate was isolated and washed thoroughly with Et_2O. H_2O was added to the filtrate and extracted with Et_2O (3 x 60 mL). The combined organic phases were dried ($MgSO_4$), filtered, and evaporated in vacuo yielding the product as a yellow oil (1.51 g, 79%). ^{1}H NMR (CD_3OD, 400 MHz) δ 7.28-7.22 (m, 2H), 7.21-7.12 (m, 3H), 3.68-3.62 (m, 2H), 2.72-2.63 (m, 1H), 2.63-2.54 (m, 2H), 2.23 (s, 6H) 1.91-1.72 (m, 2H), 1.61-1.48 (m, 2H). ^{13}C NMR (CD_3OD, 101 MHz) δ 143.49, 129.33 (4C), 126.78, 63.17, 62.28, 40.38 (2C), 34.26, 32.60, 31.93.

*3.2.45. 3-(Dimethylamino)-6-phenylhexan-1-ol (**53**)*

Compound **53** was prepared as described for **52** from a mixture of **49** (4.05 g, 15.4 mmol) and $LiAlH_4$ (0.79 g, 20.8 mmol) yielding the product as a yellow oil (3.03 g, 89%). ^{1}H NMR ($CDCl_3$, 400 MHz) δ 7.28 (d, 2H, *J* = 7.5 Hz), 7.18-7.16 (m, 3H), 3.81-3.78 (m, 2H), 2.70-2.57 (m, 3H), 2.28 (s, 6H), 1.77-1.57 (m, 4H), 1.55-1.46 (m, 2H). ^{13}C NMR ($CDCl_3$, 101 MHz) δ 142.18, 128.51 (2C), 128.44 (2C), 126.01, 66.49, 64.18, 40.05 (2C), 36.19, 31.01, 29.45, 26.19.

*3.2.46. 3-(Dimethylamino)-7-phenylheptan-1-ol (**54**)*

Compound **54** was prepared as described for **52** from a mixture of **50** (2.88 g, 10.4 mmol) and $LiAlH_4$ (0.79 g, 20.8 mmol) affording the product as a yellow oil (2.13 g, 87%). ^{1}H NMR ($CDCl_3$, 400 MHz) δ 7.30-7.27 (m, 2H), 7.20-7.16 (m, 3H), 6.30 (s, 1H), 3.79 (dd, 2H, *J* = 7.3, 3.2 Hz), 2.64-2.58 (m, 3H), 2.27 (s, 6H), 1.71-1.56 (m, 4H), 1.47 (q, 1H, *J* = 2.9 Hz), 1.44-1.42 (m, 1H), 1.26-1.07 (m, 2H). ^{13}C NMR ($CDCl_3$, 101 MHz) δ 142.54, 128.50 (2C), 128.44 (2C), 125.87, 66.65, 64.46, 40.03 (2C), 35.99, 31.75, 30.91, 27.24, 26.25.

*3.2.47. 3-(Dimethylamino)-8-phenyloctan-1-ol (**55**)*

Compound **55** was prepared as described for **52** from a mixture of **51** (1.37 g, 4.70 mmol) and $LiAlH_4$ (0.36 g, 9.40 mmol) furnishing the product as a yellow oil (0.975 g, 83%). ^{1}H NMR (CD_3OD, 400 MHz) δ 7.26-7.21 (m, 2H), 7.18-7.11 (m, 3H), 3.65 (ddd, 2H, *J* = 7.3, 5.5, 1.8 Hz), 2.61 (t, 2H, *J* = 7.5 Hz), 2.57-2.49 (m, 1H), 2.23 (s, 6H), 1.74 (sxt, 1H, *J* = 7.5 Hz), 1.64 (t, 2H, *J* = 7.3 Hz), 1.49 (dq, 2H, *J* = 5.5 Hz), 1.39-1.33 (m, 4H). ^{13}C NMR (CD_3OD, 101 MHz) δ 129.55 (2C), 129.41 (2C), 126.80, 64.12, 62.60, 40.65 (2C), 36.99, 33.01, 32.79, 29.87, 28.25, 30.60.

*3.2.48. t-Butyl 4-(6-bromopyridin-3-yl)-1,4-diazepane-1-carboxylate (**59**)*

A solution of **58**[40] (416 mg, 1.50 mmol) in dry MeCN (15 mL) was added NBS (267 mg, 1.50 mmol) and stirred for 1 h at rt. The reaction mixture was evaporated *in vacuo*. Purification by DCVC (DCM:MeOH:NH_3/100:0:0 to 97.5:2.25:0.25) afforded the product as a yellow solid (598 mg, quantitative). ^{1}H NMR ($CDCl_3$, 400 MHz) δ 7.86 (d, 1H, *J* = 3.0 Hz), 7.25 (s, 1H), 6.92-6.86 (m, 1H), 3.48-3.62 (m, 6H), 3.35 (t, 1H, *J* = 5.6 Hz), 3.25 (t, 1H, *J* = 6.0 Hz), 1.99-1.90 (m, 2H), 1.42 (s, 5H), 1.38 (s, 4H). ^{13}C NMR ($CDCl_3$, 101 MHz) δ 177.38; 155.16, 154.75 (rotamers); 142.91, 142.80 (rotamers); 133.86, 133.62 (rotamers); 127.87, 127.78 (rotamers); 121.45; 79.89; 49.94, 49.83 (rotamers); 48.62, 48.01 (rotamers); 46.15, 45.90 (rotamers); 45.84, 45.68 (rotamers); 29.56 (3C); 28.31, 28.26 (rotamers).

*3.2.49. 3-(Dimethylamino)-6-phenyl-6-((tetrahydro-2H-pyran-2-yl)oxy)hexyl methylcarbamate (**60**)* A mixture of **57**[39] (6.12 g, 26.1 mmol) and 3,4-dihydro-2*H*-pyran (4.78 mL, 52.2 mmol) was added a few drops of concentrated aq HCl solution. The reaction mixture was stirred for 2 days at rt. The reaction mixture was added Et_2O (100 mL) and extracted with sat. aq $NaHCO_3$ solution (2 x 50 mL) and H_2O (50 mL). The combined organic phases were dried ($MgSO_4$), filtered, and evaporated in vacuo. The crude product was purified by DCVC (heptane:EtOAc/2:1) giving (*E*)-ethyl 6-phenyl-6-((tetrahydro-2*H*-pyran-2-yl)oxy)hex-2-enoate as a yellow oil (6.85 g, quantitative). (Ethyl 3-(dimethylamino)-6-phenyl-6-((tetrahydro-2*H*-pyran-2-yl)oxy)hexanoate was prepared as described for **48** from a mixture of (*E*)-ethyl 6-phenyl-6-((tetrahydro-2*H*-pyran-2-yl)oxy)hex-2-enoate (6.82 g, 21.4 mmol) and dimethylamine (15.3 mL, 85.7 mmol, 33% in EtOH) yielding the product as a yellow oil (7.68 g, 99%). 3-(Dimethylamino)-6-phenyl-6-((tetrahydro-2*H*-pyran-2-yl)oxy)hexan-1-ol was prepared as described for **52** from a mixture of (ethyl 3-

(dimethylamino)-6-phenyl-6-((tetrahydro-2*H*-pyran-2-yl)oxy)hexanoate (7.68 g, 21.1 mmol) and $LiAlH_4$ (1.60 g, 42.3 mmol) affording the product as a yellow oil (6.48 g, 95%). Compound **60** was prepared as described for **13** from a mixture of 3-(dimethylamino)-6-phenyl-6-((tetrahydro-2*H*-pyran-2-yl)oxy)hexan-1-ol (1.00 g, 3.11 mmol), CDI (0.61 g, 3.73 mmol), and methylamine (2.62 mL, 31.1 mmol, 40% in H_2O) yielding the product as a yellow oil (1.08 g, 92%). ^{1}H NMR ($CDCl_3$, 400 MHz) δ 7.38-7.15 (m, 11H, diastereomers); 4.86-4.81 (m, 1H), 4.66 (ddd, 1H, *J* = 7.7, 5.7, 2.0 Hz) (diastereomers); 4.56 (t, 1H, *J* = 6.4 Hz), 4.40 (t, 1H, *J* = 3.6 Hz) (diastereomers); 4.13-4.01 (m, 4H), 3.94 (dt, 1H, *J* = 11.2, 5.7 Hz) (diastereomers); 3.60-3.45 (m, 2H), 3.32-3.23 (m, 1H) (diastereomers); 2.96-2.83 (m, 12H, diastereomers); 2.52-2.39 (m, 2H, diastereomers); 2.19, 2.18, 2.17, 2.17 (4 s, 3H, diastereomers); 1.95-1.11 (m, 27H, diastereomers). ^{13}C NMR ($CDCl_3$, 101 MHz) δ 142.39, 142.43 (diastereomers); 128.26, 128.04, 127.40, 127.38, 126.95, 126.94, 126.93, 126.45, 126.44 (diastereomers); 97.87, 97.83, 95.29, 95.27 (diastereomers); 78.84, 78.80 (diastereomers); 63.85, 63.82 (diastereomers); 62.92, 62.40, 61.88 (diastereomers); 60.84, 60.80, 60.78 (diastereomers); 40.28, 40.23, 40.21, 40.19 (diastereomers); 35.64, 35.58 (diastereomers); 34.12, 34.07 (diastereomers); 30.76, 30.71 (diastereomers); 28.91, 28.79, 28.69, 28.60 (diastereomers); 26.21, 25.88, 25.55, 25.42, 25.30 (diastereomers); 19.55, 19.19 (diastereomers). LC-MS m/z = 379.1 $[M+H]^+$.

*3.2.50. 3-(Dimethylamino)-6-phenyl-6-((tetrahydro-2H-pyran-2-yl)oxy)hexyl dimethylcarbamate (**61**)*

Compound **61** was prepared as described for **22** from a mixture of 3-(dimethylamino)-6-phenyl-6-((tetrahydro-2*H*-pyran-2-yl)oxy)hexan-1-ol (1.00 g, 3.11 mmol) (described above), CDI (0.61 g, 3.73 mmol), and dimethylamine (3.94 mL, 31.1 mmol, 40% in H_2O) yielding the product as a yellow oil (0.92 g, 75%). ^{1}H NMR ($CDCl_3$, 400 MHz) δ

7.40-7.21 (m, 13H, diastereomers); 7.20-7.09 (m, 2H, diastereomers); 4.88-4.80 (m, 1H), 4.72-4.52 (m, 4H), 4.42-4.35 (m, 1H) (diastereomers); 4.18-4.00 (m, 5H), 3.99-3.84 (m, 1H) (diastereomers); 3.61-3.45 (m, 3H), 3.33-3.23 (m, 1H) (diastereomers); 2.81-2.73 (m, 6H, diastereomers); 2.52-2.38 (m, 2H, diastereomers); 2.19, 2.18 (2s, 3H, diastereomers); 2.16 (s, 6H, diastereomers); 1.96-1.09 (m, 31H, diastereomers). ^{13}C NMR ($CDCl_3$, 101 MHz) δ 129.02, 128.28, 128.21, 128.06, 127.42, 126.99, 126.96, 126.94, 126.52, 126.48, 125.28 (diastereomers); 97.80, 95.43, 95.35, 94.66 (diastereomers); 78.73, 77.23 (diastereomers); 63.37, 62.93, 62.52, 62.44 (diastereomers); 61.93, 61.58 (diastereomers); 60.86, 60.81, 60.68 (diastereomers); 40.34, 40.28, 40.23 (diastereomers); 35.64; 34.07; 30.81, 30.78, 30.70 (diastereomers); 28.97, 28.84, 28.78, 28.68 (diastereomers); 26.04, 25.56 (diastereomers); 25.44,.25.30, 25.00 (diastereomers); 19.81, 19.76, 19.62, 19.58, 19.20, 19.12 (diastereomers). LC-MS m/z = 393.0 $[M+H]^+$.

3.3 Pharmacology

3.3.1. Materials

Culture media, serum, antibiotics and buffers for cell culture were obtained from Invitrogen (Paisley, UK). (*S*)-Nicotine was obtained from Sigma (St. Louis, MO) and [^{3}H]epibatidine from PerkinElmer (Boston, MA). The FLIPR™ Membrane Potential Blue (FMP) dye was purchased from Molecular Devices (Crawley, UK). The HEK293 cell lines stably expressing the rat α3β4 and rat α4β4 were generous gifts from Drs. K. Kellar and Y. Xiao (Georgetown University School of Medicine, Washington DC), and the stable mouse α4β2-HEK293T cell line and the rat α4β2-HEK293 cell line were generously provided by Dr. J.A. Stitzel (University of Colorado, Boulder, CO) and Dr. J.H. Steinbach (Washington University School of Medicine, St. Louis, MO), respectively [47-49].

3.3.2. Cell culture

The tsA201 and HEK293 cells lines were maintained at 37 °C in a humidified 5% CO_2 incubator in culture medium [Dulbecco's Modified Eagle Medium supplemented with penicillin (100 U/ml), streptomycin (100 mg/ml) and 10 % fetal bovine serum]. The culture medium used for the stable HEK293 cell lines expressing rat α4β2, α4β4 and α3β4 nAChRs were supplemented with 1 mg/ml G-418, and the culture medium used for the α4β2-HEK293T cells were supplemented with 0.1 mg/ml zeocin and 0.5 mg/ml hygromycin B.

3.3.3. [^{3}H]Epibatidine Binding

The binding experiments with stable HEK293 cell lines expressing rat α4β2, α3β4 and α4β4 nAChRs were performed essentially as previously described [41]. Briefly, cells were harvested at 80-90 % confluency and scraped into assay buffer [140 mM NaCl/1.5 mM KCl/2 mM $CaCl_2$/1 mM Mg_2SO_4/25 mM HEPES (pH 7.4)], homogenized using a polytron for 10 sec and centrifuged for 20 min at 50.000 × *g*. Cell pellets were resuspended in fresh assay buffer, homogenized and centrifuged at 50.000 × *g* for another 20 min. Then the cell pellet were resuspended in the assay buffer, and the cell membranes were incubated with 10 pM [^{3}H]epibatidine in the presence of various concentrations of compounds in a total assay volume of 2 mL. Nonspecific binding was determined in reactions with 100 mM (*S*)-nicotine. The reactions were incubated for 4 h at room temperature while shaking. Whatman GF/C filters were presoaked for 1 h in a 0.2 % polyethyleneimine solution, and binding was terminated by filtration through these filters using a 48-well cell harvester and washing with 3 × 4 ml ice-cold isotonic NaCl solution. Following this, the filters were dried, 3 ml Opti-Fluor™ (Packard) was added, and the amount of bound radioactivity was determined in a scintillation counter.

The fraction of specifically bound radioligand was always <10% of the total amount of radioligand. The binding experiments were performed in duplicate at least three times for each compound.

3.3.4. The FLIPR Membrane Potential Blue assay

The functional characterization of the compounds at the α3β4-HEK293 and α4β2-HEK293T cell lines in the assay was performed essentially as previously described.[50] The cells were split into poly-D-lysine-coated black 96-well plates with clear bottom (BD Biosciences, Bedford, MA). On the day of the experiment the medium was aspirated, and the cells were washed with 100 µl Krebs buffer (140 mM NaCl/4.7 mM KCl/2.5 mM $CaCl_2$/1.2 mM $MgCl_2$/11 mM HEPES/10 mM D-glucose, pH 7.4). Then 100 µl Krebs buffer supplemented with FMP dye (0.5 mg/ml) was added to the wells (in the antagonist experiments, various concentrations of the antagonists were dissolved in the buffer). After an incubation at 37°C in humidified 5% CO_2 for 30 min, the plate was then assayed in a FlexStation^3 Benchtop Multi-Mode Microplate Reader (Molecular Devices, Sunnyvale, CA) measuring emission at 565 nm [in fluorescence units (FU)] caused by excitation at 525 nm 20 sec before and 70 sec after addition of ligand solution. In the antagonist experiments, EC_{70}-EC_{80} ACh was used as the final agonist concentration. Experiments were performed in duplicate at least three times for each of the receptors.

3.3.5. Data Analysis

Data from the binding experiments were fitted to the equation % Bound = 100% Bound/(1+([L]/IC_{50})^n). Since the concentrations of [^{3}H]epibatidine and [^{3}H]GR65630 used in the binding experiments were lower than the K_D values determined for the radioligands the respective receptors, it was deduced from the Cheng-Prusoff equation

[51] that the K_i values for the compounds were similar to the obtained IC_{50} values. The concentration-response curves for agonists and concentration-inhibition curves for antagonists in the FLIPR Membrane Potential Blue assay were constructed based on the differences in the fluorescence units (△FU) between the maximal fluorescence levels recorded before and after addition of eight different concentrations of the various ligands.

3.3.6. Two-electrode voltage clamp

Whole-cell currents were measured using a two-electrode voltage clamp with a Geneclamp 500B amplifier together with a Powerlab/200 (AD Instruments, Sydney, Australia) and Chart version 3.5 for PC as previously described.[52] In brief, lobes from ovaries of

female adult *Xenopus laevis* were removed and defolliculated to obtain isolated oocytes. Oocytes were injected with a total of ;25 ng of cRNA encoding rat α4 and β2, in the ratios 1:4 and 10:1, respectively, and were then incubated 15–18°C. Recording microelectrodes were filled with 3 M KCl and had resistance between 0.2 and 1 MΩ. Two to 5 days post-injection, oocytes held at −60 mV were used for recording. To prevent the activation of Ca^{2+}-activated chloride currents, oocytes were superfused with calcium-free buffer (115 mM NaCl, 2.5 mM KCl, 1.8 mM $BaCl_2$, 10 mM HEPES, pH 7.4) while recording until a stable base current was reached. Concentration-response curves for **30** were constructed by measuring the peak current responses elicited from a range of agonist concentrations (10 nM – 10 mM). Responses were normalized to the maximum ACh currents (I/Imax) to compare data from different oocytes. Oocytes were washed for 10 min between agonist applications the α4β2 to ensure receptors were not desensitized from the previous agonist application.

3.3.7. SPR biosensor analyses

SPR biosensor interaction experiments were performed on a Biacore T200 apparatus (GE Healthcare, General Electric Co.) as described previously.[27] Briefly, *Ac*-AChBP and *Ls*-AChBP in Acetate 5.0 solution (10mM NaAc, pH 5.0, Biacore AB, Sweden) were immobilized on separate flow channels on a CM5 sensor chip (Series S, GE Healthcare Bio-Sciences AB, Sweden) using the Amine Coupling Kit (Biacore AB, Sweden) to give ~10000 response units (RUs). This step was followed by injection of ethanolamine HCl-NaOH (1M solution, pH 8.5, Biacore AB, Sweden) to give a final immobilization of ~3000 RU for *Ac*-AChBP and ~5000 RU for *Ls*-AChBP. On a separate flow channel, a reference surface was prepared using the same conditions and its signals were subtracted from the other channels during analysis. The signals obtained by blank injections were used to correct analyte curves, and solvent correction curves were recorded to assess solvent effects. Freshly prepared running buffer (phosphate buffered saline (PBS (1X) solution; 5% DMSO; 0.005% Surfactant P20 (GE Healthcare, Bio-Sciences AB) in deionized, filtered and degassed ultrapure water) was used in all experiments and solutions. Compounds were diluted using a 4-fold dilution scheme to six concentrations. Compounds were injected for 60 s and allowed to dissociate for 300 s where after regeneration (10% DMSO in running buffer) and wash (50% DMSO in running buffer) steps were run. Sensorgrams were analyzed with Biacore T200 Evaluation Software v1.0 (GE Healtcare Bio-Sciences AB).

Acknowledgements

We thank Drs. J. Patrick and D. Julius are thanked for providing us with various cDNAs, and Drs. Steinbach, Xiao, Kellar and Stitzel are thanked for their kind gifts of stable nAChR cell lines. Javairia Mian and Stefania C. Ghio are thanked for technical

laboratory assistance. This work was supported by the Lundbeck Foundation, the Carlsberg Foundation and the Novo Nordisk Foundation and the Australian National Health & Medical Research Council (NH&MRC Grant No. APP1069417).

ASSOCIATED CONTENT

Supporting Information. Results from elemental analysis of all target compounds, ^{1}H- and ^{13}C-NMR of representative compounds and co-crystal structures of *Ls*-AChBP with **4** and **6**.

REFERENCES

[1] A.A. Jensen, B. Frølund, T. Liljefors, P. Krogsgaard-Larsen, Neuronal Nicotinic Acetylcholine Receptors: Structural Revelations, Target Identifications, and Therapeutic Inspirations, Journal of medicinal chemistry, 48 (2005) 4705-4745.

[2] D. Kalamida, K. Poulas, V. Avramopoulou, E. Fostieri, G. Lagoumintzis, K. Lazaridis, A. Sideri, M. Zouridakis, S.J. Tzartos, Muscle and Neuronal Nicotinic Acetylcholine Receptors. Structure, Function and Pathogenicity, The FEBS Journal, 274 (2007) 3799-3845.

[3] D. D'Hoedt, D. Bertrand, Nicotinic Acetylcholine Receptors: An Overview on Drug Discovery, Expert Opinion on Therapeutic Targets, 13 (2009) 395-411.

[4] R.M. Eglen, Overview of Muscarinic Receptor Subtypes, Handbook of Experimental Pharmacology, 208 (2012) 3-28.

[5] S. Zappettini, M. Grilli, F. Lagomarsino, A. Cavallero, E. Fedele, M. Marchi, Presynaptic Nicotinic α7 and Non-α7 Receptors Stimulate Endogenous GABA Release from Rat Hippocampal Synaptosomes through Two Mechanisms of Action, PLoS One, 6 (2011) 1-9.

[6] T.S. Rao, L.D. Correa, P. Adams, E.M. Santori, A.I. Sacaan, Pharmacological Characterization of Dopamine, Norepinephrine and Serotonin Release in the Rat Prefrontal Cortex by Neuronal Nicotinic Acetylcholine Receptor Agonists, Brain Research, 990 (2003) 203-208.

[7] K.T. O'Leary, F.M. Leslie, Enhanced Nicotinic Acetylcholine Receptor-Mediated [^{3}H]Norepinephrine Release from Neonatal Rat Hypothalamus, Neuropharmacology, 50 (2006) 81-88.

[8] B.N. Cohen, E.D. Mackey, S.R. Grady, S. McKinney, N.E. Patzlaff, C.R. Wageman, J.M. McIntosh, M.J. Marks, H.A. Lester, R.M. Drenan, Nicotinic Cholinergic Mechanisms Causing Elevated Dopamine Release and Abnormal Locomotor Behavior, Neuroscience, 200 (2012) 31-41.

[9] M.S. D'Souza, A. Markou, Neuronal Mechanisms Underlying Development of Nicotine Dependence: Implications for Novel Smoking-Cessation Treatments, Addiction Science & Clinical Practice, 6 (2011) 4-16.

[10] J.W. Coe, P.R. Brooks, M.G. Vetelino, M.C. Wirtz, E.P. Arnold, J. Huang, S.B. Sands, T.I. Davis, L.A. Lebel, C.B. Fox, A. Shrikhande, J.H. Heym, E. Schaeffer, H. Rollema, Y. Lu, R.S.

Mansbach, L.K. Chambers, C.C. Rovetti, D.W. Schulz, F.D. Tingley, 3rd, B.T. O'Neill, Varenicline: An α4β2 Nicotinic Receptor Partial Agonist for Smoking Cessation, Journal of medicinal chemistry, 48 (2005) 3474-3477.

[11] R. West, W. Zatonski, M. Cedzynska, D. Lewandowska, J. Pazik, P. Aveyard, J. Stapleton, Placebo-Controlled Trial of Cytisine for Smoking Cessation, The New England Journal of Medicine, 365 (2011) 1193-1200.

[12] R. Hurst, H. Rollema, D. Bertrand, Nicotinic Acetylcholine Receptors: From Basic Science to Therapeutics, Pharmacology & Therapeutics, 137 (2013) 22-54.

[13] M.N. Romanelli, P. Gratteri, L. Guandalini, E. Martini, C. Bonaccini, F. Gualtieri, Central Nicotinic Receptors: Structure, Function, Ligands, and Therapeutic Potential, ChemMedChem, 2 (2007) 746-767.

[14] C. Gotti, F. Clementi, Neuronal Nicotinic Receptors: From Structure to Pathology, Progress in Neurobiology, 74 (2004) 363-396.

[15] K. Harpsøe, P.K. Ahring, J.K. Christensen, M.L. Jensen, D. Peters, T. Balle, Unraveling the High- and Low-Sensitivity Agonist Responses of Nicotinic Acetylcholine Receptors, The Journal of Neuroscience, 31 (2011) 10759-10766.

[16] K. Brejc, W.J. van Dijk, R.V. Klaassen, M. Schuurmans, J. van Der Oost, A.B. Smit, T.K. Sixma, Crystal Structure of an ACh-Binding Protein Reveals the Ligand-Binding Domain of Nicotinic Receptors, Nature, 411 (2001) 269-276.

[17] S.B. Hansen, G. Sulzenbacher, T. Huxford, P. Marchot, P. Taylor, Y. Bourne, Structures of *Aplysia* AChBP Complexes with Nicotinic Agonists and Antagonists Reveal Distinctive Binding Interfaces and Conformations, The EMBO Journal, 24 (2005) 3635-3646.

[18] S.B. Hansen, T.T. Talley, Z. Radic, P. Taylor, Structural and Ligand Recognition Characteristics of an Acetylcholine-Binding Protein from *Aplysia californica*, The Journal of biological chemistry, 279 (2004) 24197-24202.

[19] T. McCormack, R.M. Petrovich, K.A. Mercier, E.F. DeRose, M.J. Cuneo, J. Williams, K.L. Johnson, P.W. Lamb, R.E. London, J.L. Yakel, Identification and Functional Characterization of a

Novel Acetylcholine-Binding Protein from the Marine Annelid *Capitella teleta*, Biochemistry, 49 (2010) 2279-2287.

[20] B. Billen, R. Spurny, M. Brams, R. van Elk, S. Valera-Kummer, J.L. Yakel, T. Voets, D. Bertrand, A.B. Smit, C. Ulens, Molecular Actions of Smoking Cessation Drugs at α4β2 Nicotinic Receptors Defined in Crystal Structures of a Homologous Binding Protein, Proceedings of the National Academy of Sciences of the United States of America, 109 (2012) 9173-9178.

[21] N.L. Puskar, X. Xiu, H.A. Lester, D.A. Dougherty, Two Neuronal Nicotinic Acetylcholine Receptors, α4β4 and α7, Show Differential Agonist Binding Modes, The Journal of biological chemistry, 286 (2011) 14618-14627.

[22] RCSB Protein Data Bank - RCSB PDB, in.

[23] H.M. Berman, T. Battistuz, T.N. Bhat, W.F. Bluhm, P.E. Bourne, K. Burkhardt, Z. Feng, G.L. Gilliland, L. Iype, S. Jain, P. Fagan, J. Marvin, D. Padilla, V. Ravichandran, B. Schneider, N. Thanki, H. Weissig, J.D. Westbrook, C. Zardecki, The Protein Data Bank, Acta Crystallographica Section D, 58 (2002) 899-907.

[24] P.H. Celie, S.E. van Rossum-Fikkert, W.J. van Dijk, K. Brejc, A.B. Smit, T.K. Sixma, Nicotine and Carbamylcholine Binding to Nicotinic Acetylcholine Receptors as Studied in AChBP Crystal Structures, Neuron, 41 (2004) 907-914.

[25] Y. Bourne, T.T. Talley, S.B. Hansen, P. Taylor, P. Marchot, Crystal Structure of a Cbtx-AChBP Complex Reveals Essential Interactions Between Snake α-Neurotoxins and Nicotinic Receptors, EMBO Journal, 24 (2005) 1512-1522.

[26] C. Ulens, R.C. Hogg, P.H. Celie, D. Bertrand, V. Tsetlin, A.B. Smit, T.K. Sixma, Structural Determinants of Selective α-Conotoxin Binding to a Nicotinic Acetylcholine Receptor Homolog AChBP, Proceedings of the National Academy of Sciences of the United States of America, 103 (2006) 3615-3620.

[27] E. Edink, P. Rucktooa, K. Retra, A. Akdemir, T. Nahar, O. Zuiderveld, R. van Elk, E. Janssen, P. van Nierop, J. van Muijlwijk-Koezen, A.B. Smit, T.K. Sixma, R. Leurs, I.J. de Esch, Fragment Growing Induces Conformational Changes in Acetylcholine-Binding Protein: A Structural and Thermodynamic Analysis, Journal of the American Chemical Society, 133 (2011) 5363-5371.

[28] J.I. Ambrus, J.I. Halliday, N. Kanizaj, N. Absalom, K. Harpsoe, T. Balle, M. Chebib, M.D. McLeod, Covalent attachment of antagonists to the alpha7 nicotinic acetylcholine receptor: synthesis and reactivity of substituted maleimides, Chemical communications, 48 (2012) 6699-6701.

[29] N.L. Absalom, G. Quek, T.M. Lewis, T. Qudah, I. von Arenstorff, J.I. Ambrus, K. Harpsoe, N. Karim, T. Balle, M.D. McLeod, M. Chebib, Covalent trapping of methyllycaconitine at the alpha4-alpha4 interface of the alpha4beta2 nicotinic acetylcholine receptor: antagonist binding site and mode of receptor inhibition revealed, The Journal of biological chemistry, 288 (2013) 26521-26532.

[30] J. Wu, Q. Liu, K. Yu, J. Hu, Y.-P. Kuo, M. Segerberg, P.A. St John, R.J. Lukas, Roles of Nicotinic Acetylcholine Receptor β Subunits in Function of Human α4-Containing Nicotinic Receptors, The Journal of Physiology, 576 (2006) 103-118.

[31] C.P. Hansen, A.A. Jensen, T. Balle, K. Bitsch-Jensen, M.M. Hassan, T. Liljefors, B. Frølund, Carbamoylcholine Analogs as Nicotinic Acetylcholine Receptor Agonists - Structural Modifications of 3-(Dimethylamino)butyl Dimethylcarbamate (DMABC), Bioorganic & Medicinal Chemistry Letters, 19 (2009) 87-91.

[32] C.P. Hansen, A.A. Jensen, J.K. Christensen, T. Balle, T. Liljefors, B. Frølund, Novel Acetylcholine and Carbamoylcholine Analogues: Development of a Functionally Selective $\alpha_4\beta_2$ Nicotinic Acetylcholine Receptor Agonist, Journal of medicinal chemistry, 51 (2008) 7380-7395.

[33] A.A. Jensen, I. Mikkelsen, B. Frølund, K. Frydenvang, L. Brehm, J.W. Jaroszewski, H. Bräuner-Osborne, E. Falch, P. Krogsgaard-Larsen, Carbamoylcholine Homologs: Synthesis and Pharmacology at Nicotinic Acetylcholine Receptors, European Journal of Pharmacology, 497 (2004) 125-137.

[34] K. Audouze, E.Ø. Nielsen, G.M. Olsen, P. Ahring, T.D. Jørgensen, D. Peters, T. Liljefors, T. Balle, New Ligands with Affinity for the $\alpha_4\beta_2$ Subtype of Nicotinic Acetylcholine Receptors. Synthesis, Receptor Binding, and 3D-QSAR Modeling, Journal of medicinal chemistry, 49 (2006) 3159-3171.

[35] C.A. Ussing, C.P. Hansen, J.G. Petersen, A.A. Jensen, L.A. Rohde, P.K. Ahring, E.Ø. Nielsen, J.S. Kastrup, M. Gajhede, B. Frølund, T. Balle, Synthesis, Pharmacology, and Biostructural

Characterization of Novel $\alpha_4\beta_2$ Nicotinic Acetylcholine Receptor Agonists, Journal of medicinal chemistry, 56 (2013) 940-951.

[36] L.A. Rohde, P.K. Ahring, M.L. Jensen, E.Ø. Nielsen, D. Peters, C. Helgstrand, C. Krintel, K. Harpsøe, M. Gajhede, J.S. Kastrup, T. Balle, Intersubunit Bridge Formation Governs Agonist Efficacy at Nicotinic Acetylcholine α4β2 Receptors: Unique Role of Halogen Bonding Revealed, The Journal of biological chemistry, 287 (2012) 4248-4259.

[37] K. Halligan, V. Nair, A Highly Efficient Procedure for the Oxidation of the 5 '-Position of Adenosine Analogues, Arkivoc, (2006) 101-106.

[38] K. Namba, H. Yamamoto, I. Sasaki, K. Mori, H. Imagawa, M. Nishizawa, $Hg(OTf)_2$-Catalyzed Arylene Cyclization, Organic Letters, 10 (2008) 1767-1770.

[39] A.K. Ghosh, K. Shurrush, S. Kulkarni, Asymmetric Synthesis of *anti*-Aldol Segments via a Nonaldol Route: Synthetic Applications to Statines and (-)-Tetrahydrolipstatin, The Journal of Organic Chemistry, 74 (2009) 4508-4518.

[40] U. Schön, J. Messinger, M. Buckendahl, M.S. Prabhu, A. Konda, An Improved Synthesis of *N*-Aryl and *N*-Heteroaryl Substituted Homopiperazines - From Conventional Thermal Conditions to Scaling-Up Using Microwave Heating, Tetrahedron, 65 (2009) 8125-8131.

[41] A.A. Jensen, I. Mikkelsen, B. Frølund, H. Bräuner-Osborne, E. Falch, P. Krogsgaard-Larsen, Carbamoylcholine Homologs: Novel and Potent Agonists at Neuronal Nicotinic Acetylcholine Receptors, Molecular Pharmacology, 64 (2003) 865-875.

[42] D. Flammia, M. Dukat, M.I. Damaj, B. Martin, R.A. Glennon, Lobeline: structure-affinity investigation of nicotinic acetylcholinergic receptor binding, Journal of medicinal chemistry, 42 (1999) 3726-3731.

[43] P. Tosco, P.K. Ahring, T. Dyhring, D. Peters, K. Harpsoe, T. Liljefors, T. Balle, Complementary three-dimensional quantitative structure-activity relationship modeling of binding affinity and functional potency: a study on alpha4beta2 nicotinic ligands, Journal of medicinal chemistry, 52 (2009) 2311-2316.

[44] R.A. Friesner, J.L. Banks, R.B. Murphy, T.A. Halgren, J.J. Klicic, D.T. Mainz, M.P. Repasky, E.H. Knoll, M. Shelley, J.K. Perry, D.E. Shaw, P. Francis, P.S. Shenkin, Glide: A New Approach

for Rapid, Accurate Docking and Scoring. 1. Method and Assessment of Docking Accuracy, Journal of medicinal chemistry, 47 (2004) 1739-1749.

[45] J.F. O'Connell, J. Parquette, W.E. Yelle, W. Wang, H. Rapoport, Convenient Synthesis of Methyl 1-Methyl-2,4-dibromo-5-imidazolecarboxylate, Synthesis, 1988 (1988) 767-771.

[46] J.R. Davies, P.D. Kane, C.J. Moody, The Diazo Route to Diazonamide A. Studies on the Indole Bis-Oxazole Fragment, The Journal of Organic Chemistry, 70 (2005) 7305-7316.

[47] Y. Xiao, E.L. Meyer, J.M. Thompson, A. Surin, J. Wroblewski, K.J. Kellar, Rat α3/β4 Subtype of Neuronal Nicotinic Acetylcholine Receptor Stably Expressed in a Transfected Cell Line: Pharmacology of Ligand Binding and Function, Molecular Pharmacology, 54 (1998) 322-333.

[48] K. Sabey, K. Paradiso, J. Zhang, J.H. Steinbach, Ligand Binding and Activation of Rat Nicotinic a4b2 Receptors Stably Expressed in HEK293 Cells, Molecular Pharmacology, 55 (1999) 58-66.

[49] M.S. Karadsheh, M.S. Shah, X. Tang, R.L. Macdonald, J.A. Stitzel, Functional Characterization of Mouse α4β2 Nicotinic Acetylcholine Receptors Stably Expressed in HEK293T Cells, Journal of Neurochemistry, 91 (2004) 1138-1150.

[50] C.J. Armishaw, N. Singh, J.L. Medina-Franco, R.J. Clark, K.C. Scott, R.A. Houghten, A.A. Jensen, A Synthetic Combinatorial Strategy for Developing α-Conotoxin Analogs as Potent α7 Nicotinic Acetylcholine Receptor Antagonists, The Journal of biological chemistry, 285 (2010) 1809-1821.

[51] D.A. Craig, The Cheng-Prusoff Relationship: Something Lost in the Translation, Trends in Pharmacological Sciences, 14 (1993) 89-91.

[52] G.X.J. Quek, D. Lin, J.I. Halliday, N. Absalom, J.I. Ambrus, A.J. Thompson, M. Lochner, S.C.R. Lummis, M.D. McLeod, M. Chebib, Identifying the Binding Site of Novel Methyllycaconitine (MLA) Analogs at α4β2 Nicotinic Acetylcholine Receptors, ACS Chemical Neuroscience, 1 (2010) 796-809.

Abbreviations

Ac, *Aplysia californica*; ACh, acetylcholine; AChBP, acetylcholine binding protein; CNS, central nervous system; CDI, 1,1'-carbonyldiimidazole; *Ct*, *Capitella teleta*; DMABC, 3-(dimethylamino)butyl dimethylcarbamate; *Ls*, *Lymnaea stagnalis*; mAChRs, muscarinic acetylcholine receptors; nAChRs, nicotinic acetylcholine receptors; PNS, peripheral nervous system; SARs, structure-activity relationships; SPR, surface plasmon resonance; THP, tetrahydropyranyl; DCVC, dry column vacuum chromatography; FLIPR, fluorescent imaging plate reader; FMP, FLIPR membrane potential; FCC, flash chromatography; TEVC, two-electrode-voltage-clamp.

Figure 1. Chemical structures of ACh (**1**), Lobeline (**2**), **3**–**6** and general structures of the novel analogs of **4** (**7**–**27**) and **6** (**28–36)**. (1 column)

Figure 2. AChBP co-crystal structures with (*S*)-nicotine and elongated ligands **2** and **3** displayed with a calculated molecular interaction field (*upper row*) and surfaces (*lower row*) to illustrate size and shape of the cavities. A) and D) *Ls*-AChBP co-crystallised with (*S*)-nicotine (green carbons) [24]; B) and E) *Ac*-AChBP co-crystallised with **2** (orange carbons) [17]; C) and F) *Ac*-AChBP co-crystallised with **3** (deep purple carbons) [27]. Residues constituting the aromatic box are shown as sticks. Molecular interaction fields (C3 probe) is shown as a grey mesh contoured at -1 kcal/mol. Surface representation is shown in grey. Residues are named in accordance with Dougherty *et al* [21] and the amino acid numbering for *Ls*-AChBP (1UW6), *Ac*-AChBP (2BYS), *Ac*-AChBP (2Y58) and α4β2 (according to Harpsøe *et al* [15]) corresponds to TyrA1: 185/188/186/223, TyrA2: 192/195/193/230, TrpB: 143/147/145/182, TyrC: 89/93/91/126 and Trp/TyrD: 53/55/53/82 respectively. (2 columns)

Figure 3. Overlay of co-crystal structures of agonists **4** and **6** on co-crystal structures with elongated ligands **2** and **3.** Overlay of X-ray structures with A) **4** (grey carbons, PDB: 3ZDG) and **2** (orange carbons, PDB: 2BYS). The overlay indicates that introduction of substituents on the amine of **4** could lead to analogs that would address the same cavity as **2**. B) Overlay of **4** and **3** (deep purple carbons, PDB: 2Y58). The overlay indicates that introduction of substituents in the C-3-position of **4** could lead to analogs that would protrude along the interfacial cleft. C) Overlay of **6** (cyan carbons, PDB: 3U8J) and **2**; D) **6** and **3**. The overlays in C and D indicate that introduction of substituents on the N-4 of the 1,4-diazepane ring of **6** potentially could address both cavities. *Ls*-AChBP structures are shown in slate/wheat and *Ac*-AChBP in cyan/olive for the principal and complementary subunit, respectively. (1.5 column)

Figure 4. Presentation of suggested binding mode of (*R*)-**15** (A) and **32** (B) docked into a homology model of the α4β2 nAChR.. A) (*R*)-**15** (light magenta carbons) docked into the model; B) **32** (green carbons) docked into the model. Residues surrounding the ligand binding site from the principal side (density carbons) and complementary side (orange carbons) are shown. Molecular interaction (C3 probe) is shown at an isocontour level of -1 kcal/mol. Residue naming is according to Dougherty *et al.*[21] and the amino acid numbering for α4β2 (according to Harpsøe *et al.*[15]) corresponds to TyrA1: 223, TyrA2: 230, TrpB: 182, TyrC126 and Trp/TyrD: 82. (1.5 column)

Figure 5. Agonist-evoked responses for compound **30** at α4β2 nAChRs expressed in *Xenopus laevis* oocyte measured by two-electrode voltage-clamp electrophysiology. To yield uniform populations of receptors in $(\alpha4)_2(\beta2)_3$ (●) and $(\alpha4)_3(\beta2)_2$ (■) stichiometries, oocytes were injected with α4 and β2 cRNA in a 1:4 and 10:1, respectively. Peak current amplitudes were recorded,

background subtracted and normalized to the amplitude evoked by300 μM at $(\alpha4)_2(\beta2)_3$ and 1 mM ACh at $(\alpha4)_3(\beta2)_2$ (ACh_control) on the same oocyte. Calculated percentage activation were depicted as a function of the concentration ± S.E. and fitted to a monophasic Hill equation. Data points are from n = 3-6 oocytes. Regression results are presented in Table 4. (1 column)

Scheme 1. Synthesis of *N*-arylalkyl analogs of **4** (**7**-**12**). (a) methyl acetoacetate, AcOH, toluene, rt; (b) sodium, *i*-PrOH, THF, 0 °C then rt; (c) (1) CDI, toluene, rt, (2) THF, rt, (3) **9** and **10**: CH_3NH_2 (40% in H_2O), **37**: $(CH_3)_2NH$ (33% in EtOH), rt; (d) Pd/C (5% (w/w)), H_2, AcOH, rt; (e) **7**: 2-benzyloxirane, **11**: styrene oxide, $LiClO_4$, MeCN, reflux; (f) 3-phenylpropionaldehyde, $NaBH_3CN$, DCE, MeOH, rt.

Scheme 2. Synthesis of C-3-arylalkyl analogs of **4** (**13**–**15**, **22**–**25**, **27**) (a) $NH(CH_3)_2$ (33% in EtOH); (b) $LiAlH_4$, Et_2O, 0 °C then rt; (c) (1) CDI, toluene, rt, (2) THF, rt, (3) **22**-**25**: NH_2CH_3 (40% in H_2O), **13**-**15**: $NH(CH_3)_2$ (33% in EtOH), rt; (d) (1) NaH (60% in mineral oil), 2,4,5-tribromo-1-methyl-1*H*-imidazole, THF, reflux, (2) *n*-BuLi, THF, -78 °C, (3) H_2O, -78 °C. (1 column)

Scheme 3. Synthesis of C-3-arylalkyl analogs of **4** (**16**–**21**, **26**) (a) **17**: iodobenzene, **18**: 1-fluoro-4-iodo-benzene, CuI, 3,4,7,8-tetramethyl-1,10-phenanthroline, Cs_2CO_3, toluene, reflux; (b) (1) NaH (60% in mineral oil), DMF, 0 °C, (2) **19**: 2-fluoropyridine, **20**: benzylbromide, **21**: 2-bromothiazole, rt; (c) $NH(CH_3)_2$ (33% in EtOH); (d) 3,4-dihydro-2*H*-pyran, concentrated HCl, rt; (e) $LiAlH_4$, Et_2O, 0 °C then rt; (f) (1) CDI, toluene, rt, (2) THF, rt, (3) **22**-**25**: NH_2CH_3 (40% in H_2O), **13**-**15**: $NH(CH_3)_2$ (33% in EtOH), rt; (g) *p*-toluenesulfonic acid monohydrate, MeOH, rt. (1 column)

Scheme 4. Synthesis of *N*-arylalkyl 3-pyridyl diazacycle analogs **28**–**36**. (a) NBS, MeCN, rt; (b) TFA, DCM, rt; (c) **28**, **32**, and **36**: hydrocinnamaldehyde, **30** and **34**: benzaldehyde, **31** and **35**: phenylacetaldehyde, **33**: 2-(3-bromophenyl)acetaldehyde, **29**: cinnamaldehyde, $NaBH(OAc)_3$, DCE, rt. (1 column)

Table 1. Binding characteristics of **7**–**27** and reference compounds **1, 2, 4** and **5** to rat α4β2, α4β4, and α3β4 nAChRs stably expressed in HEK293 cells in a [^{3}H]-epibatidine binding assay.[a] (2 columns)

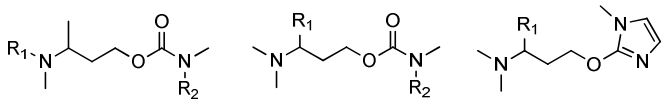

7-12 13-26 27

			Competition binding,[b] K_i (μM)						Competition binding,[b] K_i (μM)		
Compd	R_1	R_2	α4β2	α4β4	α3β4	Compd	R_1	R_2	α4β2	α4β4	α3β4
1[c]	-	-	0.033 [7.48 ± 0.11]	0.058 [7.24 ± 0.12]	0.62 [6.21 ± 0.08]	**16**	3-hydroxy-3-phenylpropyl	methyl	~30 [~4.5]	6.7 [5.17 ± 0.03]	5.9 [5.22 ± 0.06]
2[c]	-	-	0.0022 [8.7 ± 0.22]	0.12 [6.9 ± 0.21]	0.48 [6.3 ± 0.13]	**17**	phenoxymethyl	methyl	~100 [~4.0]	~100 [~4.0]	~300 [~3.5]
4[d]	-	-	0.020 [7.70 ± 0.04]	0.15 [6.82 ± 0.04]	0.42 [6.38 ± 0.06]	**18**	4-fluorophenoxy-methyl	methyl	~500 [~3.3]	~100 [~4.0]	~300 [~3.5]
5[c]	-	-	0.013 [7.89 ± 0.21]	2.6 [5.58 ± 0.08]	10 [4.98 ± 0.07]	**19**	pyridin-2-yloxymethyl	methyl	~100 [~4.0]	~300 [~3.5]	~300 [~3.5]
7	2-hydroxy-3-phenylpropyl	methyl	~500 [~3.3]	~100 [~4.0]	>1000 [<3.0]	**20**	Benzyloxy-methyl	methyl	~30 [~4.5]	~100 [~4.0]	~300 [~3.5]
8	phenylpropyl	methyl	~300 [~3.5]	>1000 [<3.0]	>1000 [<3.0]	**21**	thiazole-2-yloxymethyl	methyl	~30 [~4.5]	~300 [~3.5]	~300 [~3.5]
9	benzyl	H	~300 [~3.5]	~300 [~3.5]	~300 [~3.5]	**22**	phenethyl	H	7.1 [5.2 ± 0.1]	~100 [~4.0]	~100 [~4.0]
10	phenethyl	H	~30 [~4.5]	~300 [~3.5]	~300 [~3.5]	**23**	phenylpropyl	H	11 [4.95 ±	~30 [~4.5]	~100 [~4.0]

11	2-hydroxy-2-phenylethyl	H	~300 [~3.5]	~300 [~3.5]	~1000 [~3.0]	**24**	phenylbutyl	H	0.01] 3.6 [5.45 ± 0.03]	~30 [~4.5]	~100 [~4.0]
12	phenylpropyl	H	~50 [~4.3]	>1000 [<3.0]	>1000 [<3.0]	**25**	phenylpentyl	H	2.7 [5.6 ± 0.1]	4.5 [5.3 ± 0.1]	~50 [~4.3]
13	phenylpropyl	methyl	1.9 [5.73 ± 0.07]	4.9 [5.31 ± 0.07]	13 [4.88 ± 0.09]	**26**	3-hydroxy-3-phenypropyl	H	~100 [~4.0]	~100 [~4.0]	>300 [<3.5]
14	phenylbutyl	methyl	1.1 [5.96 ± 0.04]	4.4 [5.36 ± 0.04]	11 [4.97 ± 0.07]	**27**	phenylbutyl	-	0.76 [6.12 ± 0.03]	3.7 [5.43 ± 0.06]	8.3 [5.08 ± 0.05]
15	phenylpentyl	methyl	0.90 [6.04 ±0.11]	0.65 [6.18 ± 0.04]	6.9 [5.16 ± 0.10]						

[a]Binding affinities are given as K_i in µM with pK_i ± SEM values in brackets based on three experiments for each compound. [b]K_i values were determined in a [^{3}H]epibatidine binding assay with HEK293 cells stably expressing rat α4β2, α4β4, and α3β4 as previously described.[32] [c]Binding data from Jensen *et al*.[41] [d]Binding data from Hansen *et al*.[31] [e]Binding data from Rohde *et al*.[36]

Table 2. Binding characteristics of **28**–**36** and reference compound **6** to rat α4β2, α4β4, and α3β4 nAChRs stably expressed in HEK293 cells in a [^{3}H]-epibatidine binding assay.[a] (1 column)

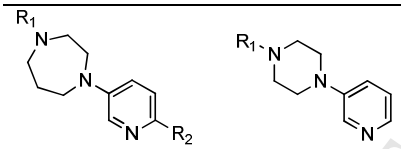

28-33

34-36

			Competition binding,[b] K_i (µM)			Selectivity ratio
Compd	R_1	R_2	α4β2	α4β4	α3β4	α3β4/α4β2
6[e]	-	-	0.00072 [9.14 ± 0.09]	n.d.	n.d.	
28	phenylpropyl	Br	0.82 [6.08 ± 0.07]	1.5 [5.82 ± 0.05]	2.2 [5.66 ± 0.02]	3
29	cinnamyl	H	0.099 [7.00 ± 0.12]	1.6 [5.79 ± 0.13]	2.9 [5.53 ± 0.07]	29
30	benzyl	H	0.104 [6.98 ± 0.06]	3.4 [5.47 ± 0.03]	2.6 [5.59 ± 0.03]	25
31	phenethyl	H	0.11 [6.98 ± 0.03]	2.4 [5.63 ± 0.05]	3.4 [5.47 ± 0.03]	31
32	phenylpropyl	H	0.082 [7.09 ± 0.02]	3.8 [5.42 ± 0.07]	3.8 [5.42 ± 0.07]	46
33	(3-bromo-phenyl)ethyl	H	0.13 [6.88 ± 0.06]	1.9 [5.72 ± 0.05]	0.78 [6.11 ± 0.05]	6

34	benzyl	-	9.6 [5.02 ± 0.02]	~100 [~4.0]	>300 [<3.5]	>31
35	phenethyl	-	0.56 [6.25 ± 0.02]	8.9 [5.05 ± 0.05]	8.2 [5.08 ± 0.04]	15
36	phenylpropyl	-	0.49 [6.30 ± 0.09]	3.5 [5.46 ± 0.06]	~20 [~4.7]	~41

[a]Binding affinities are given as K_i in µM with pK_i ± SEM values in brackets based on three experiments for each compound. [b]K_i values were determined in a [^{3}H]epibatidine binding assay with HEK293 cells stably expressing rat α4β2, α4β4, and α3β4 as previously described.[32] [c]Binding data from Jensen *et al*.[41] [d]Binding data from Hansen *et al*.[31] [e]Binding data from Rohde *et al*.[36]

Table 3. Functional properties of target compounds **13-15**, **23-25**, **27**, **29**, **35**, and **36** at mouse α4β2-HEK293T and rat α3β4-HEK293 HEK293 cell lines in the FLIPR Membrane Potential Blue assay. (1 column)

	α4β2[a]		α3β4[a]	
Compound	EC_{50} (µM) [pEC_{50}±S.E.M.]	IC_{50} (µM) [pIC_{50}±S.E.M.]	EC_{50} (µM) [pEC_{50}±S.E.M.]	IC_{50} (µM) [pIC_{50}±S.E.M.]
13	Agonist[b]	-	Agonist[c]	-
14	Agonist[b]	-	Agonist[c]	-
15	Agonist[d]	-	Agonist[e]	-
23	Agonist[b]	-	Agonist[c]	-
24	Agonist[b]	-	Agonist[c]	-
27	Agonist[d]	-	Agonist[e]	-
29	-	1.1 [5.96 ± 0.09]	-	Weak antagonist[f]
35	Agonist[g]	-	Agonist[g]	-
36	Agonist[e]	-	Agonist[c]	-

[a]EC_{50} and IC_{50} values are given in µM with pEC_{50} ± SEM and pIC_{50} ± SEM values in brackets. The data are the means of three individual experiments performed in duplicate. [b,c,d,e,f]Complete concentration-response or concentration-

inhibitions curves could not be obtained for the compounds in the tested concentration ranges. [b] The compound elicited a significant agonist response at 100 µM and higher concentrations. [c] The compound elicited a significant agonist response at 300 µM. [d] The compound elicited a significant agonist response at concentrations of 30 µM and higher. [e] The compound elicited a significant agonist response at concentrations of 100 µM and higher. [f] The compound exhibited antagonist activity at concentrations of 100 µM and higher.

Table 4. Functional activity of **30** in two-electrode voltage clamp at $(\alpha4)_2(\beta2)_3$ and $(\alpha4)_3(\beta2)_2$ nAChRs expressed in *Xenopus* oocytes.[a] (1 column)

	Activity $(\alpha4)_2(\beta2)_3$		Activity $(\alpha4)_3(\beta2)_2$	
Compound	EC_{50} (µM) [pEC_{50} ± SEM]	R_{max}	EC_{50} (µM) [pEC_{50} ± SEM]	R_{max}
30	1.8 [5.75 ± 0.07]	16±0.8	7.9 [5.1 ± 0.20]	6 ± 0.7

[a]The $(\alpha4)_2(\beta2)_3$ receptors were expressed by a 1:4 ratio of α:β. The $(\alpha4)_3(\beta2)_2$ receptors were expressed by a 10:1 ratio of α:β.

Table 5. Dissociation constants of **30** and **32** and reference compounds (*S*)-nicotine and **2**.[a] (1 column)

	K_D (µM)[a]		K_i (µM)[b]
Compound	*Ls*-AChBP	*Ac*-AChBP	α4β2
(*S*)-Nicotine	0.32 [6.5 ± 0.2]	3.16 [5.5 ± 0.1]	0.0076 [8.12 ± 0.05][c]
2	0.63 [6.2 ± 0.1]	0.013 [7.9 ± 0.1]	0.0050 [8.3 ± 0.1][d]
30	0.16 [6.8 ± 0.1]	>1.0 [<6][e]	0.104 [6.98 ± 0.06]

32	0.020 [7.7 ± 0.1]	>1.0 [<6][e]	0.082 [7.09 ± 0.02]

[a]SPR binding affinity values for *Ls*- and *Ac*-AChBP represented as K_D (μM) with pK_D ± SEM values shown in brackets, determined by steady-state affinity analysis as previously described.[27] [b]Receptor binding affinity values for α4β2 represented as K_i (μM) with pK_i ± SEM values shown in brackets, determined in a [^{3}H]epibatidine binding assay with HEK293 cells stably expressing rat α4β2 as previously described.[32] [c]Data from Ussing *et al*.[35] [d]Data from Edink *et al*.[27] [e]Binding isotherm did not reach plateau within the tested range.

Figure 1

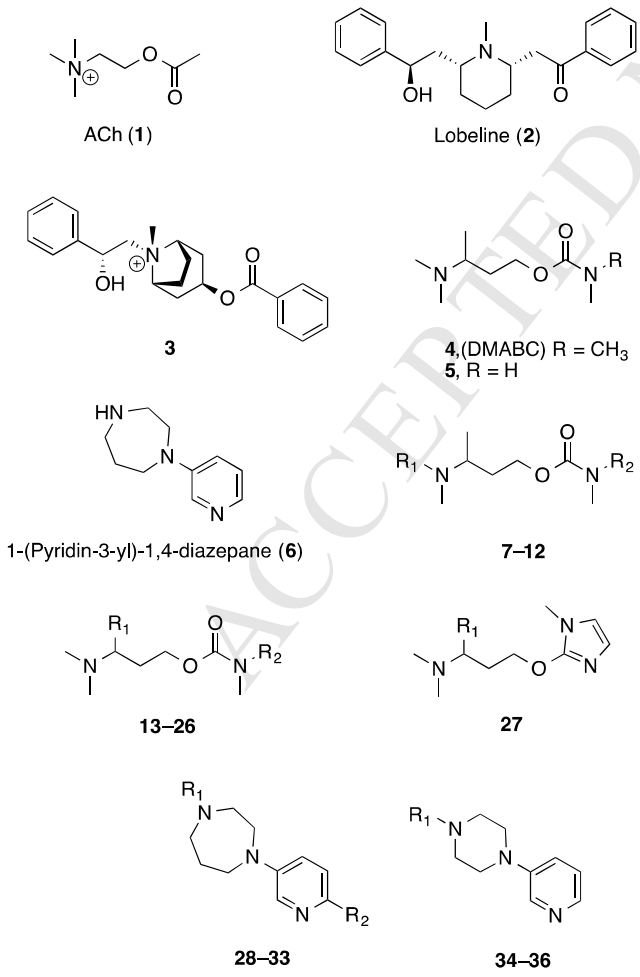

Figure 2

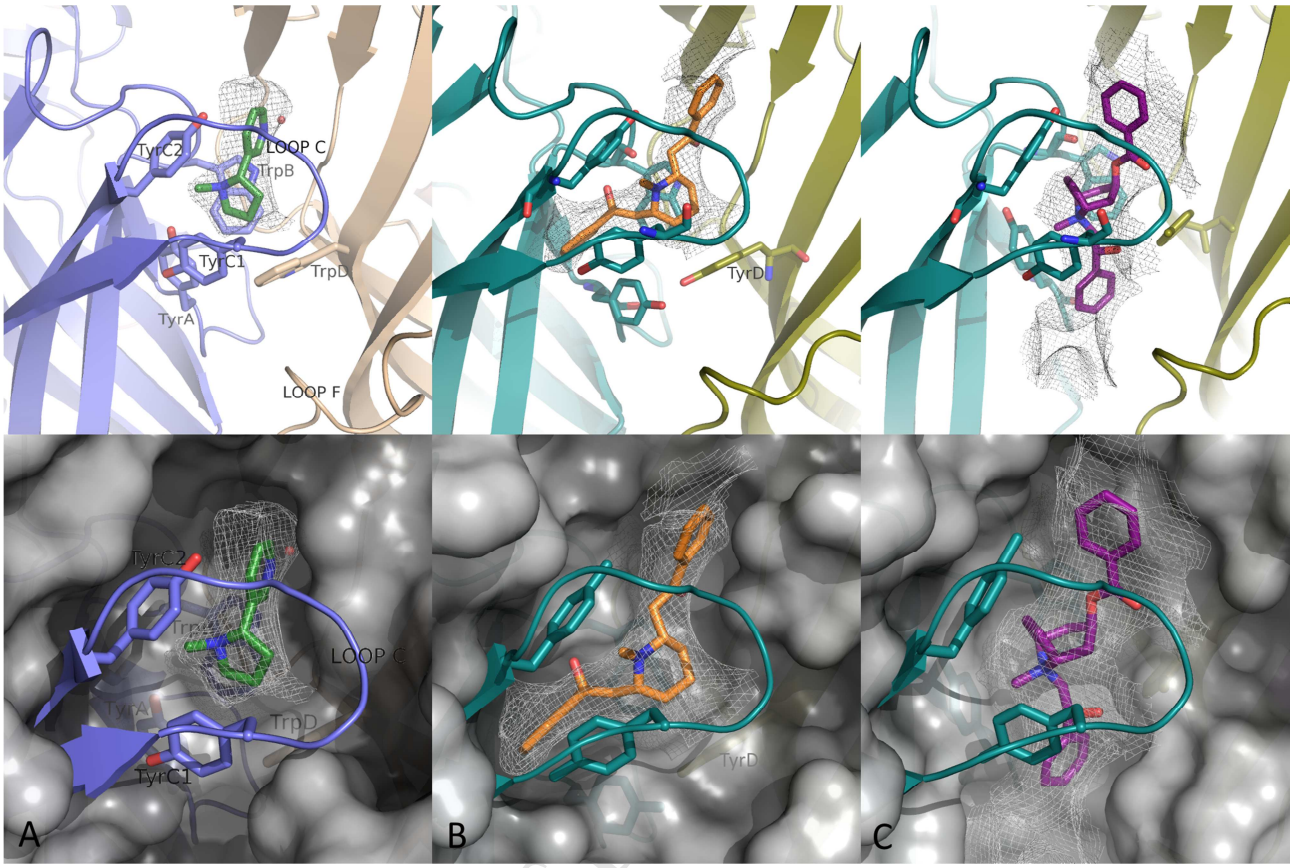

Figure 3

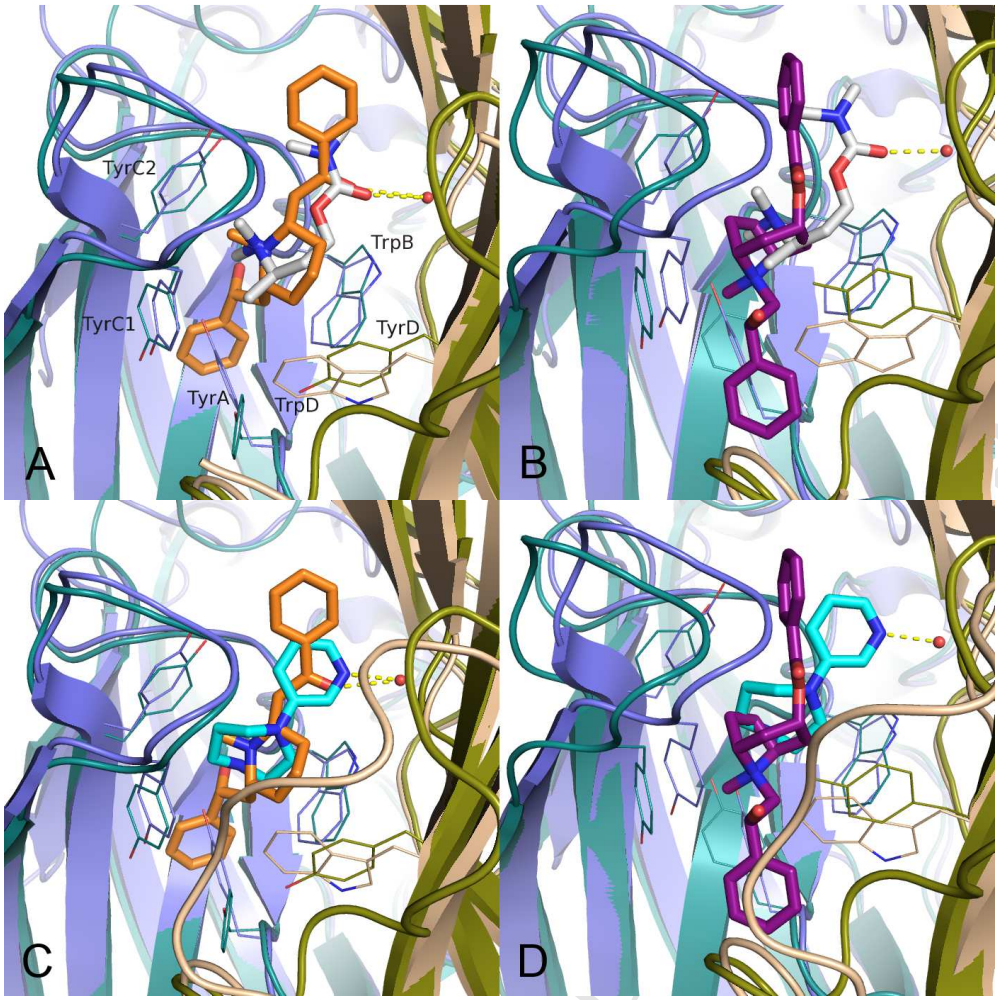

Figure 4

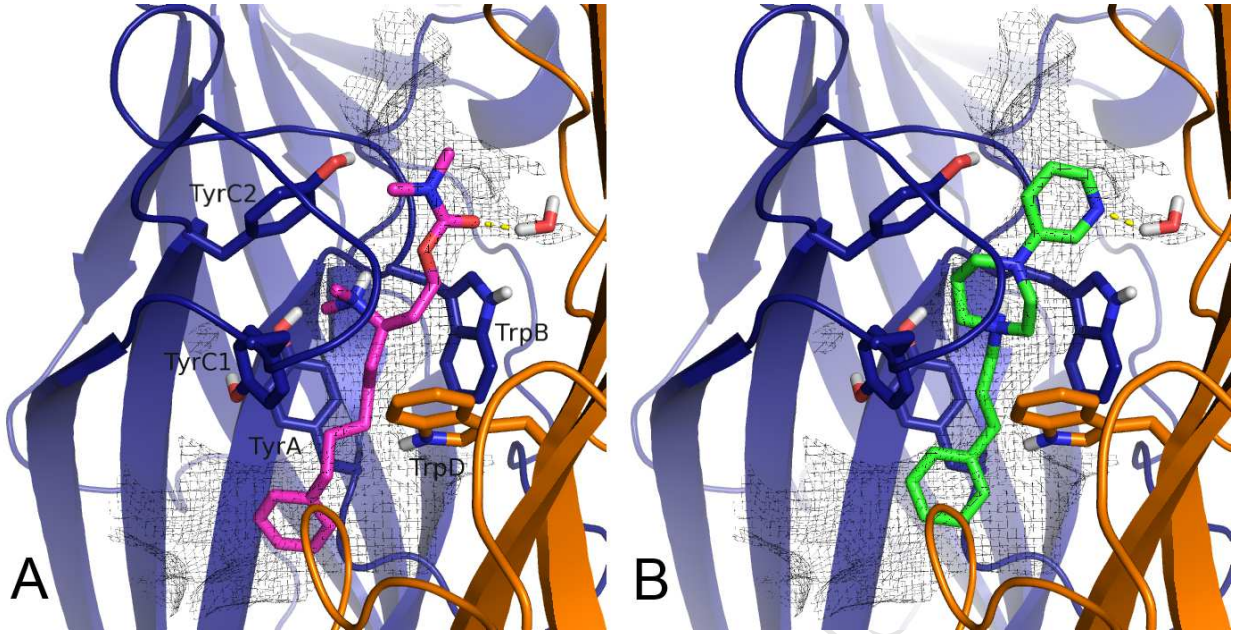
TyrC2
TrpB
TyrC1
TyrA
TrpD
A
B

Figure 5

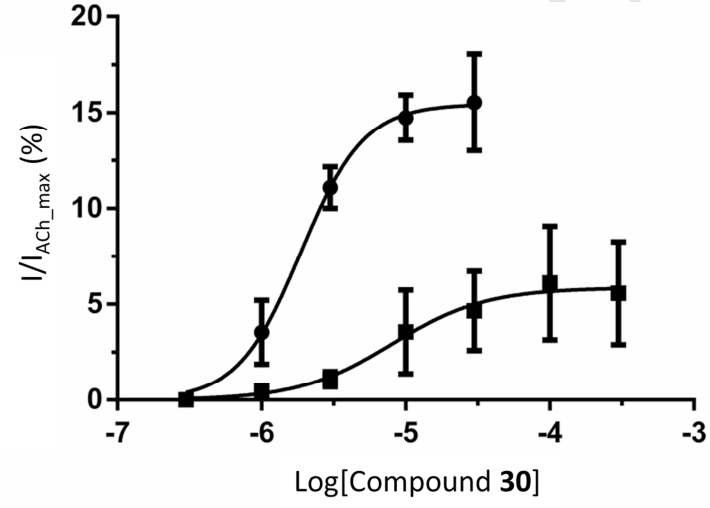
20
15
10
5
0
-7
-6
-5
-4
-3
I/I_ACh_max (%)
Log[Compound 30]

Scheme 1

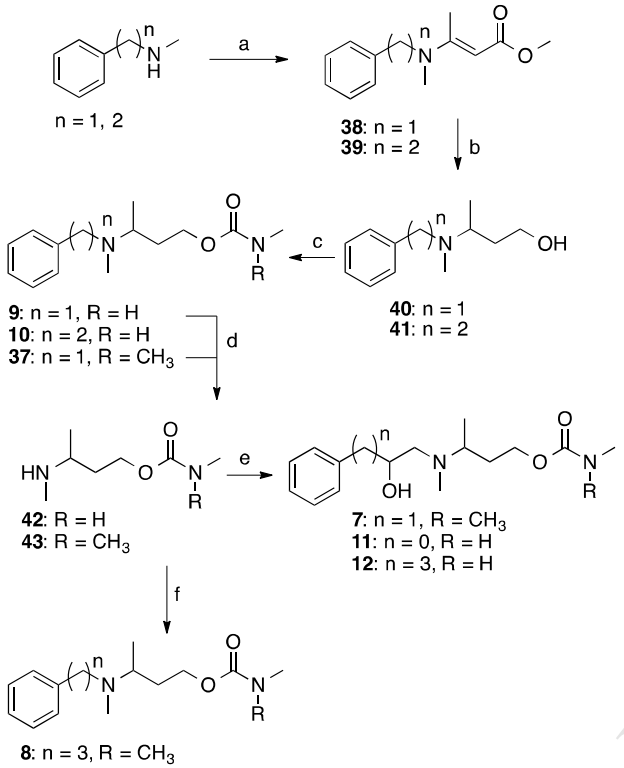

Scheme 2

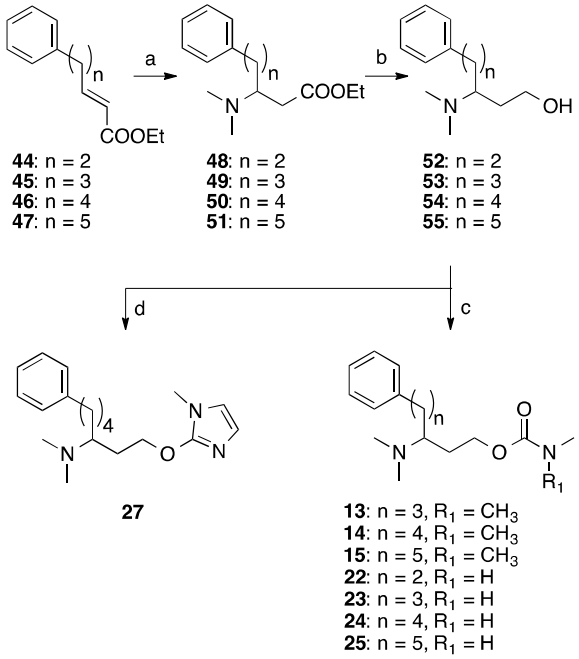

Scheme 3

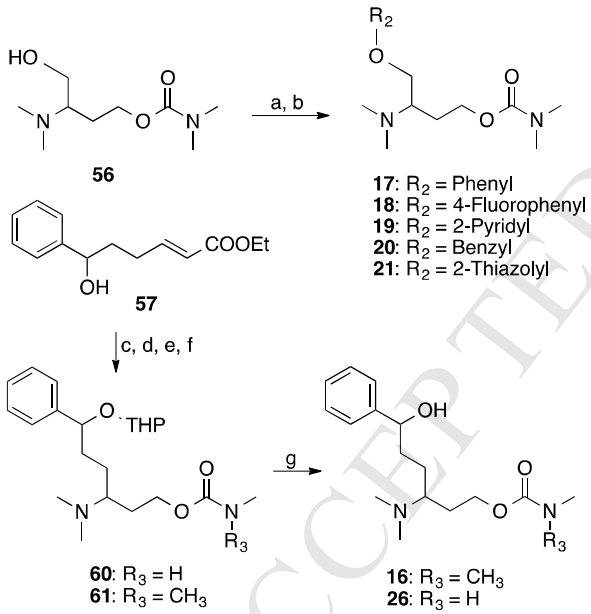

Scheme 4

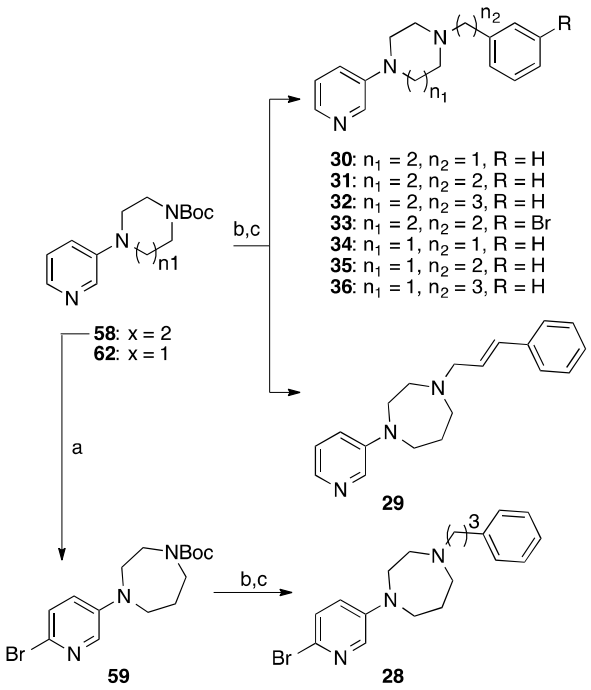

Highlights:

- Elongated α4β2 nAChR ligands have retained partial agonist profile
- SAR indicate classical binding mode for the core agonist part of the molecule
- Substituents bind along the subunit interface
- Ligands showing preference for *Ls*-AChBP over *Ac*-AChBP

Supporting Information

Exploration of the Molecular Architecture of the Orthosteric Binding Site in the α4β2 Nicotinic Acetylcholine Receptor with Analogs of 3-(Dimethylamino)butyl Dimethylcarbamate (DMABC) and 1-(Pyridin-3-yl)-1,4-diazepane

Tinna B. Bach,[#] Anders A. Jensen,[#] Jette G. Petersen,[#] Troels E. Sørensen,[#,†] Serena Della Volpe,[#] Jun Liu,[†] Antoni R. Blaazer,[º] Jacqueline E. van Muijlwijk-Koezen,[º] Thomas Balle,[†,] and Bente Frølund[#,]**

[#]Department of Drug Design and Pharmacology, Faculty of Health and Medical Sciences, University of Copenhagen, Universitetsparken 2, DK-2100 Copenhagen, Denmark

[†]Faculty of Pharmacy, The University of Sydney, Sydney, NSW 2006, Australia

ºDivision of Medicinal Chemistry, Amsterdam Institute for Molecules, Medicines and Systems, Faculty of Sciences, VU University Amsterdam, De Boelelaan 1105, 1081 HV Amsterdam, The Netherlands

Table of Contents

Figure S1. Co-crystal structures of *Ls*-AChBP with **4**[1] and **6**[2].[a]

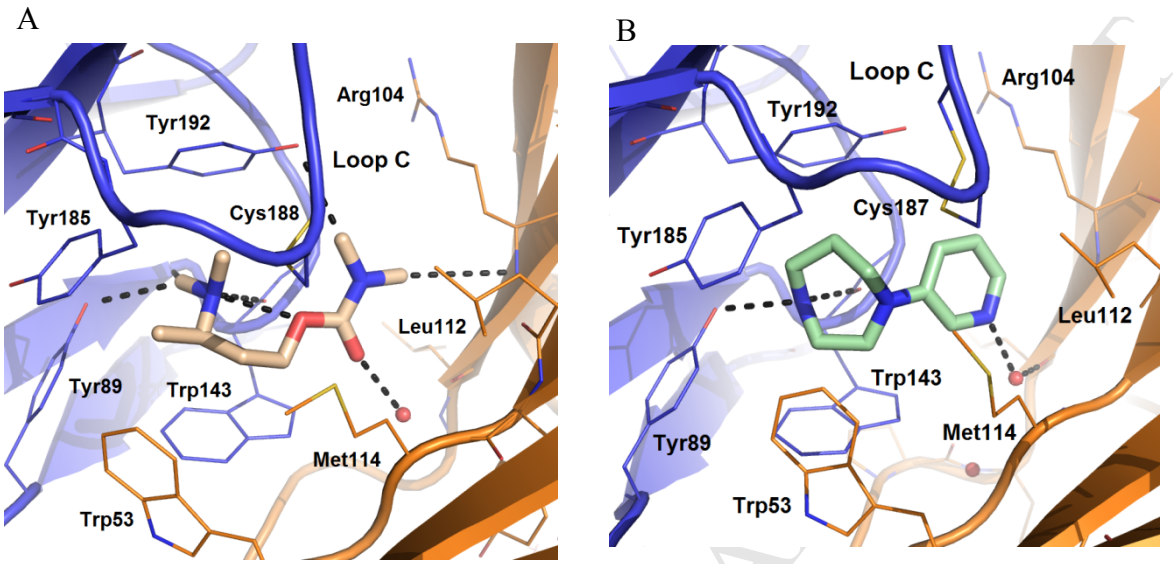

[a]Residues at the principal and complementary side are colored blue and orange, respectively. Dashed lines indicate short contact distances (< 3.5 Å) representing ionic or electrostatic interactions between ligands and the protein or a water molecule (red sphere). A) **4** (wheat carbons) in complex with *Ls*-AChBP. A polarised hydrogen on one of the methyl groups on the protonated nitrogen forms a direct interaction to Tyr89. B) **6** (pale green) in complex with *Ls*-AChBP. **6** forms a direct hydrogen bond to Tyr89.

Elemental analysis data

Compound		**Elemental analysis calculated (found)**			**Deviation**
		C	H	N	
7	$C_{17}H_{27}N_2O_3 \cdot C_2H_2O_4$	57.42 (57.14)	7.35 (7.66)	7.05 (6.97)	<0.4

8	$C_{17}H_{28}N_2O_2 \cdot C_2H_2O_4$	59.67 (59.55)	7.91 (7.56)	7.32 (7.32)	<0.4
9	$C_{14}H_{22}N_2O_2 \cdot C_2H_2O_4$	56.46 (56.49)	7.11 (6.98)	8.23 (8.13)	<0.4
10	$C_{15}H_{24}N_2O_2 \cdot C_2H_2O_4$	57.61 (57.28)	7.39 (7.26)	7.90 (8.02)	<0.4
11	$C_{15}H_{24}N_2O_3 \cdot 1.1C_2H_2O_4$	54.45 (54.26)	6.96 (6.92)	7.38 (7.08)	<0.4
12	$C_{16}H_{26}N_2O_2 \cdot 1.1C_2H_2O_4$	57.92 (57.62)	7.53 (6.98)	7.42 (7.94)	0.55
13	$C_{17}H_{28}N_2O_2 \cdot C_2H_2O_4$	59.67 (59.68)	7.91 (7.72)	7.32 (7.37)	<0.4
14	$C_{18}H_{30}N_2O_2 \cdot C_2H_2O_4$	60.59 (60.53)	8.14 (7.92)	7.07 (7.06)	<0.4
15	$C_{19}H_{32}N_2O_2 \cdot C_2H_2O_4 \cdot 0.1H_2O$	61.17 (60.92)	8.36 (8.11)	6.79 (6.88)	<0.4
16	$C_{17}H_{28}N_2O_3 \cdot C_2H_2O_4$	57.27 (57.15)	7.59 (7.38)	7.03 (7.03)	<0.4
17	$C_{15}H_{24}N_2O_3 \cdot C_2H_2O_4$	55.13 (54.86)	7.08 (6.78)	7.56 (7.28)	<0.4
18	$C_{15}H_{23}FN_2O_3 \cdot C_2H_2O_4$	52.57	6.49	7.21	<0.4

		(52.40)	(6.59)	(7.11)	
19	$C_{14}H_{23}N_3O_3 \cdot 1.1C_2H_2O_4$	51.15 (51.08)	6.68 (6.79)	11.05 (11.05)	<0.4
20	$C_{16}H_{26}N_2O_3 \cdot C_2H_2O_4$	56.24 (56.30)	7.34 (7.37)	7.29 (7.36)	<0.4
21	$C_{12}H_{21}N_3O_3S \cdot 1.2C_2H_2O_4 \cdot 0.1H_2O$	43.54 (43.60)	5.99 (6.08)	10.58 (10.53)	<0.4
22	$C_{15}H_{24}N_2O_2 \cdot C_2H_2O_4 \cdot 0.1C_3H_6O$	57.69 (57.91)	7.44 (7.24)	7.78 (7.75)	<0.4
23	$C_{16}H_{26}N_2O_2 \cdot C_2H_2O_4$	58.68 (58.89)	7.66 (7.52)	7.60 (7.62)	<0.4
24	$C_{17}H_{28}N_2O_2 \cdot C_2H_2O_4 \cdot 0.2H_2O$	59.11 (58.77)	7.94 (7.59)	7.26 (7.60)	<0.4
25	$C_{18}H_{30}N_2O_2 \cdot C_2H_2O_4$	60.59 (60.54)	8.14 (8.04)	7.07 (7.00)	<0.4
26	$C_{16}H_{26}N_2O_3 \cdot C_2H_2O_4$	56.24 (55.87)	7.34 (7.10)	7.29 (7.25)	<0.4
28	$C_{19}H_{24}BrN_3 \cdot 1.4C_2H_2O_4 \cdot 0.2C_3H_6O$	52.55 (52.77)	5.51 (5.29)	8.21 (7.97)	<0.4
29	$C_{19}H_{23}N_3 \cdot 2.5C_2H_2O_4 \cdot 0.4C_3H_6O$	55.87 (55.89)	5.66 (5.79)	7.76 (7.85)	<0.4

30	$C_{17}H_{21}N_3 \cdot 1.6C_2H_2O_4 \cdot 0.4C_4H_{10}O$	59.36 (59.66)	6.44 (6.39)	9.53 (9.75)	<0.4
31	$C_{18}H_{23}N_3 \cdot 1.5C_2H_2O_4$	60.57 (60.57)	6.29 (6.18)	10.09 (10.01)	<0.4
32	$C_{19}H_{25}N_3 \cdot 1.8C_2H_2O_4 \cdot 0.1C_3H_6O$	59.37 (59.39)	6.35 (6.51)	9.07 (9.16)	<0.4
33	$C_{18}H_{22}BrN_3 \cdot 2.0C_2H_2O_4$	48.90 (48.67)	4.85 (4.69)	7.78 (7.56)	<0.4
34	$C_{16}H_{19}N_3 \cdot 2.6C_2H_2O_4$	52.24 (52.56)	5.00 (4.70)	8.62 (8.72)	<0.4
35	$C_{17}H_{21}N_3 \cdot 2.7C_2H_2O_4 \cdot 0.1C_3H_6O$	52.81 (52.87)	5.27 (5.19)	8.14 (8.21)	<0.4
36	$C_{18}H_{23}N_3 \cdot 2.2C_2H_2O_4$	56.11 (56.11)	5.76 (5.62)	8.76 (8.68)	<0.4

1. Ussing, C. A.; Hansen, C. P.; Petersen, J. G.; Jensen, A. A.; Rohde, L. A.; Ahring, P. K.; Nielsen, E. Ø.; Kastrup, J. S.; Gajhede, M.; Frølund, B.; Balle, T. Synthesis, Pharmacology, and Biostructural Characterization of Novel $\alpha_4\beta_2$ Nicotinic Acetylcholine Receptor Agonists. *J. Med. Chem.* **2013**, *56*, 940-951.

2. Rohde, L. A.; Ahring, P. K.; Jensen, M. L.; Nielsen, E. Ø.; Peters, D.; Helgstrand, C.; Krintel, C.; Harpsøe, K.; Gajhede, M.; Kastrup, J. S.; Balle, T. Intersubunit Bridge

Formation Governs Agonist Efficacy at Nicotinic Acetylcholine α4β2 Receptors: Unique Role of Halogen Bonding Revealed. *J. Biol. Chem.* **2012**, *287*, 4248-4259.